Influence of reaction conditions on hydrothermal carbonization of monosaccharides

Pierpaolo Modugno

Submitted in partial fulfilment of the

requirements of the Degree of

Doctor of Philosophy

School of Engineering and Materials Science,

Queen Mary University of London

London, United Kingdom

Statement of originality

I, Pierpaolo Modugno, confirm that the research included within this thesis is my own work or that where it has been carried out in collaboration with, or supported by others, that this is duly acknowledged below and my contribution indicated. Previously published material is also acknowledged below.

I attest that I have exercised reasonable care to ensure that the work is original, and does not to the best of my knowledge break any UK law, infringe any third party's copyright or other Intellectual Property Right, or contain any confidential material.

I accept that the College has the right to use plagiarism detection software to check the electronic version of the thesis.

I confirm that this thesis has not been previously submitted for the award of a degree by this or any other university.

The copyright of this thesis rests with the author and no quotation from it or information derived from it may be published without the prior written consent of the author.

Pierpaolo Modugno

November 13th, 2021

Details of publications:

- Nicolae, S. A., Au, H., **Modugno, P**., Luo, H., Szego, A. E., Qiao, M., ... & Titirici, M. M. (2020). Recent advances in hydrothermal carbonisation: from tailored carbon materials and biochemicals to applications and bioenergy. Green Chemistry, 22(15), 4747-4800.
- **Modugno, P.,** & Titirici, M. M. Influence of reaction conditions on hydrothermal carbonization of fructose. ChemSusChem.

Acknowledgements

Firstly, I want to thank my first supervisor Professor Magda Titirici for having allowed me to become a part of her research group. I am grateful to her for the inspiration she has given me with her work, the constant support, the great tips and advices, the infinite supply of trust and the of energy she has provided to me in times when I needed it.

My most sincere gratitude goes also to my second supervisor Dr Petra Szilágyi for her invaluable support in times of need.

I consider myself very lucky to have had the chance of working, spending time, sharing moments of fun, happiness, enthusiasm, doubts and concern with Sabina and Anthony. The memory of the moments spent together will always warm my heart.

I want to thank all my colleagues at the Titirici group, Jingyu, Hui, Servann, Philip, Alain, Anders, Heather, Richard, Jesus. Maria, Hande, Lin, and to those from other groups, like Szymon, Pavel, Yamin and Alex for their friendship, their precious help, the laughs and the good times spent together.

Thank you to Prof. Dr. Joan J. Manyà and Dr. Belén González García and my colleagues from Green Carbon project spread throughout Europe for the great lesson of shared knowledge.

Thank you to Simone and Vito, friends in life and science and fellow PhD students, for their incredible and patient support both for scientific and human matters.

Thank you to Mario for being close despite distances.

To my friends in London, Giuseppe, Gioia, Ilaria, Tina, Davide, my second family who never made me feel alone in a huge and sometimes intimidating city like London.

Finally, to my first family, my mother and my father, my brothers and my sister for their love.

Abstract

The grim perspective of a near future when out-of-control global warming caused by $C0_2$ emissions will threaten to put human lives in serious danger is pushing the scientific community to seek for alternatives to fossil fuels to counteract this negative trend. At the moment, fossil fuels are the main source of energy and chemical building blocks for the synthesis of plastics. Hydrothermal carbonization is a process that aims to replace fossil fuels with renewable biomass as source of energy (biofuels) and materials (platform chemicals and hydrothermal carbon).

The process of hydrothermal carbonization has been known for a little more than a century as a way to mimic the natural process of coalification of biomass. It consists in a conversion of wet biomass in water, at subcritical temperatures (180-250°C) and autogenous pressure. Biomass is made of lignin, a polymer of alkylphenol derivatives, cellulose and hemicellulose (polysaccharides). These materials, in hydrothermal conditions, undergoes a series of reaction: hydrolysis of large polymer chains, solubilisation of monomers in water, dehydration, fragmentation and ring opening reaction, oxidation and formation of organic acids and re-polymerization to amorphous carbonaceous materials.

This process is extremely interesting because some of its products have been recognised as strategic for a future emancipation from fossil fuels: furan derivatives like furfural, 5-hydroxymethylfurfural and levulinic acid can be a source for the synthesis a great variety of chemicals, including biofuels. The amorphous carbonaceous materials (hydrothermal carbon) has been successfully employed as a starting material for the development of electrode in batteries, supercapacitors and fuel cells, or gas capture.

However, a thorough understanding of the underlying mechanisms of hydrothermal carbonization still needs to be achieved. The aim of this research project is to evaluate the effect of the chosen parameters on the sugar conversion, the change of the product yields and the morphological and chemical properties of HT carbon; to highlight the correlation between chemicals in the liquid phase and HT carbon; to get a deeper understanding on the chemical structure of HT carbon.

The attention was focused on three monosaccharides: fructose, glucose and xylose.

Hydrothermal conversion of fructose was tested by varying the reaction time (2-12h), acid catalysis (H_2SO_4, HNO_3, HCl, HBr, HI) and headspace feed gas (air, N_2, CO_2). The soluble and insoluble products were collected and the results discussed. Fructose proved to be a very reactive substrate for hydrothermal conversion also in plain water and absence of catalyst, leading to a maximum HMF yield of HMF of 52% after 3 h. Strong acids strongly accelerate fructose conversion to carboxylic acids but they have a less pronounced effect on HT carbon formation. A pressurized system has also a positive effect in terms of conversion. Morphological and chemical analysis of HT carbon produced showed that the alkylfuran skeleton evolves through time to a more condensed and cross-linked structure. The presence of a family of oligomers formed by units with a mass of 211 Da suggests that HT formation proceeds via progressive polymerization of a well-defined monomer.

Hydrothermal conversion of glucose was performed in conditions of increasing reaction time (2-12h) and different acid catalysis (H_2SO_4, HNO_3, HCl, HBr, HI). In this case, glucose proved to be a less sensitive substrate to dehydration than fructose. Acid catalysis greatly increase its conversion and it is possible to distinguish the different contribution of the anions in the ability to catalyse the reaction. Morphological and chemical analysis of HT carbon produced showed similar results to those obtained from fructose but also suggest that HMF concentration throughout time plays a key role in the growth rate of carbon particles. Oligomers species were also detected in this case.

Finally, the effect of reaction time (2-12h) was evaluated for the hydrothermal conversion of xylose. The structural difference between xylose and the previously studied fructose and glucose has a profound impact on its reactivity in hydrothermal conditions. Although the time scale of its conversion to FF is roughly comparable to glucose conversion to HMF, FF is notably more stable than its hexose-derived furan analogous. Its relative stability depends on the fact that there is no reaction occurring on FF that is similar to the HMF ring opening. Lower HT carbon yields also suggest that carbon formation is less efficient with FF molecules. The slight difference of the FF molecule has repercussions on the structure of carbon spheres as well as their chemical structure. HT carbon particles have a reduced

tendency to aggregate as reaction time proceeds. Chemical characterization showed similarities with C_6 HT carbon but also a distinctive more aromatic character that once again can be ascribed once the different chemistry of FF. In this case, a few species in the mass range between 800 Da and 1500 Da were found, whose masses increase with time, with little evidence of oligomeric nature.

The kinetic modelling of the data of concentration *versus* reaction time allowed to find the reaction rate constants associated with glucose, fructose and xylose degradation to their dehydration products (HMF and furfural respectively) as well as the constants related to levulinic acid and hydrothermal carbon formation. These constants are in good agreement with previous studies and proves that glucose dehydration is the slowest ($k=1.8 \cdot 10^{-5}\ s^{-1}$), followed by xylose ($k=3.9 \cdot 10^{-5}\ s^{-1}$) and fructose ($k=7.6 \cdot 10^{-5}\ s^{-1}$).

Contents

List of abbreviations

AA	acetic acid
FA	formic acid
FF	Furfural
fru	Fructose
FTIR	Fourier-transform infrared spectroscopy
glu	Glucose
HMF	5-hydroxymethylfurfural
HT	Hydrothermal
LacA	lactic acid
LevA	levulinic acid
MALDI-TOF-MS	Matrix-Assisted Laser Desorption/Ionization - Time of flight - Mass spectrometry
NMR	Nuclear magnetic resonance spectroscopy
SEM	Scanning electron microscopy
xyl	Xylose

List of figures

List of schemes

List of tables

Chapter 1 Introduction

The illusion of an economic system based on unrenewable resources and aiming for indefinite growth is starting to take its toll on earth. For the first time, mankind is confronting with the fact that the consequences of its actions might not only heavily impact the environment, they can also pose a threat to its own existence. Climate change is the major threat of our time. Caused the greenhouse effect, triggered by massive release in the atmosphere of CO_2 that had been sequestered by photosynthetic organisms in ancient times and stored underground for millions of years, climate change has now reached a point in which it is expected to cause irreversible damage unless a drastic reduction of greenhouse gas emission is accomplished.[1] The most feared effects are desertification of dry lands[2] and out-of-control acceleration in the rise of the sea level, due to polar ice sheets melting.[3] The Paris climate agreement in 2015 has set, among the international community, the goal of keeping the increase in the global mean temperature below 2 °C, in order to avoid the most serious consequences. In the long term, the ambition is to reach net-zero by the middle of the 21st century.

In order to fulfil these ambitious requirements, we need to resolutely and definitively steer away from exploitation of fossil resources. It is estimated that more than 90% of the raw material extracted from fossil deposits is intended for energetic purposes.[4] Therefore, our entire economic and productive system must be re-thought and converted in the key of sustainability. This implies a series of challenges: firstly, diversification of energy sources and sustainable exploitation of local renewable sources of energy, such as solar, wind, tidal or geothermal power.

The intrinsic discontinuity of these energy sources represents the second challenge in this radical transformation: in order to overcome this limitation and secure a constant supply of energy, we must develop very efficient ways to capture it and an increased capacity to store it using sustainable materials. Unfortunately, many technologies to exploit renewable sources of energy can hardly be defined as renewable or sustainable, as they make use of

materials or metals whose scarcity[5] and extremely localized availability[6] seriously hinders the global spread of these systems. Furthermore, the aforementioned discontinuity of renewable energies forces us to rely heavily on batteries to store electric power. Lithium batteries are the widest spread batteries nowadays, consisting of two electrodes, typically lithium cobalt oxide ($LiCoO_2$) cathode and graphite (C_6) anode.[7] In this case, both of its two main components, lithium and graphite cause concern not only about their limited overall availability,[8], [9] but also because the exploitation of these resources comes at the cost of impoverishment of people, health issues and pollution of the nearby environment.[10] Such a grim scenario can hardly been juxtaposed to words like "green" or "sustainable". A truly sustainable technology for large scale energy storage solutions should involve cheap, environmentally friendly and widely available materials such as molten salts or bio-derived carbon materials.

Among all renewable sources of energy, solar energy is a special case. In fact, the whole life on earth is based on the developed ability of some organism to catch the energy coming from the solar radiation through photosynthesis. Photosynthesis, in a nutshell, is a wonderful and extremely efficient process to capture solar energy and store it in the form of highly energetic chemical bonds of saccharides. After all, the molecules that make up fossil fuels are remnants of ancient biomass which captured and stored solar energy in their chemical bonds for millions of years. It obvious, then, to turn again to biomass in the perspective of a shift from fossil fuels. Unfortunately, both two traditional forms of biofuels, namely bio-alcohols (ethanol or longer chain alcohols) and biodiesels, presents some drawbacks in their use. Bio-alcohols, derived from bacterial or fungal fermentation of sugars, are less energy-dense than traditional fuels; moreover, their production is a slow process that employs microorganisms, which are costly to bio-engineer.[11] Biodiesels are methyl esters of fatty acids. They are compatible for the use in current car engines and they are much safer in terms of polluting emissions. First generation biodiesels are obtained from transesterification of non-edible oils. In order to be sustainable, non-edible oil farming should not subtract space or water to food crops.[12] Unfortunately, even if all cultivated land was repurposed and dedicated exclusively to energy crops farming, the output would never satisfy the current demand for fuel.[13] Second generation biodiesels are obtained from waste cooking oil or animal fats

and therefore do not compete with food production, but the number of impurities that these type of feedstock carries has a negative impact on the manufacturing costs.[14] For these reasons, bio-alcohols and biodiesels are unlikely to impose themselves as a solid alternative to traditional fuels.

Finally, not all fossil fuels are employed to produce energy. In fact, we must remember that around 10% of it is needed to make chemicals to make petrochemicals, such as plastics.[15], [16] Besides energy, then, the rising demand for plastic is a major driving force that pushes towards fossil fuel consumption.[16] Another threat deriving from plastic is its very poor biodegradability that is causing accumulation in the environment. Plastic pollution is alarmingly pervasive, it is able to severely impact ecosystems and it is almost irreversible.[17] Taking for granted that all kind of efforts must be done in order to reduce plastic production and disposal and promote recycling, we must admit that plastic materials possess some characteristics, like light weight and extreme versatility, which makes its production and utilization impossible to discontinue. The third challenge is therefore to identify new starting materials and develop new processes to convert these materials into valid and renewable alternatives to traditional plastics.

These three challenges require an immediate response and a strong effort to seek for innovative solutions. Hydrothermal carbonization (HTC) is a sustainable technology that aims to address them all.

The expression hydrothermal carbonization describes a thermal treatment of biomass that takes place in an aqueous medium heated at subcritical temperatures (180-250°C), under self-generated pressure. Earliest studies on HTC date back to over a century ago and they were carried out by pioneers such as Bergius, Specht, Berl and Schmidt; this process was initially meant to mimic the natural process of coal and fossil fuels formation from biomass, motivated by concerns about the temporary shortage of fossil fuel supplies.[18] Last two decades of increasing awareness about the necessity of moving away from fossil fuels have brought the topic back to attention of the scientific community.[19]–[21] As a substitute for natural coalification, HTC is able to convert a complex matrix like lignocellulosic material into coal-like materials and a vast range of light chemicals. These chemicals can be used for

energy generation or for plastic synthesis, while the coal-like materials can be employed in sophisticated applications such as electrodes. The main advantages of HTC are two: firstly, the starting material, waste biomass, is ubiquitous, it is free and its use does not imply new CO_2 emissions; secondly, as the process takes place in water, biomass does not require a preliminary drying step, thus saving great amounts of energy and time, and furthermore allowing processing of wet mixtures, including aqueous waste and sewage sludge.

Despite the huge progress made by research in unveiling the details of the process, the characteristic of the outcomes and their possible uses, there is still a perceived need to deepen the knowledge about the complex network of transformation occurring on biomass during the hydrothermal conversion, particularly concerning the mechanism of formation of carbonaceous species and the influence of reaction parameters on the overall conversion.[22], [23]

This thesis is a report of the results obtained from an investigation on the impact of varying conditions and reaction parameters on the hydrothermal conversion of fructose, glucose and xylose. These three monosaccharides, chosen as a model of cellulose- and hemicellulose-based biomass, were subjected to hydrothermal treatment under different conditions of reaction time, acid catalysts or pressure and feed gas. Their conversion products were collected, quantified and characterised.

The goals of this research project were:

- To evaluate the effect of the chosen parameters on the sugar conversion, the change of the product yields and the morphological and chemical properties of HT carbon;
- To highlight the correlation between chemicals in the liquid phase and HT carbon;
- To get a deeper understanding on the chemical structure of HT carbon.

This thesis consists of five chapter. Chapter 1 is a brief introduction on the necessity of developing an economic and productive system based on renewable resources such as biomass, which can provide a source of energy, platform chemicals and carbonaceous materials for sophisticated applications.

Chapter 2 provides an introduction on topic of hydrothermal carbonization of biomass, explaining the current understanding of the mechanism of formation of the different products in the liquid phase and the hydrothermal carbon, the studies on the influence of reaction parameters on the reaction and a brief mention on the proposed uses for the reaction products.

Chapter 3 is focused on hydrothermal conversion of fructose, glucose and xylose. Their conversion in hydrothermal conditions was tested at fixed temperature (200 °C) and increasing reaction time (2-12h). Glucose and fructose reactivities were also tested in acid conditions at fixed time and temperature (200 °C, 3 h) in presence of five different strong inorganic acids (H_2SO_4, HNO_3, HCl, HBr, HI). Finally, fructose reactivity was tested at fixed time and temperature (200 °C, 3 h) in a reactor with three different headspace feed gas (air, N_2, CO_2) at two levels of pressure (1 bar and 2 bar). The soluble and insoluble products were collected and the results discussed.

Chapter 4 presents the results of a kinetic modelling of the experimental data in function of time and offers a final summary of this study, with conclusive observations and suggestions for future investigations based on this research project.

Chapter 5 presents synthesis methods and characterization techniques used in this thesis.

Chapter 2 Literature review

The following chapter will serve as description of process of hydrothermal carbonization, with a discussion of the current understanding on the mechanisms of conversion of saccharides and an overview of the main products and their applications.

Hydrothermal carbonization

Lignocellulosic biomass consists in three main components, namely cellulose, hemicellulose and lignin. Cellulose and hemicellulose are both made of polysaccharides chains. Cellulose is a linear polymer of glucose units bonded together by β-(1,4)-glucosidic bonds. Hemicellulose is a polysaccharide too, but it differs from cellulose in that it contains a variety of saccharides, hexoses like glucose, mannose and galactose and pentoses like xylose. The presence of different sugars allows the structure to be branched but it also causes the chains to be shorter and less strong than cellulose chains. Lignin, finally, is an amorphous heteropolymer consisting of phenylpropane units joined together by different types of linkages. Although lignin structure is generally explained as being derived by the disordered polymerization of three phenyl propionic alcohols (monolignols), namely coniferyl alcohol, coumaryl alcohol, and sinapyl alcohol,[24] several other monomers are often encountered in substantial amounts or in traces in normal plants.[25]

Lignocellulosic materials undergo a vast series of transformations like hydrolysis, dehydration, bonds cleavage and formation of new bonds when they are subject to hydrothermal treatment in an aqueous medium, at subcritical temperatures and pressures.

The products of this conversion process can be divided in three groups: water-soluble compounds, solid carbonaceous species (primary and secondary chars, carbon dots) and gases (water vapour, CO, CO_2, CH_4).[26]

Water-soluble compounds include hydrolysis products of the natural polymers (monosaccharides and phenyl propionic alcohols), furan derivatives (furfural and 5-hydroxymethylfurfural) and aldehydes, ketones and carboxylic acids. Some of these compounds have receive special attention due to studies that demonstrated their strategic

importance as bio-derived platform chemicals.[27] Solid carbonaceous species can be furtherly divided in different categories: primary chars (sometimes called hydrochars) are the result of direct dehydration and pyrolysis occurring on biomass without an intermediate hydrolysis step. The result of this treatment is a charred appearance and an increased higher heating value compared to that of the original biomass that makes this material fit for combustion and energy generation, with zero net CO_2 emissions.[28], [29]

Secondary chars derive from further dehydration, condensation and polymerization of water dissolved compounds. They appear as isolated or clustered solid spheres with a range of size between hundreds of nanometres to a few micrometres. This material is often referred to humins[18], [30] or, more accurately, as hydrothermal carbon. Hydrothermal carbons are by-products in the hydrothermal carbonization of all lignocellulosic biomass, mono- and polysaccharides, hexoses and pentoses.[31], [32] The interest in hydrothermal carbon arises from the great versatility of this material has showed. Its porosity can be modified by means of natural templates or activation steps; it can be doped with heteroatoms or easily functionalized due to the plenty of oxygenated groups on the surface of the spheres.[33] Finally, carbon dots, despite being solid particles, deserve a separate mention because of their distinctive features that distinguish them from hydrothermal carbons. Carbon dots are quasi-spherical fluorescent carbon particles,[34], [35] with diameters of few nanometres,[36] an amorphous or nanocrystalline structure with sp^2 carbon clusters[37] and a large number of hydroxyl and carboxyl group on the surface.[38] The mechanism of formation of this particle is still under investigation but some interesting applications have already emerged in the detection of metal ions[39]–[42] or other chemicals,[43]–[45] as catalyst[43] or for imaging of cells.[46]

Soluble products

The hydrothermal decomposition of cellulosic materials can be divided in three phases. An initial phase of depolymerization, breaking of hydrogen bonds between cellulose fibres and hydrolysis of the glycosidic bond between sugars, with progressive shortening of the polymeric chains and dissolution of the biomass in water in its simplest constituents, namely C_5 and C_6 monosaccharides (glucose, xylose, etc.) from cellulose and hemicellulose[47] and

phenols from lignin.[48] The next phase is an intricate network of transformations that is initiated by the decomposition of monosaccharides through dehydration reactions (with formation of furan species) or retro-aldol condensations and consequent formation of shorter saccharides.

Both furans and short saccharides can undergo further conversion through ring-opening reaction or oxidation, respectively, to form carboxylic acids;[49] 3. A condensation and re-polymerization phase during which hydrothermal carbon is formed.[50]

The complex network of transformations and reaction pathways taking place during hydrothermal carbonization of lignocellulosic biomass is made apparent by the large

Table 1 *. Products of decomposition of lignocellulosic biomass in hydrothermal conditions*[58]–[61]

Aldehydes, ketones, monosaccharides	**Furan derivatives**	**Carboxylic acids**	**Phenols**
glucose fructose xylose erythrose dihydroxyacetone levoglucosan pyruvaldehyde glyceraldehyde formaldehyde acetaldehyde 2,5-dioxo-6-hydroxyhexanal	furfural HMF furfuryl alcohol 2-methylbenzofuran soluble polymers	pyruvic acid glycolic acid acetic acid lactic acid formic acid levulinic acid propionic acid	guaiacol catechol cresol

number of species that have been identified as products of this process. Without taking into account HT carbon and gaseous products (H_2, CO_2, CO),[49] we can group all water-soluble

compounds into four classes: aldehydes/ketones (including saccharides), furan derivatives, carboxylic acids and phenols (**Table 1**).[51]–[57]

The main furan derivatives formed in hydrothermal conversion of cellulosic biomass are furfural (FF) and 5-hydroxymethyl furfural (HMF). FF is found in hydrothermal conversion of hemicellulose and it derives from the dehydration of pentoses such as xylose, whereas, HMF is a product of dehydration of hexoses like fructose or glucose.[58], [62]

It is believed that glucose conversion to HMF and its subsequent products proceeds through a necessary step of isomerization of the aldose form to the relative ketose form, fructose, as it is been demonstrated in different studies.[62], [63] The rate constant of this isomerization step was found to be one order of magnitude smaller than the rate constant of dehydration of fructose to HMF,[63] thus proving that this is indeed the rate determining step in the whole reaction pathway. This isomerization, named Lobry de Bruyn–Alberda van Ekenstein transformation after the two scientists who first reported it, also encompasses the epimerization of aldoses.[64] In its original formulation, the Lobry de Bruyn–Alberda van Ekenstein transformation describes a based-catalyzed process that proceeds via enediol intermediate (**Scheme 1**), thus also explaining the chiral inversion of the C2 and the subsequent formation of mannose from glucose.[65] Soon after its discovery, the same reactivity has been observed in the presence of strong acids.[66] Later, by means of isotopic labelling, the mechanism of the acid-catalyzed isomerization was described as a 1,2 hydride shift occurring on glucose in its acyclic form (**Scheme 2**).[67] In more recent times, some studies have demonstrated the thermodynamic feasibility of different pathways connecting glucose to HMF in hydrothermal conditions without involving any fructose intermediate. Assary *et al.* reported two mechanisms: one cyclic pathway initiated by the protonation of the C2–OH group of the pyranose ring and dehydration leading to a carbo-cation rearrangement to form a furanose ring, very similar to fructose dehydration; a second acyclic one with ring opening and enolization.[68] Yang *et al.* confirmed this hypothesis, indicating the first dehydration, following C2-OH protonation, as the rate limiting step.[69] Both aforementioned studies described a secondary mechanism of glucose dehydration initiated by C2-OH protonation and forming furfuryl alcohol, with loss of one carbon atom as formic acid.[68], [69]

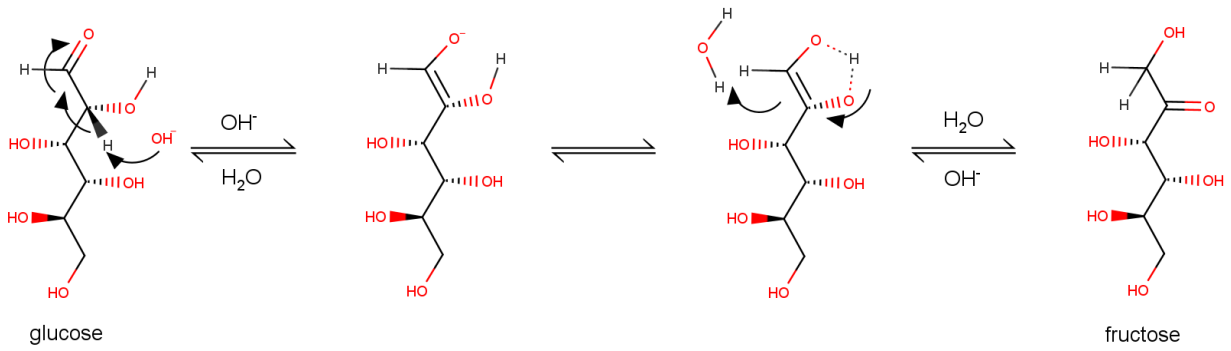

Scheme 1 *Mechanism of base-catalyzed glucose isomerization to fructose.*[70]

(a)

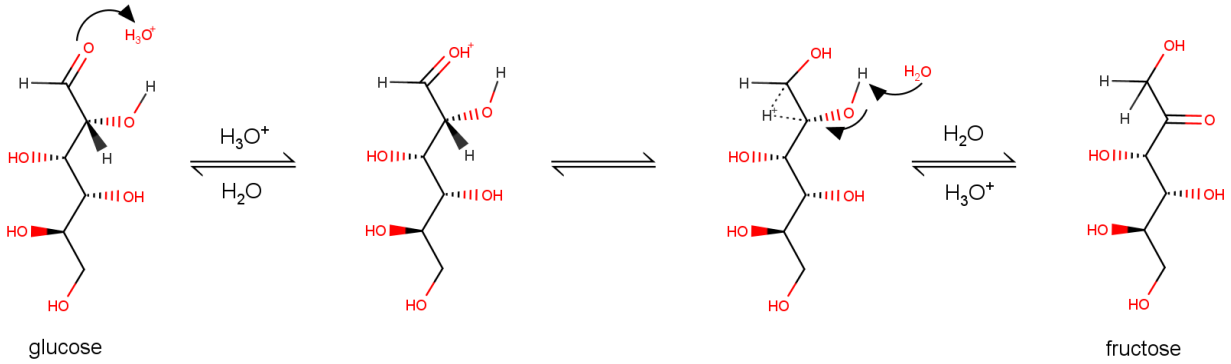

Scheme 2 *Mechanism of acid-catalyzed glucose isomerization to fructose.*[67]

The mechanism of formation of HMF *via* dehydration of fructose [Equation (1)] is explained in **Scheme 3:**[62]

$$fructose \rightarrow HMF + 3H_2O \qquad (1)$$

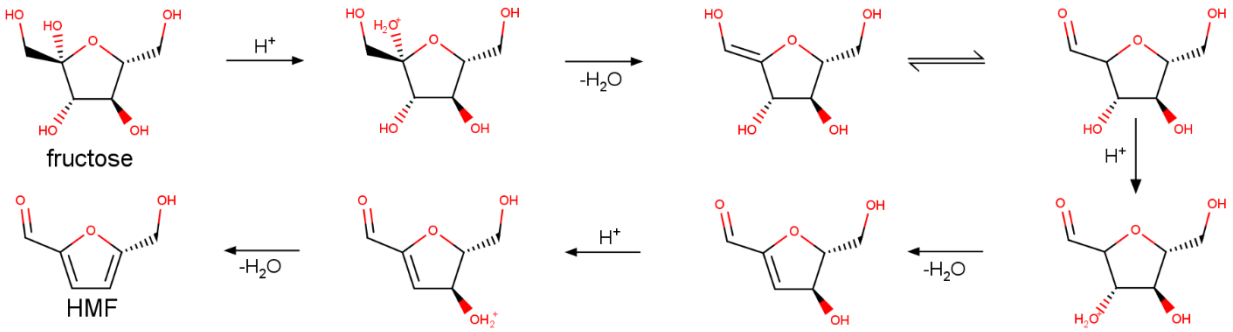

Scheme 3 *Mechanism of dehydration of fructose to HMF.*

This mechanism is supported by Zhang and Weitz studies, who demonstrated that C1 and C6 carbon atoms in D-fructose maps respectively onto the aldehyde and methoxy groups of HMF.[71] Amarasekara at al. were also able to identify the intermediate (4R,5R)-4-hydroxy-5-hydroxymethyl-4,5-dihydrofuran-2-carbaldehyde to furtherly support this mechanism.[72]

HMF has attracted a huge interest because of the reactivity of its two functional groups, methoxy- and aldehydic, and the possibilities of derivatisation that they offer. In fact, this chemical has been recognized as a valuable bio-based chemical building block[27] which can play a key role not only as intermediate for the production of the biofuel dimethylfuran (DMF),[73] but also for other biomass-derived intermediates for polymers synthesis, such as 2,5-furan-dicarboxylic acid,[74], [75] adipic acid[76] and levulinic acid (LA).[77], [78] As a consequence, a few processes for large scale synthesis of HMF from monosaccharides have already been patented. AVA Biochem, a Swiss-based company, has developed a continuous process based on carbonization of fructose that allows increased HMF yields through recycling of unreacted sugar[79] and has been producing HMF at commercial small scale since 2014;[80] in its pilot plant in Amsterdam, Netherlands, Avantium is using a technology based on solvolysis of sugars in methanol to obtain HMF ethers that are catalytically oxidized to 2,5-furandicarboxylic acid (FDCA).[81], [82]

Levulinic acid (LevA), also named 4-oxopentanoic acid, is derived from the rehydration and ring opening reaction of HMF. In this reaction, HMF undergoes a fission of the formyl group and formic acid (FA) is formed [Equation (**2**)] and Scheme 4.[69]

$$HMF + 2H_2O \rightarrow LevA + FA \quad (2)$$

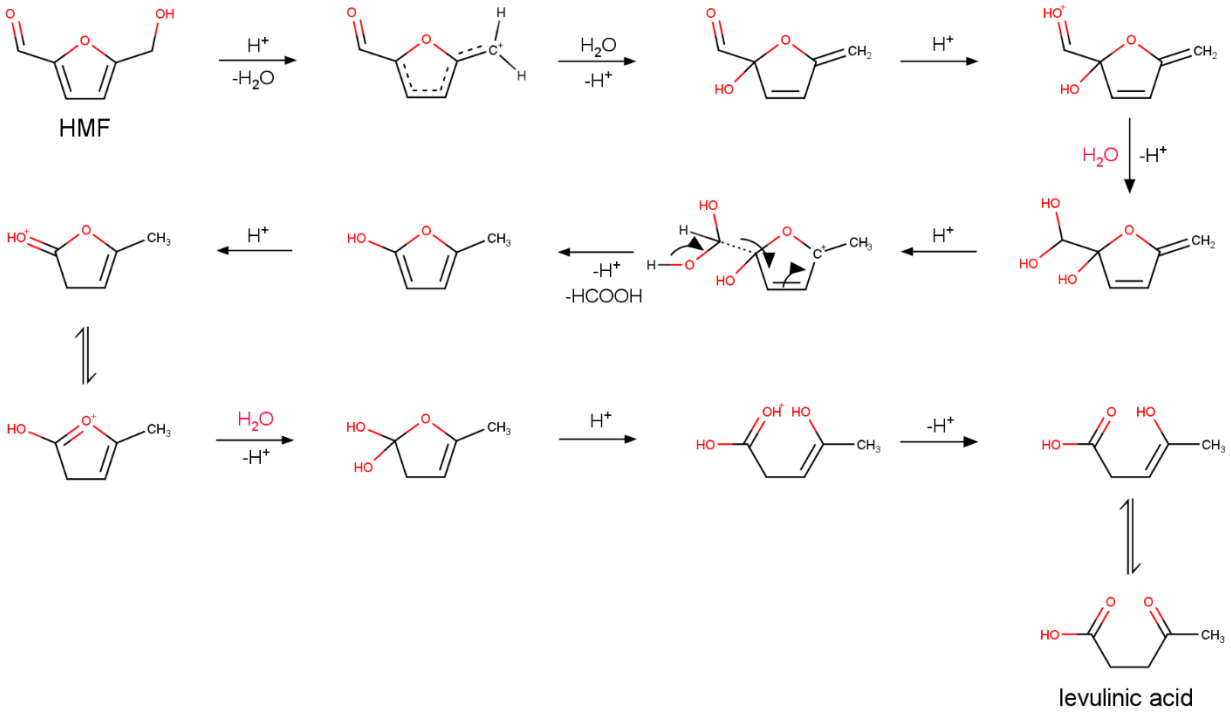

Scheme 4 *Mechanism of rehydration of HMF to levulinic acid with loss of a carbon atom as formic acid.*

LevA and FA are already commercially produced by GFBiochemicals[83] through the Biofine process. This process employs cellulosic biomass for the in a two-step conversion: in the first step, the ground biomass is converted in a few seconds to HMF with dilute sulfuric acid at a temperature of 210-220 °C and a pressure of 25 bar. Subsequently, the mixture is transferred to a second reactor where HMF is converted to LevA and FA, in milder conditions of temperature and pressure, using the same catalyst. Furfural and other by-products are removed at this stage. Water is subsequently boiled off, along with the remaining volatiles, and levulinic acid is extracted from the resulting mixture by distillation. In this process, approximately 50% of the initial mass of C6 sugars is converted to LA, 20% to formic acid and 30% to tar (i.e. hydrothermal carbons).[78] Levulinic acid (LevA) is considered as one of the most promising bio-derived platform chemicals because of its applications as starting material for the production of fuels, solvents, polymers, plasticisers, resins, anti-freeze agents, food-flavourings, herbicides and pharmaceuticals.[84], [85]

Furfural is largely produced by dehydration of pentose sugars, of which hemicellulose is rich. Hemicellulose is the one of the most abundant polymers in nature, along with cellulose, chitin and lignin,[86] making up about 20-50% of the total weight of plant biomass.[87], [88] It differs from cellulose in that other species of C_5 and C_6 monosaccharides, besides glucose, and uronic acids participate to its structure.[87] Interestingly, bio-derived FF produced to commercial scale vastly predates the recent resurgence of interest for bioderived chemicals like HMF. In fact, FF was studied as way to make use of oat hulls, a cheap and low value by-product of oats.[89] Early studies on acid-catalysed dehydration of water solutions of xylose to FF date back to almost a century ago[90], [91] and commercial production of FF from biomass even predates those studies,[92] while a more focused investigation on the FF formation from xylan during thermal treatment of wood has been reported in more recent times.[93]

First attempts at understanding the kinetics of xylose conversion in acidic medium comes from studies of Garrett[94] and Feather[95] who both proposed an acyclic pathway of formation. A more recent study by Antal Jr. contradicted these early explanations and concluded that a cyclic route of acid-catalyzed xylose dehydration initiated by C1 hydroxyl protonation was more fitting to experimental data.[96] A later study by Nimlos, however, specified that a protonation on C2 hydroxyl group is energetically favoured.[97]

Secondary products of hydrothermal degradation of xylose in plain water or acid-catalyzed conditions are glyceraldehyde, pyruvaldehyde, lactic acid, glycolaldehyde, hydroxyacetone [96]and formic acid.[96], [98] Oefner observed that basic catalysis drove xylose conversion away from conversion to FF and towards the production of aldehydes, ketones and organic acids (formic, glycolic, lactic, and acetic acid). This alternative pathway is initiated by Lobry de Bryn-Alberda van Ekenstein rearrangement of xylose, forming the C2 epimer lyxose and other pentoses, whose fission by means of retro-aldol condensation is responsible for the formation of C_1, C_2, C_3 and C_4 species.[99]

In more recent times, the interest towards the hydrothermal conversion of cellulosic biomass has brought back bio-derived furan species under the spotlights, including FF.

Xylose, consequently, has been studied alongside fructose and glucose from the point of view of hydrothermal conversion.

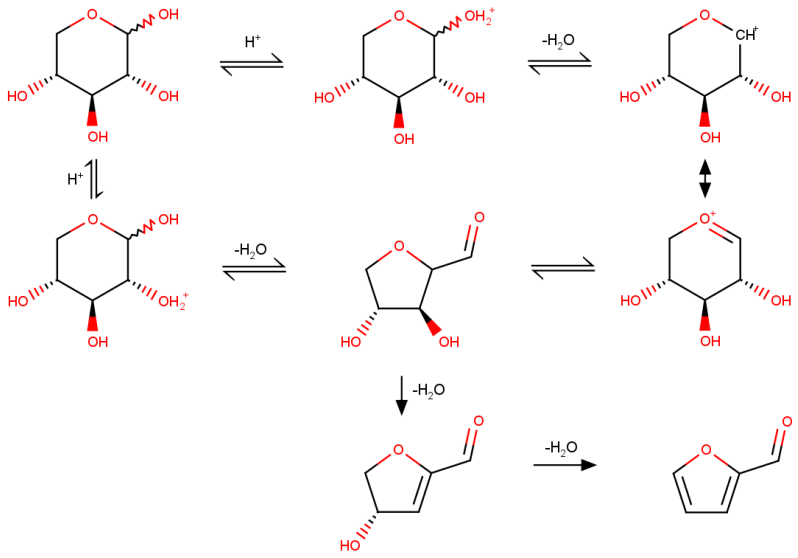

Scheme 5 *Mechanism of acid-catalyzed xylose dehydration to furfural.*

Nowadays, the method of conversion of biomass into furfural traditionally involves a two-step process:[100]

1. Hydrolysis of lignocellulosic biomass using acid (mainly sulfuric acid) and heat to release the pentoses (mainly xylose) from the biomass stock, and
1. Cyclodehydration of the pentoses using acid and steam for the production of furfural.

The typical process involves the breaking down of the hemicellulose fraction of a lignocellulosic biomass in a sulfuric acid solution 3% for 3 hours, in a range of temperatures between 170-185 °C. In these conditions, 40-50% of the potential furfural is obtained. The undissolved residual solid, composed of lignin and cellulose, is recovered and employed for energy recovery, while the acid catalyst is recycled.[101] Several mechanisms have been speculated to explain pentoses dehydration to furfural including both acyclic[102] and

cyclic[96] intermediates. The interest in bio-derived furfural arises from the many possibilities that this molecule or its derivatives offers for the synthesis of solvents, plastics, resins or as a building block for the synthesis of pharmaceuticals.[100] Moreover, the special chemical properties of this molecule allow for multiple condensation reactions and formation of long chain alkanes that can be exploited for bio-derived, carbon neutral fuels.[103]

Furfural, like HMF, is regarded as a good candidate molecule to serve as a platform chemical. Li *et al.* noted that the use of furfural as a functionalized renewable platform compound allows the sustainable production of value-added chemicals through fewer steps than those required when starting from fossil feedstocks.[104] Among the value-added chemicals cited in their study, there are C_5 derivatives like levulinic acid and γ-valerolactone and C_4 derivatives like succinic acid. An increase in the demand for high-value bioderived chemical might push to a growth of furfural market capacity. Nonetheless, a reduction in the cost of bio-derived furfural is necessary to win the competition against traditional fossil fuel derived chemicals.[105] Diversification of products obtained from biomass can be the key to tackle this issue. Zang suggests the possibility of reducing the cost of furfural by 37% with respect to market price by producing it from biomass in a bio-refinery along with lignin and ethanol.[106] Alternatively, according to Dalvand, repurposing existing production sites to produce furfural derivatives (such as 1,5-pentanediol, 2-methyltetrahydrofuran) would lead to profits that are five times higher than those made by selling furfural.[107] In any case, all these changes are based on a better understanding of the fundamentals of hemicellulose conversion to furfural.

The above-mentioned compounds have received a great deal of attention because of their primary role in the transition to sustainable, bio-based fuels and materials. However, there are many other interesting chemicals produced during hydrothermal carbonization of biomass that, despite their limited strategic relevance, can still have commercial value due to their abundance as by-products in the hydrothermal conversion of biomass. Retro-aldol condensation of aldohexoses like glucose produces short-chained carbohydrates like erythrose and glycolaldehyde if the cleavage occurs on the C2-C3 bond or dihydroxyacetone and glyceraldehyde or if the cleavage occurs on the C3-C4 bond. In the latter case, both of

these trioses can be dehydrated to pyruvaldehyde, which in turn is converted to lactic acid (LacA) with a benzylic acid rearrangement.[108] LacA is usually found in higher concentrations when basic conditions are employed for hydrothermal conversion of cellulosic biomass.[109], [110] However, its presence has been detected also in acidic conditions.[108] LacA is a promising platform chemical for its synthesis of solvents (ethyl lactate), biodegradable plastics (polylactic acid, PLA) and other polymer precursors (acrylic acid).[111] FA, a less valuable by-product in the synthesis of LevA, has been extensively used in the preparation of organic esters and in the manufacture of drugs, dyes, insecticides, and refrigerants and green solvents,[78] as well as an excellent liquid hydrogen storage material.[112], [113] Acetic acid (AA) has been reported previously in hydrolysis and oxidation of glucose[114] and cellulose[115] in hot compressed water. Its synthesis has been explained by two alternative pathways. The first route involves decarbonylation or decarboxylation of lactic acid with production of acetaldehyde which is then oxidized to AA.[116]–[118] Lactic acid derives, in turn, from fructose, via retro-aldol condensation and base-catalyzed benzylic acid rearrangement of pyruvaldehyde (Error! Reference source not found.).[110]

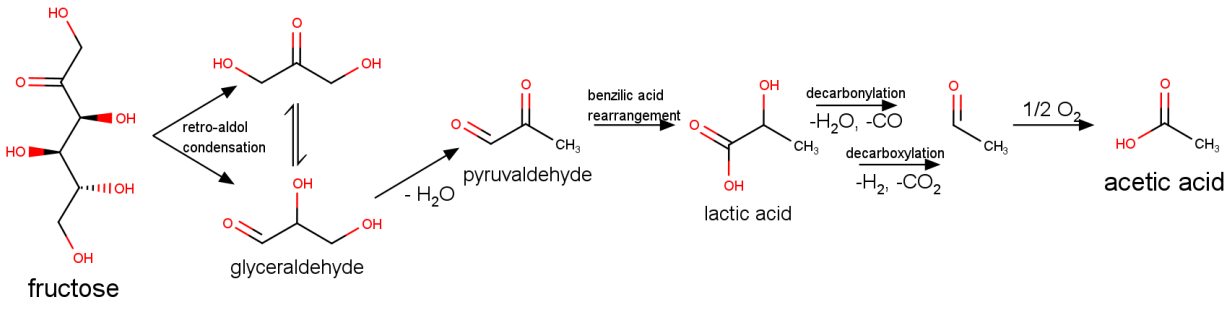

Scheme 6 *Mechanism of formation of acetic acid from fructose through lactic acid intermediate.*

The second route involves the oxidation of furfural and HMF.[119] A general formula for the oxidation of an aliphatic chain of *n* carbon atoms to acetic acid is given by Equation (**3**):

$$CH_3 - (CH_2)_{n-2} - CH_3 + \frac{3}{2}(n-1)O_2 \rightarrow CH_3 - COOH + (n-2)CO_2 + (n-1)H_2O \quad (\mathbf{3})$$

Bio-derived AA could be employed for the production of calcium/magnesium acetate.[119] Ca-Mg acetate salts are a viable and more environmentally friendly alternative to conventional inorganic road de-icers such as chlorides, as they are less toxic than chlorides, easily biodegradable and less harmful to plants and aquatic life.[120], [121]

Hydrothermal carbon

Hydrothermal carbon (HT carbon) is the amorphous carbonaceous material consisting of micro- or nano-scaled spherical particles[19] which are by-products in the hydrothermal carbonization of all lignocellulosic biomass, mono- and polysaccharides, hexoses and pentoses.[31], [32] An investigation on its chemical structure has proved to be fundamental to get a better understanding of its mechanism of formation. A great contribution to the ongoing research about formation and chemical structure of HT carbons has come from the efforts of Baccile et al.[122] and Falco et al.,[32] who identified the structural motif of furan rings connected aliphatic and vinyl linkers that clearly betrays the derivation of HT carbon as a result of disordered polymerization via aldol addition/condensation of furan and other organic species.[59] Sumerskii *et al.* confirmed these observation and proposed a polycondensation of HMF molecules with formation of ethers and acetals as the origin of HT carbon, also noting the possibility of formation of C-C coupling between furan rings in the case of FF-derived HT carbon.[123] Patil et al. assigned a pivotal role in the formation of HT carbon to a HMF-derived fleeting species, 2,5-dioxo-6-hydroxy-hexanal (DHH).[124] Moreover, they noted that different concentrations of HMF may affect HT carbon chemical structure.[124] Following these early studies, van Zandvoort et al. provided several more details about the relation between processing parameters such as feedstock, reaction temperature and acid concentration and the molecular structure of carbon spheres and revealed their furan structure with alcohol, acid, ketone and aldehyde functional

groups.[125], [126] By means of 1D and 2D solid state NMR and ^{13}C labelling, they identified abundant C_{α}-$C_{aliphatic}$ and C_{α}-C_{α} linkages between furan units and rarer C_{β}-C_{β} and C_{β}-$C_{aliphatic}$

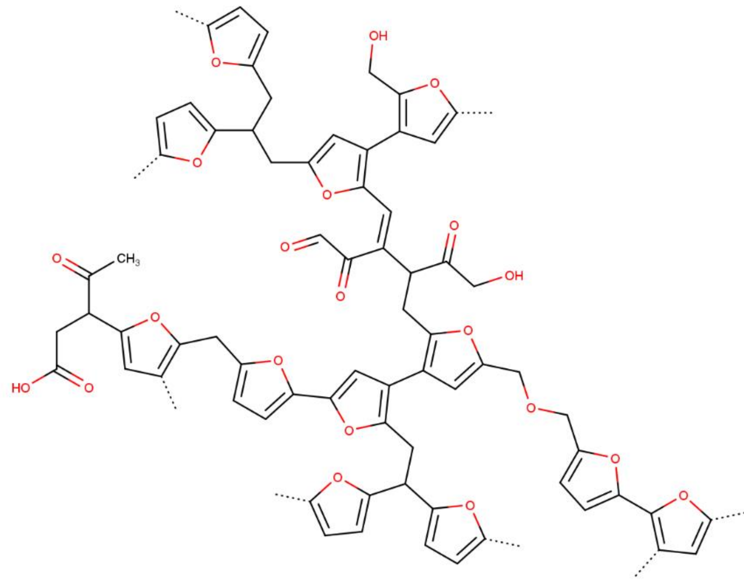

***Figure 1** Chemical structure of C_6 sugars-derived hydrothermal carbon as proposed by can Zandvoort et al.*

cross-links. Thus, they were able to elaborate a refined molecular structure (**Figure 1**). This model is also notable for including covalently bonded LevA in the HT molecular structure,[125] an observation that has found more confirmations in later studies.[127] The more the investigations on this topic has progressed, the more it has become apparent that HT carbon composition is not homogenous throughout a whole spherical particle, but rather composite-like, comprising of many different structural units such as aliphatic, furans, condensed benzene rings (occasionally) and other functional groups). Brown at al, made use of DFT fitting of experimental data to propose two models of structure: 1. arene domains comprised of 6-8 rings connected *via* aliphatic chains; 2. a furan/arene structure consisting primarily of single furans and 2 or 3 ring arenes.[128] Striking evidence of a core/shell structure was found in glucose-derived hydrothermal carbon, where the core composition is richer in C whereas functional groups such as aldehydes and carboxylic dominate the outer shell.[129] There is a possibility that this outer and "softer" shell coincides with the non-aqueous solvent soluble fraction identified by Cheng et al. made by oligomers that have mass numbers ranging from 200 to 600 Da.[130] In general, longer reaction times are known to

have a positive effect on both growth of particles and final yields.[131], [132] The growth of HT particles also seems not to be limited by HMF availability, as significant increase in the particles size was also observed after complete consumption of HMF, pointing to a growth mechanism based on coalescence.[133][133] Their size, eventually, reaches a maximum after which no further growth is observed.[132]

The question over the growth mechanism of HT carbon raises another question: what is the connection between the water-soluble precursors and the insoluble, amorphous HT carbon? Are there any intermediates in this polymerization process and what do they look like? To answer these questions, some studies have focused their attention to a large group soluble compounds found in trace in the water phase after hydrothermal conversion of sugars. These chemicals, despite comprising only 5% of the precursor's carbon content,[134] are of great interest as they may provide some insight on the intricate sugar dehydration pathways and the early mechanisms of HT carbon formation. Poerschmann et al. have detected a large number of chemical species in the mass range between 120 Da and 300 Da by means of GC-MS; among the proposed identifications, there are many keto- and benzo-furan species.[134] Shi et al. have investigated a similar mass range, between 150 Da and 270 Da. Besides identifying many species rich in furan, benzofuran and phenolic and moieties, they have gone further to propose a mechanism that challenges common conception of HT carbon formation through polymerization of furan derivatives. Instead, they proposed a mechanism based primarily on polymerization of sugar-derived α-carbonyl aldehydes, followed by cyclization and formation of aromatic domains.[135] In this model, many of the small and medium-sized water-soluble species would form through hydrolytic C-C cleavage of early carbocyclic polymers.[136], [137]

HT carbon allows for its properties to be tuned depending on the synthetic conditions rendering it eligible for advanced applications such as supercapacitors,[138]–[141] batteries,[142], [143] fuel cell electrodes,[141], [144], [145] electrocatalysts,[146] metal ions nanosensing[147] and gas capture.[33], [148]–[150]

Influence of reaction conditions

HTC of biomass is usually performed in acidic conditions, because hydrolysis and dehydration reactions are catalyzed by hydronium ions. As mentioned before, HMF is the pivotal compound in the whole process of transformation, as it is the starting point for both conversions to dissolved products (levulinic acid) and solid products (hydrothermal carbon). Therefore, any consideration about the influence of reaction parameters over the final products of hydrothermal carbonization must take into account the reactivity of HMF. Rate-limiting step in the dehydration of glucose to HMF in acidic medium is the isomerization of glucose to fructose.[62], [63] This explains the reluctance of glucose, compared to fructose, in dehydrating to HMF: in fact, isomerization of glucose to fructose is base catalyzed and therefore it is slower in typical acidic condition for the synthesis of HMF.[62]

The nature of the acid used to catalyze dehydration of saccharides plays a major role in the final yield and distribution of products. Lu et al. noted a faster kinetic in HCl catalyzed hydrolysis of cellulose compared to that of H_2SO_4 in same concentration.[151] Reiche et al. described a different behaviour in HTC of 20 wt% glucose solutions treated with HCl or HNO_3 to the same synthesis pH. Nitric acid in fact, due to the oxidizing properties of NO_3^-, drives the conversion towards higher yields of hydrothermal carbon in spite of HMF, levulinic acid and formic acid. Hydrochloric acid, conversely, catalyzes more efficiently conversion of glucose to HMF and levulinic acid subsequently, with much lower HTC carbon yields. It is also worth pointing out to a strong imbalance between levulinic and formic acid, in favour of the former, for both HCl and HNO_3 acidified samples, despite a theoretical ratio of 1:1. This effect is particularly strong when at synthesis pH 0. In these conditions, the strong acidity is causing formic acid and other carboxylic acids to break down into gaseous species (CO, CO_2), also causing a slight rise in the final pH.[152]

Hydrothermal treatment of poly- and monosaccharides in basic conditions leads to quite significant change in the scenario. In fact, although bases such as NaOH, KOH and $Ca(OH)_2$ are all able to accelerate the hydrolysis of cellulose to glucose, they somehow change the pathway of carbonization, slowing down its dehydration to HMF, with consequent build-up of glucose concentration and lower yields of levulinic acid.[61], [151] On the other hand, a

rise in formic acid and lactic acid concentration is observed with higher synthesis pH,[151] pointing out the preferred pathway of degradation of the hexoses, involving retro aldol condensation, as shown in **Figure 2**.

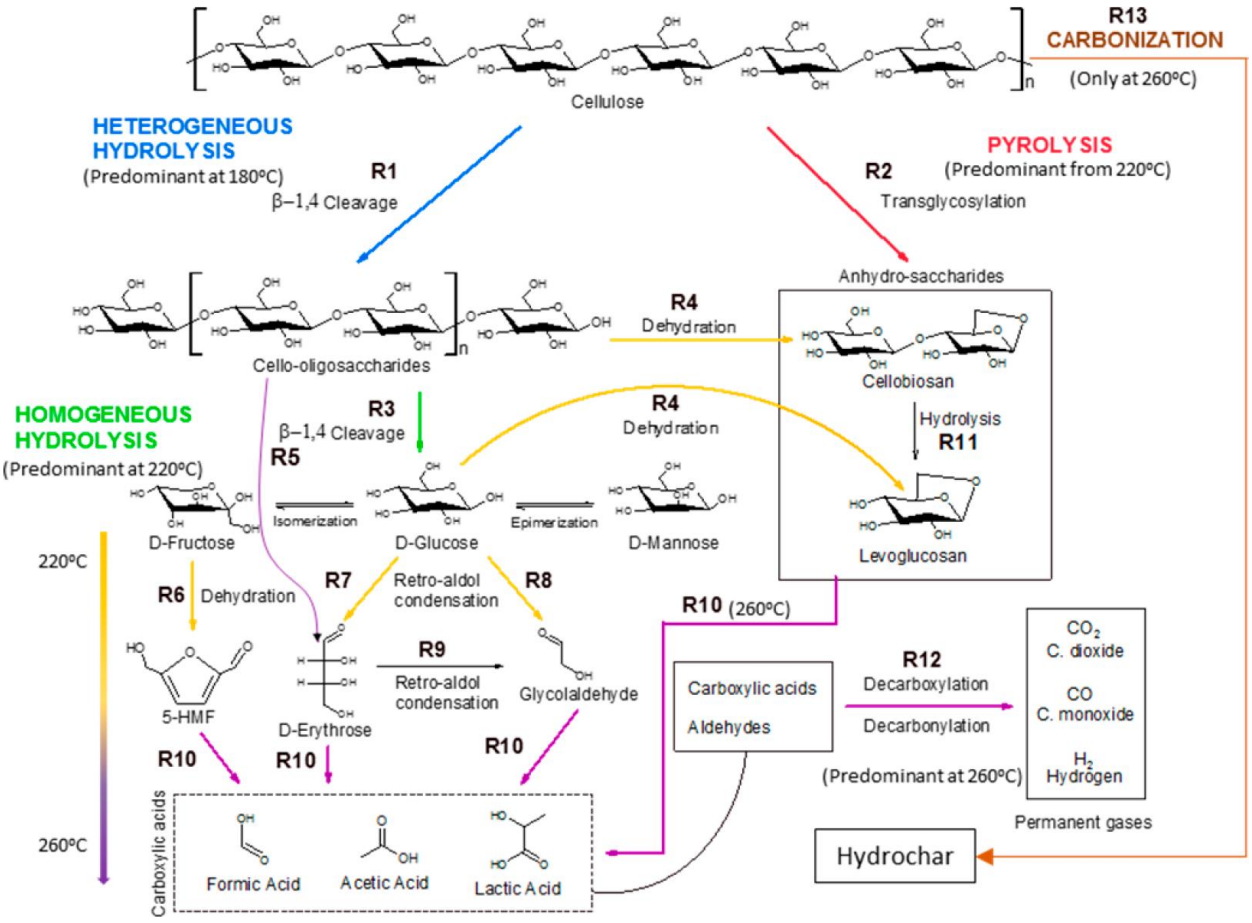

Figure 2 *Schematic of main reaction pathways of cellulose decomposition in hydrothermal conditions. Reproduced from Buendia-Kandia et al.*[49] *Copyright 2017 American Chemical Society*

Salt anions too can affect the conversion of sugars in hydrothermal conditions. In fact, anions with good leaving group qualities can strongly accelerate the rate of dehydration of fructose to HMF, provided that they are also small and good nucleophiles. This is due to their intervention in the first step of dehydration of the fructose, which involves substitution and elimination reaction on the C2 carbon.[153] Lewis acids are also of interest in the homogeneous catalysis of dehydration reaction as substitutes of traditional Brønsted acids, due to their lower corrosivity. Various Lewis acids have been studied for carbohydrate conversion. Dehydration of glucose has been achieved using $CrCl_2$ in ionic liquid with 70%

yield of HMF;[154] $CrCl_3$ and HCl with 59% yield HMF in water (NaCl)/THF biphasic medium;[155] $SnCl_4$ in ionic liquid to afford 64% yield of HMF.[156] More recently, Jiang et al.363 have achieved a 88% yield of LevA in biphasic medium (water : MeTHF) at 200 °C in 60 min (pH 1) with $FeCl_3$ and a yield of 56% for HMF in a biphasic solution at higher pH (pH = 2) in 180 min with $FeSO_4$.[157] Weiqi et al. have studied the synergist effect of coupling $CrCl_3$ and H_3PO_4 on glucose conversion to LA compared to single use of $CrCl_3$ or H_3PO_4. The highest LA yield of 54.24% was obtained from 100% glucose conversion at 170 °C for 240 min.[158]

CO_2 in hydrothermal application can be considered as Lewis acid in gaseous form or Brønsted acid in its hydrated form. In any case, it has proved to be effective in catalyzing carbohydrates to HMF. Lin et al. have obtained a HMF yield of 60.33% from fructose conversion at 190 °C for 20 min with a CO_2 pressure of 2 MPa.[159] There is also evidence that compressed CO_2 is also effective in hindering the formation of undesired HMF oligomers, thus improving the conversion yield of sugar to HMF.[160] The use of heterogeneous catalysis has the significant advantage of avoiding time and energy-consuming recovery steps that are necessary for homogeneous catalysts. A large variety of heterogeneous catalysts have been proposed, including transition metal oxides,[161] phosphates,[162], [163] zeolites,[164] organic polymers,[165] and sulfonated carbons.[166]–[168]

Influence of reaction time and temperature on soluble carbonization products

Several studies have investigated the effect of reaction time and temperature on products yields in the liquid phase after hydrothermal carbonization of carbohydrates and lignocellulosic feedstock. **Table 2** provides a summary of the reaction conditions used in the papers taken into account. Seen from the perspective of reaction time, in the early stages of polysaccharides conversion, HTC liquid phase is characterized by relatively high concentration of sugars (glucose) and furan species (HMF). Temperature has a big impact on hydrothermal decomposition of cellulose. Depolymerization of microcrystalline cellulose in water-soluble compounds is known to start at 180°C[169] and becoming predominant at 220°C; a further increase of the temperature to values as high as 260°C causes a decline of sugar oligomers in favour of decomposition products such as HMF or carboxylic acids.[49]

Table 2 *A summary of carbon precursors and reaction conditions of a collection of studies on the impact of process parameters on the hydrothermal carbonization of biomass and saccharides.*

Carbon precursor	Biomass/water ratio (wt. %)	Reaction temperature (°C)	Reaction time	Ref.
Starch	10%	180, 200, 220, 240	2 to 40 min	
Biomass (Jeffrey pine and white fir)	12.5%	215, 235, 255 275, 295	30 min	
		255	5 to 60 min	
Cellulose	20%	225, 250, 275	0 to 96 h	
Cellulose Wheat straw Poplar	12.5%	200, 230, 260 (fixed)	0 to 8 h	
		160-260 (dynamic)	/	
Coconut husk Rice husk	10%	140, 160, 180, 200	4 h	
		200	1, 2, 3 h	
Cassava rhizome	20%, 10%, 6.6%	160, 180, 200	1, 2, 3 h	
Corncomb	20%, 10%, 6.6%	160, 180, 200	1, 2, 3 h	
Sucrose, glucose, fructose	2% (sucrose) 1.05% (glu., fru.)	180	2 to 24 min	
		200, 220	2 to 18 min	

As general picture, it appears that hydrolysis of polysaccharides to simple sugars consistently increases with temperature, with maximum yields being achieved in shorter reaction time as temperature increases.[51], [52] Highest sugars yields are generally found between 180 °C and 230 °C and between 1 hour and 2 hours.[53]–[56] Fructose yields are generally poor in comparison to glucose yields in experiments that involves cellulose or starch thermal hydrolysis,[52], [53] due to the obstacle of isomerization. The hindering effect of glucose isomerization to fructose causes glucose concentration to build up in the reaction medium, whereas fructose is readily consumed. HMF yield is very dependent on both reaction time and temperature and its production is strictly connected to sugars content in the liquid phase. Although time scale of HMF concentration peak may vary from few minutes to hours, depending on the type and size of reactor,[52], [53], [55], [56] it always follows the maximum in monosaccharides concentration. HMF reaches optimal yields in a temperature range of 180-220 °C,[53], [55], [56] while higher temperatures cause faster conversion but lower yields, due to increase of secondary reactions. Experiments on conversion of simple

sugars monomers (glucose, fructose) and dimers (sucrose), although being conducted in presence of acid catalyst and therefore being kinetically faster, lead to a similar conclusion.[63] Xylose and FF are only detected as trace products of hydrothermal conversion of hexoses.[63] On the other hand, FF yields grow significantly when hemicellulose-rich biomass is employed; interestingly, its concentration decays more slowly than that of HMF with increasing reaction time, indicating a higher stability.[53] Finally, the formation of organic acids becomes more relevant as reaction time proceeds and higher temperatures are used, with acetic acid being particularly high in concentration in HTC of lignin-rich biomass.[51], [53]–[56]

Chemical isolation

At the end of a hydrothermal conversion, all chemical products like carboxylic acids, aldehydes, ketones and furfural derivatives need to be extracted from the water medium. Despite efforts to maximize yields, these products are always found in diluted concentration, making separation by direct distillation unfavourable. Every process designed to convert cellulosic biomass into platform chemicals will have to confront with this challenge, often opting for a liquid-liquid extraction step. A good solvent for liquid-liquid extraction must fulfil some basic requirements: it must extract effectively and selectively the compound of interest; it must be recoverable by distillation, in order to be recycled, thus lowering the production costs; it must be poorly soluble in water, in order to minimize losses during extraction; it must have a fairly different density from water, to allow a quick separation. In addition to these fundamental features, in the perspective of a greener process, it should also be inexpensive and non-toxic.[170] Several organic solvents have been successfully employed for liquid-liquid extraction of HMF, LevA and FF. Some of them are more traditional solvents, like methyl isobutyl ketone (MIBK),[171], [172] 2-butanol,[73], [171] tetrahydrofuran[173] and 2-methytetrahydrofuran;[173] some other less obvious alternative solvents such as dimethylcarbonate,[163] o-propylphenol[174] or hexafluoroisopropanol[175] have also been proposed due to their remarkably high partitioning coefficient. Among the traditional ones, MIBK in particular has proved to be the best solvent for the extraction of HMF in counter current, due to the combined effect of it

high partition coefficient and its lower solubility in water, compared to other solvents. Addition of sodium chloride furtherly improves the partition coefficient.[176]

The performances of solvents in liquid-liquid extraction can be improved by exploiting the salting-out effect of some common salts. Salting-out efficiency appears to be roughly independent of the nature of the cations and the extracting solvent, in the liquid-liquid extraction of HMF; in fact, it only depends on the anion.[177] Therefore, "green" solution can be applied also to this problem. A waste material like pentasodium phytate, derived from cereal, has also been considered as an alternative to inorganic salts as a cheap salting-out agent, thanks to its promising performances in a water/1-butanol/HMF system, in terms of separation of HMF.[178] Other strategies to achieve better extraction yields involves the use of a mixture of solvents and salts,[179] or different solvents in separate stages of extraction.[180] The downside of using salts to improve HMF extraction is an increased risk of corrosion of the production lines as well as a higher boiling point of water, thus requiring a higher amount of energy to be distilled and recycled back in the system. The increased demand of energy and maintenance costs hinder the scalability of these processes to industrial scale.[181]

Alternative approaches to synthesis of HMF in non-aqueous medium, such as the employment of organic solvents, ionic liquids or deep eutectic solvents, still rely on a necessary extraction phase with a second solvent in order to concentrate the product and minimize secondary reaction. Once HMF is extracted, this solvent need to be separated again in order to get the desired product.[171], [182] Extraction with supercritical CO_2 is a way to circumvent this problem by employing a cheap and non-toxic solvent that can be easily separated from the HMF once the extraction is complete, by simple depressurization. Supercritical CO_2, however, is only used as extraction solvent when ionic liquids are employed as reaction medium solvent.[183]

Other methods such as filtration can allow to completely skip the extraction step from the reaction medium and a good recovery of the reaction solvent.[184]

Influence of feedstock, reaction time and temperature on hydrothermal carbon properties

Feedstock

As highlighted in the previous section, furfural and HMF, originating from the dehydration of pentoses and hexoses respectively, play a key role in the formation of hydrothermal carbon spheres, due to their reactivity. Consequently, it is reasonable to expect chars with similar morphology and structure, regardless of the carbon precursor, as long as any of the aforementioned compounds are present in the reaction medium. Titirici *et al.* showed that carbon spheres derived from hexoses like glucose, maltose or hexose-based polysaccharides like sucrose or starch have the same morphology among themselves and with HMF-derived HT carbon. Similarly, carbon spheres obtained from the HTC of xylose and furfural are indistinguishable in shape. A relevant difference in morphology was instead found by comparing hexose- and pentose-derived carbons: the former had a more clustered or interconnected shape while the latter had a more dispersed appearance.[31] A study by Falco *et al.* confirmed these findings by comparing the morphology of the HTC secondary char derived from glucose, cellulose and rye straw. It also noted that hydrothermal treatment of real biomass causes disruption of fibres and formation of microsphere on the surface of the fragmented fibres.[32]

Reaction time and temperature

Reaction time and temperature have been shown to influence hydrothermal carbon morphology. Sevilla *et al.*, studying hydrothermal carbon yields from the HTC of glucose, sucrose and starch, noted that in any case, a rise of the precursor concentration, reaction time or reaction temperature resulted in an increased yield of hydrothermal carbon and in the diameter of the microspheres.[185] Romero-Anaya have substantially confirmed the observation, noting also that carbon sphere growth reaches a maximum (at fixed reaction time and precursor concentration) at 200°C.[132] Reaction time seems to have an impact on morphology and size of carbon spheres only up to a certain point. In fact, it has been noted

that, over a treatment time of 12, 24 and 48 h, sugars derived carbon spheres achieve bigger and more uniform sizes from 12 h to 24 h, but longer reaction times do not produce any change in size or morphology.[132] Moreover, it has been demonstrated that a second subsequent HTC of the carbon spheres results in the uniform growth of the pre-existing particles without any relevant formation of new ones.[186] Simsir *et al.* have studied the effect of different reaction time on HTC of different kind of feedstocks (glucose, cellulose, chitin, chitosan, wood chips) at a fixed temperature of 200°C. In this study, glucose-derived carbon spheres are not observed before a 12 hours long treatment, with an average diameter of around 800 nm for a residence time between 12 h and 36 h, and a slightly lower average diameter of 500-600 nm with increasing residence time to 48 h.[187] This has been explained with the plausible existence of an equilibrium between growing and decomposition of spherical carbon particles for longer residence times. Chitin is insensible to HTC, while cellulose and wood chips produce hard carbon spheres, too. Finally, chitosan derived hydrothermal carbon appears in the form of densely aggregated structures.

Chapter 3 Hydrothermal conversion of fructose, glucose and xylose

Introduction

Several recent reviews, covering the topic of hydrothermal conversion of biomass, insist on the necessity of a deeper theoretical comprehension of the mechanisms of carbon formation.[22], [23], [188], [189] Nevertheless, the majority of hydrothermal carbonization studies have been focused on elucidating either the liquid[58]–[61], [84] or solid phase[31], [185], [190]–[193] independently, while in fact, not only HT carbon formation is strictly connected to HMF, the latter being reckoned as its most likely building block;[31], [133], [194] HT carbon formation competes with carboxylic acids synthesis for the consumption of HMF;[32], [131], [133] finally, HT carbon is known to chemically incorporate in their structure some of these carboxylic acids in the liquid phase.[127] A synergistic study investigating mutual interdependencies between the two classes of products, chemicals in the liquid phase and solid HT carbons would be of paramount importance for a better understanding of the entire process, which in turn would allow its optimization. For this study, fructose, glucose and xylose were chosen as substrates to investigate their reactivity in hydrothermal conversion. Glucose and xylose are the main building blocks of cellulose[131], [195]–[197] and hemicellulose.[87] As for fructose, it is believed to be an intermediate in the hydrothermal conversion of glucose [62], [63]; a study of his behaviour allows to reduce the complexity of the system and compare the reactivities of a furanose sugar and a pyranose sugar. Time is an obvious key parameter to test. In order to make this process more efficient we must understand the time scales of formation of the chemicals involved and their evolution through time. Acid catalysis is strictly related to kinetic of the process, as it is necessary to maximize conversion and reduce the reaction time. Strong mineral acids, however, such as H_2SO_4, HNO_3, HCl, HBr or HI, not only act as catalysts by lowering the pH of the reaction medium; they also possess conjugate basic anions with different features: varying pK_a, increasing basicity and nucleophilicity, different ionic size and oxidizing power. All these features may have an impact on both products yields and chemical properties of HT carbon. Finally, initial pressure and atmosphere are often overlooked parameters in a process that occurs in an autogenous pressurized environment

and involves formation of several gas species.[144] Air atmosphere is predominantly employed in the reactor headspace in these kinds of reactions, but a N_2 atmosphere could provide an inert environment and possibly prevent oxidation reactions. A CO_2 atmosphere, on the other hand, might be a suitable way to provide mild, clean and sustainable acid catalysis necessary to accelerate the process.[198]–[201] Therefore, the aim of this study is to elucidate the influence of reaction time, acid catalysts and pressure on the hydrothermal conversion products of fructose synergistically and make correlations between the composition of the liquid and solid phase.

Composition of the aqueous phase

Figure 3 shows a sequence of HPLC chromatograms relating to the aqueous media of

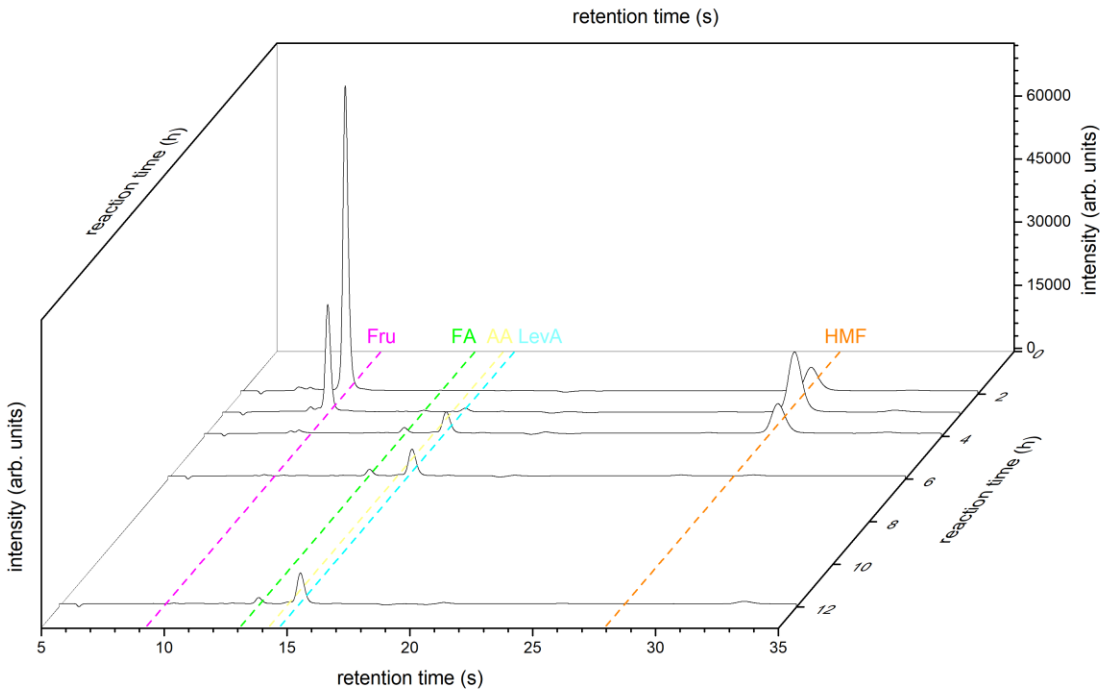

Figure 3 *HPLC chromatograms of hydrothermal aqueous solution versus reaction time, displaying the consumption of sugar precursor (fructose), the appearance and disappearance of HMF in the time range between 2 and 4 h an the rising of FA and LevA peaks at longer reaction times.*

reaction time series of experiments, with an identification of the main products: fructose (starting material), formic acid (FA), acetic acid (AA), levulinic acid (LevA) and HMF (5-hydroxymethyl furfural). Although hydrothermal conversion of sugars is known to produce a vast variety of chemical species beyond the ones mentioned above,[144] in the present study these five species only were identified as major components of the aqueous phase and therefore quantified in the experiments. Any other trace species was not included in this study.

Reaction time.

Figure 4 shows the yields of products of conversion of fructose and residual unreacted precursor. Secondary y axis shows the pH of aqueous phase at the end of the reaction. Yields are expressed as ratio of product moles over reagent moles. HT carbon molarity is calculated by assuming a molar mass of 108.1 g mol-1. This assumption has been already employed in previous kinetic studies on the formation of HT carbon.[133], [202] It is based on a model that treats HT carbon as a polymer made of HMF units condensed with loss of a molecule of water, with simplified stoichiometry as given by [Equation (**4**)]:

$$n\,HMF \rightarrow hydrothermal\ carbon + n\,H_2O \qquad (\mathbf{4})$$

This model, however, is an oversimplified representation of the real material. In fact, considering hydrothermal carbon as a clean, straight chain of repeated HMF units, it is not taking into account the presence of ramifications, the minor involvement of other molecules in the polymerization process, nor does it consider possible post-polymerization structural modifications such as cross-linking, cyclization, dehydration and oxidation. All of these deviations from the ideal model can result in an incorrect estimation of the number of moles. In particular, the functionalization of the outer layers of carbonaceous particles may increase the final mass of HT carbon, leading to an overestimation of the moles of product. This uncertainty, in turn, will add up to the sum of uncertainties arising from HPLC detection of chemicals in the aqueous phase, leading to a sum of individual yields which is higher than 100% in a few cases.

By the observation of the HPLC data relative to the hydrothermal conversion of fructose from 2 h to 12 h (**Figure 4**), three reactions can be distinguished. The first reaction takes place from 0 to 4 h, when fructose quantitative conversion is achieved (Table 3).

Table 3 *Product yields, residual fructose and final pH versus reaction time at 200 °C.*

Time (h)	Fru (mol %)	FA (mol %)	AA (mol %)	LevA (mol %)	HMF (mol %)	HTC (mol %)	pH
2	98.1 ± 0.0	0	0	0	6.0 ± 2.0	0	3.00 ± 0.10
3	28.7 ± 0.8	8.0 ± 3.0	[a]	4.0 ± 2.0	52.7 ± 0.3	36.0 ± 3.0	2.30 0.06
4	0	23.0 ± 1.0	[a]	18.0 ± 1.0	21.0 ± 4.0	42.0 ± 3.0	2.33 ± 0.02
6	0	27.0 ± 2.0	1.8 ± 0.2	22.0 ± 1.0	0	52.0 ± 7.0	2.28 ± 0.03
12	0	23.9 ± 0.7	2.3 ± 0.0	23.9 ± 0.3	0	61.5 ± 0.3	2.16 ± 0.02

[a] below quantification limit

Between 2 and 3 h the conversion rate of fructose to HMF is very fast, reaching a maximum yield of 53% in 3 h. At this point, rehydration of HMF and consequent production of levulinic acid (LevA) and formic acid (FA). In fact, FA and LevA, can already be observed at 3 h, although in low yields (8% and 4% respectively). Conversion rate of HMF to LevA and FA grows fast from 3 h to 4 h, eventually reaching a plateau (23.9%). At a later stage of the reaction, while we observe only minor fluctuations in the yields of FA and LevA, the third process, namely HT carbon formation (Eq. 1), grows steadily. The fact that no significant increase in the yields of LevA and FA is observed from 4 h on, whereas HT carbon yields constantly increase with time, seems to suggest that, if any "new" levulinic acid and formic acid are synthetized, they are immediately consumed. This might imply a chemical

incorporation of LevA molecules in forming HT carbon particles (**Figure 4a**), as previously proposed by Qi.[127]

It must be also noted that the final pH decreases constantly as the reaction proceeds, indicating the accumulation of acidic species in the reaction medium. Acetic acid (AA) is certainly among this species. AA is present in small but appreciable amounts in the aqueous phase at long reaction times (6-12 h, **Figure 4a**). The late appearance of AA points out to its synthesis through a minor, slower chemical pathway. Jin et al. have reported a prevalence of the oxidation of furfurals over lactic acid pathway as the responsible for the production of AA, though not ruling out other unspecified synthetic routes.[119] Although lactic acid was not monitored in this study, it must be noted that HMF is totally consumed in the time rage between 4 and 6 h, but AA yield slightly increases from 6 to 12 h. This means that, in these conditions, HMF oxidation is not the main source of AA.

The accumulation of species like AA and FA accounts for the slow but constant decrease in the pH of the aqueous solution as the hydrothermal treatment proceeds. Moreover, the existence of many other oxidation pathways, other than HMF rehydration, leading to the formation of FA[119] can account for the slight but frequent deviations from equimolarity between FA and LevA.

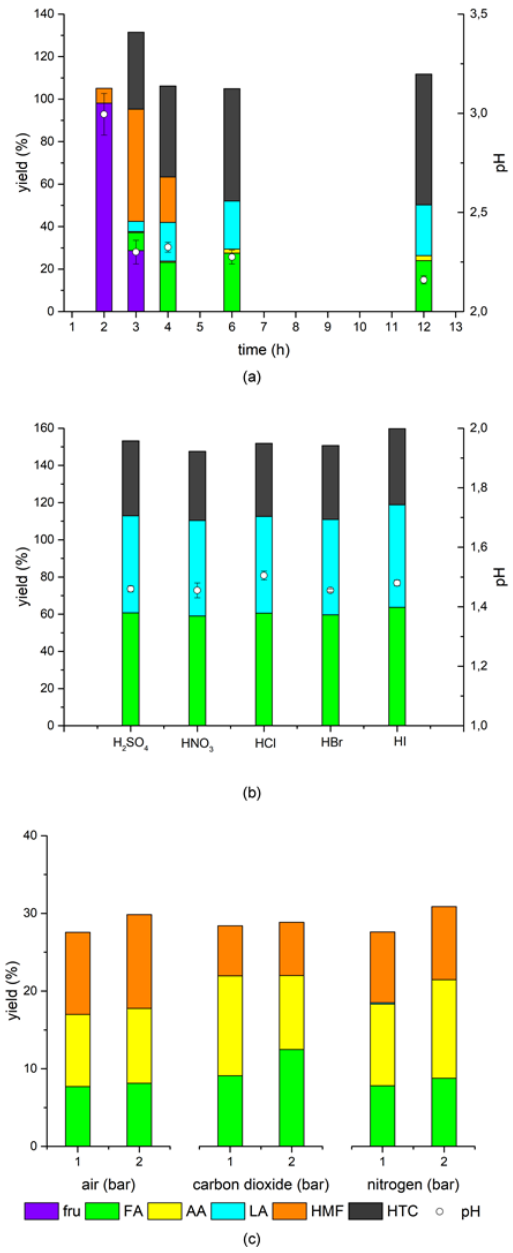

Figure 4 *Degradation products of fructose. Fructose (fru), formic acid (FA), acetic acid (AcA), levulinic acid (LevA), 5-hydroxymethylfurfural (HMF), HT carbon (HTC). Final pH of liquid phase is shown on the secondary y axis. Reaction parameters: starting solution 10% w/w fructose in water (a) 200 °C, increasing reaction time, no catalyst, air, atmospheric pressure; (b) acid-catalyzed reaction, 200 °C, 3 h, initial pH 1.5, air, atmospheric pressure; (c) controlled atmosphere (air, CO_2, N_2) and pressure (1.01 bar or 2 bar) at 200 °C for 2 h.*

Figure 5 shows the yields of conversion of glucose to soluble chemicals and insoluble particles of hydrothermal carbon. Glucose conversion starts off very slowly. Unreacted glucose still makes up roughly 80% of the initial concentration after 4 hours of reaction and the conversion is brought to completion after over 6 hours from the start of the treatment. The only conversion products observed in the time range between 2 hours and 3 hours are HMF and fructose, in extremely low yields. While the slowness of the process proves the reluctance of glucose to undergo dehydration reaction, the presence of fructose, in small but detactable amounts, indicates that the reaction pathway of isomerization of glucose to fructose is active at these reaction conditions. In this scenario, fructose acts as labile intermediate proving that gets dehydrated to HMF very easily. HMF highest yield of 15.9% is achieved at 4 hours and the first HT carbon precipitate is observed at the same time. Consequently, 6 hours time marks a fast decline in the HMF yield and the appearance of FA and LevA. HT carbon keeps growing eventually taking over at 12 hours, followed by FA and LevA. The overall chronology of reactions reflects the one observed in the previous chapter, with fructose as precursor, but it is nonetheless dominated by the extremely slower reactivity of glucose acting as a bottleneck and delaying the formation of HMF. HMF highest yield in these reaction conditions does not exceed 16%, consequently keeping LevA and FA yields low. As seen in the previous chapter, LevA and FA formation benefits more from a lower pH than HT carbon. Moreover, the same reaction produces FA, furtherly lowering the pH and proceeding in an autocatalytic way. In this case, reaction pH decreases more slowly and so does HMF rehydration. On the other hand, HMF polymerization to HT carbon is less pH-sensitive. Thanks to the reduced competition of the LevA-FA reaction pathways, HT carbon proceeds undisturbed, leading after 12 hours to a final yield that is comparatively higher than that observed at the same reaction time with fructose as carbon precursor.

This set of data confirms the sequence of trasformations that goes from glucose to HMF through fructose, and then from HMF to LevA, FA and HT carbon as well as the whole time scale. From the perspective of an industrial upgrading of the conversion of glucose to HMF, it is impractical to design a process that does not involve any catalyst, because of great amount of time it would take to obtain the desired product, the energy demand and unsatisfactory yields, resulting ultimately unsustainable. However, the weak point of using

glucose as a precursor, which is the kinetic bottleneck of slow isomerization to fructose, can be turned into a strenght if HMF is rapidly and effectively removed from the reaction medium before accumulating, thus pushing the reaction towards the desired product and avoiding further conversion at the same time.

Table 4 *Product yields, residual fructose and final pH versus reaction time at 200 °C*

Time (h)	Glu (mol %)	Fru (mol %)	FA (mol %)	LevA (mol %)	HMF (mol %)	HTC (mol %)	pH
2	104 ± 6	0	0	0	0.7 ± 0.1	0	3.51 ± 0.1
3	100 ± 4	0.8 ± 0.2	0	0	5.8 ± 0.7	0	3.09 ± 0.05
4	76.3 ± 0.7	0	0.2 ± 0.1	0*	15.9 ± 0.3	12 ± 1	2.84 ± 0.02
6	26 ± 2	0	12.5 ± 0.3	8.5 ± 0.2	12.0 ± 0.4	40 ± 7	2.48 ± 0.01
12	0	0	16.8 ± 0.7	14.6 ± 0.1	0	65 ± 1	2.30 ± 0.04

* below quantification limit

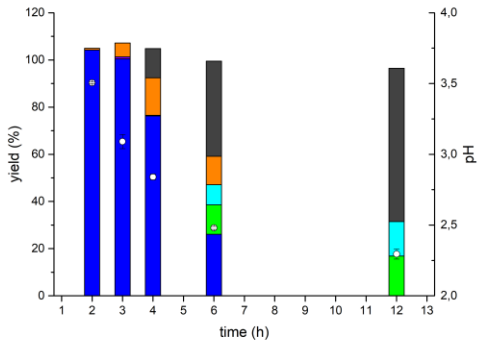

(a)

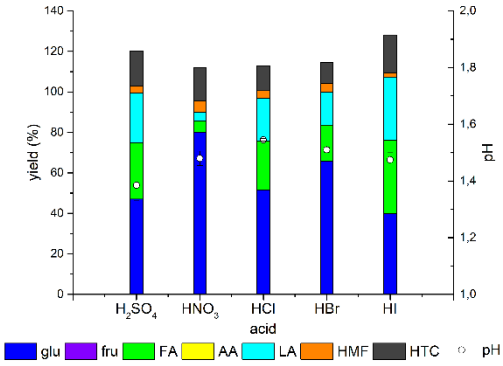

(b)

Figure 5 *Conversion products of glucose. Glucose (glu), fructose (fru), formic acid (FA), acetic acid (AcA), levulinic acid (LevA), 5-hydroxymethylfurfural (HMF), HT carbon (HTC). Final pH of liquid phase is shown on the secondary y axis. Reaction parameters:* ***(a)*** *200 °C, increasing reaction time, no catalyst;* ***(b)*** *acid-catalyzed reaction, 200 °C, 3 hours, initial pH 1.5.*

Figure 6 shows the evolution of xylose conversion and products yields between 2 h and 12 h at 200 °C in plain water. The monitored species were xylose, glucose, fructose, formic acid, acetic acid, levulinic acid, HMF and HT carbon. The calculation of the molar yield of xylose-derived HT carbon were made with an assumption similar to the one made for fructose-derived HT carbon (Chapter 3) and adapted to a FF polymer model, as in Gandini.[203] Therefore, the theoretical molar mass was assumed to be 94.07 g mol^{-1}.

Among these species, only FF, AA, FA, HTC and unreacted xylose were found in the reaction medium. FF is well known to be produced by the dehydration reaction of pentoses such as xylose.[204] Reverse aldol condensation of xylose is another decomposition pathway triggered by heat, leading to the C2-C3 cleavage and formation of glycoladehyde and glyceraldehyde, as described by Antal.[96] The decomposition pathways of glyceraldehyde has been mentioned in the previous chapters for its involvement in the formation of lactic acid that can be decarbonylated or decarboxylated to acetaldehyde, which in turn is oxidised to AA.[108], [114], [116], [205] Since AA only was monitored in these series of experiments, its presence is the only clue of the actual impact of the reverse aldol condensation synthetic pathway on the overall conversion of xylose. The other species involved can account, to some extent, for the percentage of converted xylose that is not detected in form of product. Lactic acid, in particular, can be one the organic acids that are responsible for the slow and constant decrease in the pH. As for AA, it must be noted that it is found in low concentration and at late stage of the conversion (12 h). Moreover, the sum of unreacted xylose, FF and HT carbon always represents more than 70% of the initial moles of xylose. These two observations suggest that reverse aldol condensation of xylose, if active, may be a minor degradation pathway, while the majority of the xylose is dehydrated to FF. AA has also been previously detected as a trace component in hydrothermal conversion of glucose and fructose, particularly after long reaction times. An alternative explanation for its presence at later stages of conversion is that AA may be the result of the wet oxidation of furan units the structure of HT carbon.

FF formation due to xylose dehydration is relatively slow: if compared to the observed reactivity of fructose and glucose in previous chapters, its reactivity towards dehydration can be placed somewhere between glucose and fructose, with fructose being the most

reactive species and glucose the least reactive one. In fact, complete conversion of xylose in these conditions is only achieved after 6 h, similarly to glucose. Xylose conversion to FF, however, produces much higher FF yields than those of glucose dehydration to HMF. FF highest yield of 45% is reached at 6 h, while HMF highest yield from glucose is 15% at 4 h. It is also worth noticing that, despite the time scale of xylose dehydration is more leaning to that of glucose dehydration, FF tends to accumulate in the reaction medium in a way that is notably different from the behaviour of HMF. HMF concentration, both in glucose and in fructose conversion, plummets down shortly after reaching its peak, as a joint effect of polymerization/condensation to HT carbon and rehydration to levulinic acid. No HMF was ever detected in our experiments at a reaction time of 12 h. Conversely, it appears that no significant reactions, other than HT carbon formation, occur at the expense of FF. This behaviour is not entirely unexpected. An early study by Dunlop demonstrated that pure FF is a thermally stable molecule that undergoes little to no decomposition at all after prolonged heating at 140 °C and 180 °C in vacuum, showing relevant signs of decomposition just after more than 100 h at 230 °C.[206] In another study, its relative stability in low concentrations of acids was also noted.[207] The observed behaviour of FF in the present study confirms previous findings: FF is notably far more stable than HMF in analogous conditions and it is also less prone to ring opening reactions than HMF. It follows that the only reaction that consumes FF is HT carbon formation and, also in this case, FF-derived HT carbon yields are notably lower than those of HMF-derived HT carbons. This difference in HT carbon yields must be rooted in the different chemical structure of FF and HMF and once again proves that the furan species are key molecules in the formation and chemical properties of HT carbons.

Finally, FA peculiar behaviour should be mentioned. FA sparsely appears in very low amounts at 3 h and 6 h. It is believed to be derived from hydrolytic fission of the aldehyde group, as a secondary product in the resinification[204] or oxidation[208] of furfural. Its presence here not only confirms those previous studies, but it also suggests that this kind of reaction might contribute to the notorious excess of FA with respect to LevA already observed in the hydrothermal conversion of HMF. The reason for its oscillating yields might be found in the known tendency to undergo hydrothermal decomposition to CO_2 and H_2.[209]

Table 5 *Product yields of xylose hydrothermal conversion, residual xylose and final pH versus reaction time at 200 °C*

Time (h)	Xyl (mol %)	FA (mol %)	AA (mol %)	FF (mol %)	HTC (mol %)	pH
2	94.5 ± 0.2	n.d.	n.d.	1.3 ± 0.1	n.d.	
3	78.6 ± 0.8	0.9 ± 0.4	n.d.	10.7 ± 0.8	0.7 ± 0.1	
4	43.5 ± 10.5	n.d.	n.d.	38.3 ± 5.6	8.7 ± 1.5	
6	5.2 ± 3.7	3.0 ± 0.3	*	45.1 ± 5.5	26.5 ± 1.2	
12	n.d.	n.d.	2.6 ± 0.1	29.3 ± 0.5	46.5 ± 0.2	

* below quantification limit

Acid catalysis

The acids employed in this series of experiments (H_2SO_4, HNO_3, HCl, HBr, HI) were chosen in order to have a diverse group of strong mineral acids with different features: variation along the period (HX), monoatomic and polyatomic anions (HX vs. nitric acid and sulphuric acid) and an oxidizing acid (nitric acid). Each acid was added in such a volume to reach to reach a concentration of 0.031 M. This concentration corresponds to a pH of 1.5 for monoprotic acids (HNO_3, HCl, HBr, HI) and 1.4 for H_2SO_4.In comparison to the reaction time experiments, monitoring the evolution of chemical species over reaction time, these experiments provide a static picture, not only because they were made at fixed reaction time (3 h), but also because the addition of strong inorganic acids as catalysts pins the pH to a low value that is kept practically unaltered throughout the whole reaction (**Figure 4b, Figure 5b**).

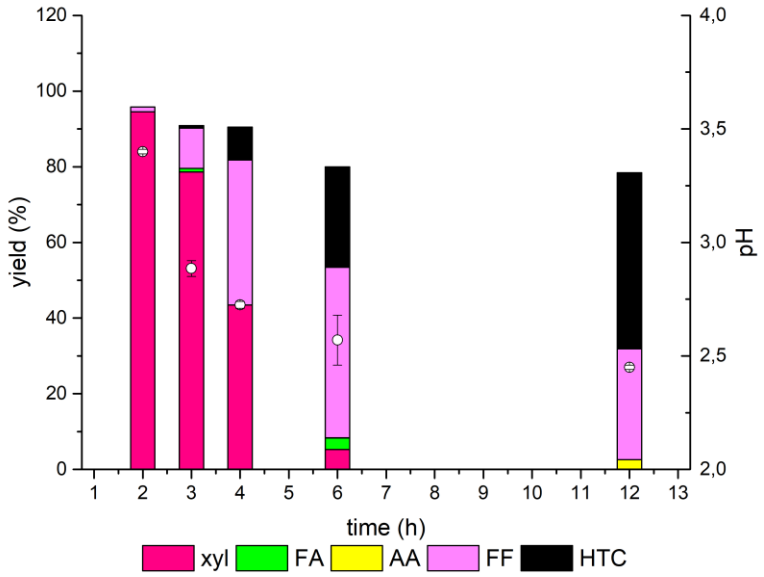

Figure 6 *Conversion products of xylose. Unreacted xylose (xyl), formic acid (FA), acetic acid (AcA), furfural (FF), HT carbon (HTC). Final pH of liquid phase is shown on the secondary y axis. Reaction parameters: 200 °C, increasing reaction time, no catalyst.*

Under these conditions, fructose is quantitatively converted, as opposed to partial conversion in uncatalyzed 3 h sample (**Figure 4a**). HMF is not detected either. The only detected products are FA, LevA and HT carbon (Table 6). Several experimental[194], [202], [210], [211] and computational studies,[68], [69] however, suggest that formation of HMF from fructose still takes place in acidic conditions and both levulinic acid and HT carbon originate from it in the same synthetic sequence observed in the previous experimental series. HT carbon yields are significantly lower than the sum of FA and LevA yields. Moreover, HT carbon yields are similar to those obtained at the same reaction time in absence of acid catalyst, whereas FA and LevA are produced in much higher amounts. This means that the polymerization of HMF to HT carbon is not greatly affected by acid catalysts, while reaction of HMF and formation of LevA and FA is faster in acidic conditions. This finding is consistent with previous studies.[133]

Table 6 *Product yields and final pH versus acid catalyst at 200 °C for 3 h.*

Acid (0.031 M)	FA (mol %)	LevA (mol %)	HTC (mol %)	pH
H_2SO_4	60.8 ± 0.0	52.1 ±1.0	40.3 ± 0.1	1.46 ±0.01
HNO_3	59.0 ± 4.0	51.0 ± 3.0	37.0 ± 1.0	1.46 ± 0.02
HCl	60.6 ±0.0	52.0 ± 0.0	39.3 ± 0.1	1.51 ±0.01
HBr	59.0 ± 2.0	51.0 ± 2.0	39.8 ± 0.6	1.46 ± 0.01
HI	63.6 ± 0.1	55.1 ± 0.1	40.9 ± 0.5	1.48 ± 0.01

It is also interesting to notice that FA is always found in slight excess with respect to LevA, apparently contradicting the theoretical assumption of these two carboxylic acids being formed in equal amount by the rehydration of HMF. However, we already noticed an increase in the yield of HT carbon in uncatalyzed condition from 4 to 6 h in absence of HMF. This is another hint that LevA can take part, along with HMF, in the polymerization process that leads to the formation of HT carbon. Finally, it must be noted that no AA is detected in any of the samples. As previously said, AA can be derived from oxidation of lactic acid[116], [117] or HMF. Lactic acid, however, requires base-catalyzed benzylic rearrangement of pyruvaldehyde to form. Two hypotheses can be made to explain this result: 1. low synthesis pH suppresses the basic-catalyzed reaction pathway of formation of AA involving lactic acid;

2. oxidation of HMF to AA is slow and all HMF is converted to LevA and FA or HT carbon before this synthetic route can take place.

The following series of experiments employs the same set of strong acids (H_2SO_4, HNO_3, HCl, HBr, HI) and reaction conditions (3 h, 200 °C) for the acid-catalyzed conversion of glucose. ***Figure 5b*** shows that this addition profoundly alters the system with respect to the analogous uncatalyzed system. The first notable fact is the great difference in the final pH (~1.5) of catalysed and uncatalyzed systems (3.09). Overall, the addition of mineral acid enhances the glucose degradation. Percentages of unreacted glucose in the reaction medium vary from 80% (nitric acid) to 40% (hydroiodic acid), marking an overall great improvement in the conversion with respect to the extremely low conversion in the uncatalyzed system. Conversion yields of FA, LevA, HMF and HT carbon changed accordingly. In fact, even if HMF yields are lower, on average, than those obtained in absence of acids at the same reaction time, it must be considered that, unlike the uncatalyzed system, FA, LevA and HT carbon yields are present in large amounts. This means that much more HMF was produced in a smaller time and the majority of it was furtherly converted to either LevA+FA or HT carbon. Looking at the performances of each single acid in terms of glucose conversion and product yields, we can see quite distinct results, pointing out to relevant contribution of the negative counter ion. Grading these values from the highest to the lowest we obtain the following scales:

$$C_G(HI) > C_G(H_2SO_4) > C_G(HCl) > C_G(HBr) > C_G(HNO_3)$$

for glucose conversion;

$$Y_{HMF}(HNO_3) > Y_{HMF}(HBr) > Y_{HMF}(HCl) > Y_{HMF}(H_2SO_4) > Y_{HMF}(HI)$$

for HMF yields;

$$Y_{LevA}(HI) > Y_{LevA}(H_2SO_4) > Y_{LevA}(HCl) > Y_{LevA}(HBr) > Y_{LevA}(HNO_3)$$

for LevA and FA;

$$Y_{HTC}(HI) > Y_{HTC}(H_2SO_4) \approx Y_{HTC}(HNO_3) > Y_{HTC}(HCl) > Y_{HTC}(HBr)$$

for HT carbon.

These four scales correspond to four main reaction steps:

1. Glucose isomerization to fructose;
2. Fructose dehydration to HMF;
3. HMF rehydration to LevA and FA;
4. HMF polymerization to HT carbon.

All these steps are based on the assumption that glucose is isomerized to fructose also in these conditions. This is implied by the direct observations made previously in uncatalyzed conditions, when fructose was clearly detected, although in very small amounts, as well as previous studies. In all of our observations, however, no fructose is detected at the end of the reaction, most probably due to its high reactivity under these conditions.

Of all the above mentioned four steps, the first three are consecutive reactions while the last two are competing reactions; moreover, the first two steps, namely isomerization and dehydration, are acid-catalyzed. Therefore, to better understand the effect of different acids on the outcomes of these reactions, the activity a_H of the proton H^+ must be take into account. a_H is defined as follows (eq. 5).

$$a_H = \gamma[H^+] \quad (\mathbf{5})$$

The coefficient of activity γ for solution with low ionic strength can be obtained from the Debye-Hückel equation (eq. 6).

$$log_{10}\gamma = -\frac{A|z_+z_-|\sqrt{I}}{1 + Ba\sqrt{I}} \quad (\mathbf{6})$$

I is the ionic strength of the solution, z is the integer charge of the ion, A and B are constants for each solvent at a given temperature and a is the effective diameter of the ion in angstrom.

Table 7 displays the calculated ionic strengths of the 5 acidified glucose solutions and the H^+ and anions coefficient of activity at 25 °C in water. Coefficients of activity are calculated as per eq. 7; values of A and B constants of 0.5085 and 0.3281 at 25 °C in water are taken from Skoog[212] and effective diameters of ions a are taken from Kielland.[213]

Table 7 *Ionic strength of 0.031 M solutions of H_2SO_4, HNO_3, HCl, HBr, HI in water an corresponding H^+ and anions coefficients of activity.*

acid	Ionic strength	γ_H	γ_A
HNO_3	$3.16\ 10^{-2}$	$8.72 \cdot 10^{-1}$	$8.38 \cdot 10^{-1}$
H_2SO_4	$4.65\ 10^{-2}$	$7.35 \cdot 10^{-1}$	$6.75 \cdot 10^{-1}$
HCl	$3.16\ 10^{-2}$	$8.72 \cdot 10^{-1}$	$8.38 \cdot 10^{-1}$
HBr	$3.16\ 10^{-2}$	$8.72 \cdot 10^{-1}$	$8.38 \cdot 10^{-1}$
HI	$3.16\ 10^{-2}$	$8.72 \cdot 10^{-1}$	$8.38 \cdot 10^{-1}$

Higher ionic strength of sulfuric acid solution depends entirely on the higher number of ionic species in solution due to diprotic nature of the acid. In turn, this higher value causes a slightly lower activity of H^+ compared to that of monoprotic acids. However, the ionic strength of a solution plays an important role in the dissociation of the acid itself. According to Kennedy,[214] the pK_a of an acid in conditions that take into account ionic strength of a solution (defined as $pK_{a(mix),n}$), is the sum of the $pK_{a(therm),n}$ (theoretical pK_a at infinite dilution) and an additional term depending on the constant A, the ionic strength, the charge of the undissociated acid z and the degree of dissociation n (eq. 7).

$$pK_{a(mix),n} = pK_{a(therm),n} + A\frac{\sqrt{I}(2z - 2n + 1)}{1 + \sqrt{I}} \qquad (\mathbf{7})$$

Eq. 8 shows that all the acid catalysts employed in these experiments (z=0) will see a slightly increased K_a as ionic strength of solution increases. K_a increase will be more pronounced in the case of sulfuric acid, due to a higher degree of dissociation (n=1), as opposed to monoprotic acids. Eq. 8 also suggests that dissociation constants of acids will increase as an effect of the higher ionic strength of the reaction medium given by the dissociation of new acidic species such as acetic acid and formic acid formed during decomposition of glucose. Anyway, it can be argued that the slight increase of pKa due to changes in ionic strengths of reaction solutions will be levelled out by the effect of water. Moreover, the variation of temperature during the reaction will also imply a change of K_a. The definite integral of the Van 't Hoff equation (eq. 9) calculated between T_1 and T_2 allows to estimate the dissociation constant $K_a^{"}$ at a given T_2, when the variation of enthalpy associated to the process (ΔH,

assumed as being constant) and the value of equilibrium constant K_a' at a temperature T_1 are known.

$$ln\frac{K_a^{"}}{K_a'} = \frac{\Delta H}{R}\left(\frac{1}{T_1} - \frac{1}{T_2}\right) \quad (\mathbf{8})$$

Variations of enthalpy ΔH for the dissociation in water of all acids included in this study are negative,[215] i.e. their dissociation is a strongly exothermic process. Hence, an increase in temperature will lead to a decrease of the dissociation constant; the effect will be more pronounced on acids with very negative enthalpy of dissociation in water and greater K_a, such as HCl, HBr and HI (**Table 8**). The reduction of K_a due to increase of temperature greatly surpasses the slight increase as an effect of the ionic strength of the solutions.

Table 8 *Enthalpies of dissolution of H_2SO_4, HNO_3, HCl, HBr, HI in water, their dissociation constants at 298 K and their estimated dissociation constants at 473 K.*

$\Delta H°$ [kJ mol^{-1}]	$K'_{a,(298\ K)}$	$K^{"}_{a,(473\ K)}$
-33.4	2.82 10^{2}	2.43 10^{-5}
-71.76	1.00 10^{3}	2.24 10^{-8}
-57	1.00 10^{6}	2.03 10^{-10}
-65	1.00 10^{9}	6.14 10^{-14}
-62	3.16 10^{9}	3.04 10^{-14}

Table 8 shows that nitric acid and sulfuric acid are less effected than halohydric acids from the shift of equilibrium due to increased temperature and therefore should have a behave as better acid catalysts. However, this is not observed in the before mentioned scales of conversion of glucose and product yields. The reason for experimental difference between yields is not entirely explained by the strength of the acids employed and other factors must play a role in different ability of each acid anion to catalyze the four reactions, such the interaction of anions in the transition states of the conversion reactions.

The mechanism hypothesized by Harris for the acid-catalyzed isomerization of glucose includes two possible transition state structures, both satisfying the observed stereochemistry. The first is a 1,2-hydride shift with a three-member ring between C1, C2

and a hydrogen atom, with a partial positive charge. The second is a 1,2 enediol structure with a proton that is partially associated with the π orbital. In both cases, the transition state is stabilized by a negatively charged counterion.[67] Qualities such as a good nucleophile character and a stronger basicity may improve the stabilization of the anion on the transition state, pushing the isomerization towards the formation of fructose. Based on the pKa of acids,[216] the strengths of conjugated bases can be graded from the highest to the lowest as follows:

$$NO_3^- > HSO_4^- > Cl^- > Br^- > I^-$$

Basicity is linked to nucleophilicity when considering atoms on the same row of the periodic table. Ion size is another very important parameter to define the nucleophilicity of anions in water, because bigger ions are less shielded by solvation shells than smaller ones and therefore more nucleophile.[217] Atomic radii and bond lengths of the ions involved are listed as follows from longer to shorter:[218], [219]

$$S - O > I^- > N - O > Br^- > Cl^-$$

These two scales show discordant and often contrasting properties. This contrast is reflected on the glucose conversion values in function of each anion. The high conversion of glucose caused by hydroiodic acid and sulfuric acid suggest that bulkier anions provide better stabilization on the positively charged transition state. However, chloride ion, the next in the series after I^- and HSO_4^-, precedes bromide, suggesting that in this case a stronger basic character of Cl^- prevails over Br^- larger ionic radius (and better nucleophile qualities) in the stabilization of the transition state. Nitric acid glucose conversion is exceptionally low, in contrast with what could be expected by both basicity and ion size. The exceptional character of nitric acid is also found in the next three series of yields and it will be discussed later in this subsection.

The series of yields, which are relative to fructose conversion to HMF as functions of the employed acid, perfectly mirrors the first series. Among the several studies that have investigated the influence of anions in hydrothermal conversion of mono- and disaccharides,[220]–[226] there is large consensus about the positive effect played by anions such as halides in the HMF formation, particularly in presence of bromide ions rather than

chloride and iodide.[225]–[228] These findings are in good agreement with what we observed by comparing HMF yields in function of different acids used. Körner et al. reported the different ability of various anions to catalyse fructose dehydration to HMF and explained that good leaving group qualities effect a strong acceleration in the reaction, provided that they also are good and small nucleophiles. In fact, the study suggested that good nucleophiles could increase the rate of the first dehydration of fructose (occurring on C2-OH) by substituting the hydroxyl group and forming a Fru-X intermediate that can undergo further elimination reaction, with an overall acceleration of the process, provided that the –X group is also a good leaving group.[220] HMF, though, acts as an intermediate before the bifurcation point in the reaction pathway that connects glucose to either LevA (and FA) or HT carbon. The poorer HMF yield is, the higher LevA, FA and HT carbon yields are, with the only exception of $Y_{HTC}(HNO_3)$. Therefore, it is not possible to conclusively establish whether what we observed here is the different ability to enhance the fructose conversion to HMF or to decrease its final yield by promoting further conversion. LevA and FA yields are higher than HT carbon yields and often exceeds the yields obtained from glucose after 12 h in uncatalyzed conditions. This proves, once more, that HMF rehydration to LevA and FA is more strongly dependent on pH than HT carbon formation.

Finally, the notable abnormal behaviour of nitric acid should be most probably ascribed to a few reasons that make this acid stand out among the others. Poor glucose conversion and HMF yield may be consequences of nitrate ion being a bad nucleophile and a bad leaving group, as hypothesized by Körner.[220] Moreover, nitric acid oxidizing power can deviate the reaction pathway from the usual one, oxidizing HMF thus blocking the LevA formation and pushing HMF conversion towards polymerization reactions, as showed by the unusual high yields of HT carbon.

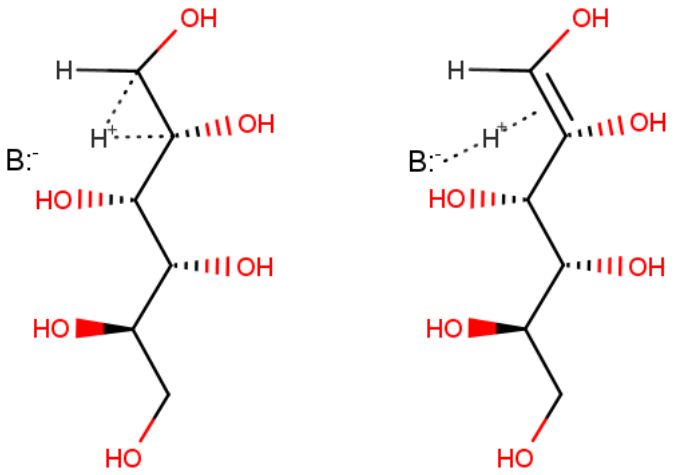

Scheme 7 *Two possible transition states hypothesized by Harris for the glucose isomerization to fructose. In both cases the stabilizing effect of the conjugate base of the acid is highlighted.*

Atmosphere and pressure

Figure 4c shows the product yields from hydrothermal conversion of fructose in air, CO_2 and N_2 atmosphere at two different pressure levels (1 bar and 2 bar). The purpose of this series of experiments was to study the possible effect of overpressure on the hydrothermal conversion of fructose, as well as to evaluate the possible chemical interaction between feed gas and liquid phase. As for the chosen feed gases, nitrogen gas was employed in order to provide a purely inert atmosphere as opposed to normal air, which is oxidizing effect, due to its O_2 content. This effect is already exploited for the decontamination of wastewaters through hydrothermal wet oxidation, a process that allows to break down large molecules into small carboxylic acid such as formic acid and acetic acid.[229] CO_2 was chosen because of its ability to dissolve in water and serve as weak acid catalyst. In fact, considering the current atmospheric concentration of CO_2 in atmosphere of 400 ppm,[230], the pH of an aqueous solution exposed to atmosphere can be calculated by means of Henry's law and dissociation constant of CO_2 in water

$$CO_{2\,(aq)} \rightleftharpoons H^{+}_{(aq)} + HCO^{-}_{3\,(aq)} \qquad (9)$$

Given Henry's constant k_H^o for CO_2 in water at 25 °C is 0.034 ml kg^{-1} bar^{-1} [231] and the pK for the above indicated equilibrium of acidic dissociation of solvated CO_2 in water is 6.352,[232] it follows that an aqueous solution exposed to atmosphere will have a pH of 5.6. It can be calculated in the same way that an aqueous solution will have a pH of 3.9 in 1 bar of CO_2 and a pH of 3.7 in 2 bar of CO_2.

It must be noted that the other gaseous species involved in this section of the study, N_2 and O_2 are very poorly soluble in water in the range of temperatures and pressures considered here; CO_2 is slightly more soluble in water than N_2 or O_2, but its solubility decreases at higher temperatures.[233], [234] Although fructose conversion in this system always proceeds to completion, the overall yield of soluble products is higher at higher pressure under all three atmospheres (**Table 9**). However, the ratio of the individual yields changes with different feed gas. Highest HMF yields are achieved in air atmosphere. HMF and FA yields slightly increase in air at 2 bar, whereas AA yields remain basically unchanged. In CO_2 atmosphere, HMF yields do not exceed 6% at both pressure values. FA yield increase as the pressure raise, while FA yield decrease. These results confirm the hypothesis of CO_2 mildly acidifying the reaction medium and thus causing an increment of acid-catalyzed FA and a decrease of base-catalyzed lactic acid formation, a precursor of AA. Yields in nitrogen atmosphere are quite similar to those achieved in air. Finally, it is also interesting to notice a strong imbalance between FA and hardly detected LevA. LevA was always detected in extremely low concentrations, below quantification limits, except for one case (N_2, 1 bar), where in theory it should be present in similar concentration to those of FA. This observation once again suggests the existence of alternative synthetic routes to FA as well as the possibility of free LevA being consumed by adsorption or chemical bonding to HT carbon.

Chemical structure and morphology of hydrothermal carbon

The second part of this study is focused on the impact of reaction time and synthesis pH on the morphology and chemical structure of HT carbon.

Table 9 *Product yields of hydrothermal conversion of fructose versus feed gas (air, CO_2, N_2) and pressure at 200 °C for 2 h.*

atmosphere	Pressure (bar)	FA (mol %)	AA (mol %)	LevA (mol %)	HMF (mol %)
air	1	7.7 ± 0.2	9 ± 1	0[a]	10.5 ±0.4
	2	8.1 ± 0.3	9 ± 2	0[a]	12 ± 1
CO_2	1	9.1 ± 0.7	12 ± 2	0[a]	6 ± 2
	2	12 ± 3	9 ± 3	0[a]	6 ± 2
N_2	1	7.80 ± 0.02	10.5 ± 0.6	0.172 ±0.004	9.1 ± 0.5
	2	8.7 ± 0.4	12.6 ± 0.9	0[a]	9 ± 1

[a] below quantification limit

Reaction time

SEM micrographs and histograms of HT carbon particles size distribution are shown in **Figure 8**. These pictures show a very rapid increase of the average diameter from 3 to 4 h (0.86 µm to 1.81 µm). In this phase, relatively low amounts of HMF formed from fructose in uncatalyzed conditions and short reaction time (**Figure 4a**) produce smaller particles with a narrow distribution of sizes. Afterwards, from 6 to 12 h, the average diameter fluctuates from 1.4 µm to 1.7 µm. At the same time, we can observe a substantial broadening in the

particle size distributions. This phenomenon can be ascribed to a process of coalescence of smaller particles. In fact, in these later stages the particles start to fuse into each other forming big agglomerates. In the meantime, last remnants of polymer precursors (HMF above all) are consumed to produce new, smaller particles. Thus, the particle size distribution broadens, reaching a bimodal distribution after 12 h, while the average size stays relatively unchanged.

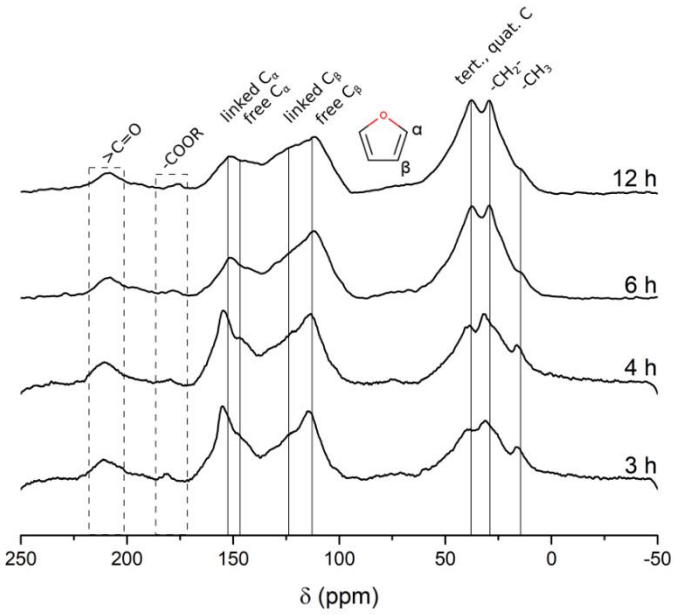

Figure 7 *Solid state ^{13}C CP-MAS spectra of hydrothermal carbon derived from fructose at increasing reaction time. Signals highlighted in the range between 0 ppm and 50 ppm belong to aliphatic carbons. Signals between 100 ppm and 160 ppm belong to sp^2 carbon atoms in furan and arene structures.*

Figure 7 shows the ^{13}C CP-MAS spectra of fructose-derived hydrothermal carbon in uncatalyzed conditions. Three main regions can be identified: signals at δ < 50 ppm belong to aliphatic carbons, whereas signals 100 ppm < δ < 160 ppm refer to aromatic or unsaturated carbons and finally signals at δ > 170 ppm belong to carbonyl groups. The same profile is roughly recognizable on each spectrum, with broad peaks that point out to a

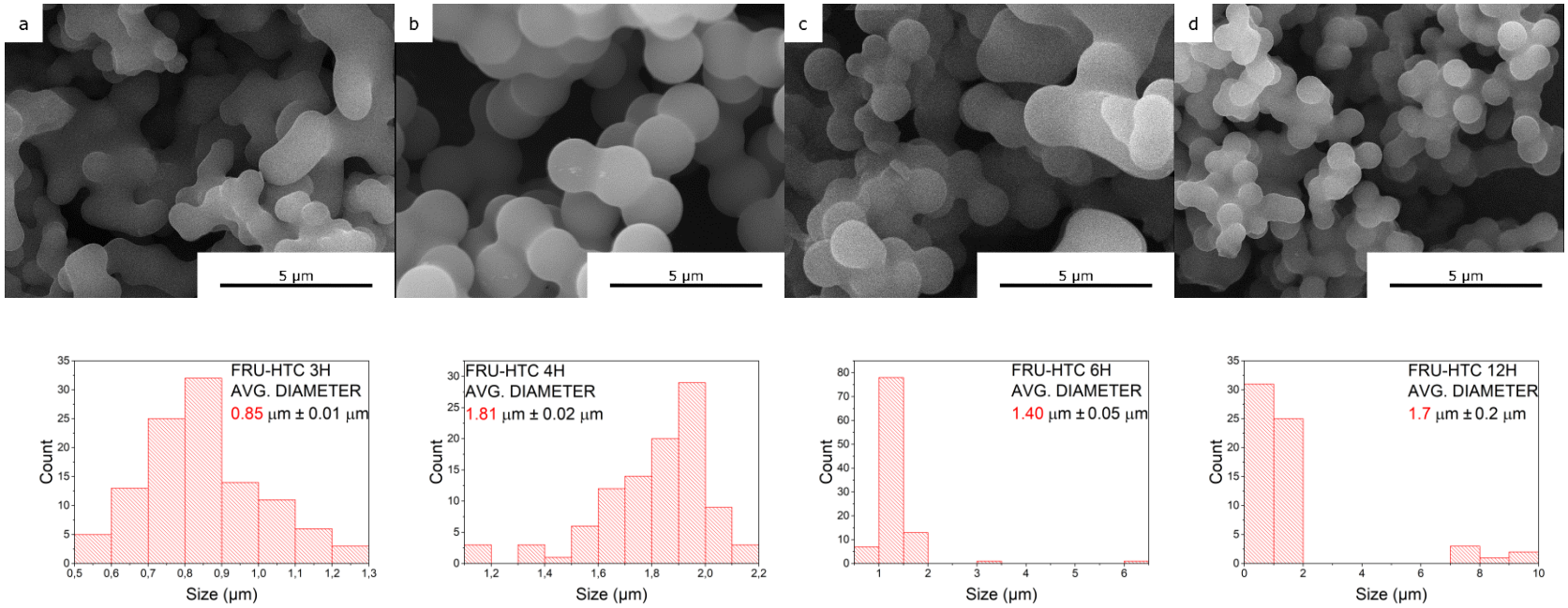

Figure 8 *SEM pictures of HT carbon obtained from fructose at 3 hours (a), 4 hours (b), 6 hours (c), 12 hours (d) with the relative histograms of particles diameter.*

complex structure with aliphatic chains, (hetero)aromatic moieties and many oxygenated functional groups (ketones, carboxylic acids, esters). Chemical shifts of the main peaks are listed in **Table 10** with the relative assignments. Many spectral features are shared in all samples, particularly in the portion of δ > 170 ppm, suggesting that ketones, carboxylic and ester functionalities are common to all HCs and they undergo little to no modifications under prolonged reaction times. Unsaturated carbon atoms dominate the middle part of all spectra with peaks that point out to a complex structure with aliphatic chains. Two main signals falling at 151 ppm and 114 ppm can be assigned respectively to a C_α furan linked and a C_β free furan. Alongside these two main peaks, we can trace the contributions of two minor peaks at 146 ppm and 121 ppm, identified as C_α free furan and linked furan C_β respectively. These four signals, found in all samples, in absence of a strong peak around 125-129 ppm commonly identified as a marker of C_6 aromatic moieties,[32], [235], [236] seem to suggest that furan units are prevalent in the chemical structure of fructose-derived HT carbons. As reaction time increases, linked C_β signal becomes more intense and overlap with the free C_β peak, resulting in a broader and smoother band. This behaviour can be explained as evidence of post-polymerization cross-linking or functionalization of furan moieties on the C_β. Three signals found in the range between 50 ppm and 100 ppm belong to primary, secondary and tertiary aliphatic C atoms. The disappearance of the 16 ppm peak (primary C) is an evidence of chemical transformation in the HC due to extended exposure to the reaction medium. FT-IR spectra of HT carbon show similar evolution through times, with disappearance of furfural aldehydic signal at long reaction times and a change in the aromatic structure, possibly due to cross-linking.

Table 10 *Peak assignments solid state ^{13}C NMR spectra*

δ [ppm]	Functional group	Chemical formula
210	ketone	C=O
181	acid, ester	COOH/COOR
151	C_α linked furan	C=*C*-OH or C=*C*-O
146	C_α free furan	C=*C*H-O
121	C_β furan linked	*C*=C-OH or C-*C*=C-O
114	C_β furan protonated	H*C*=C-OH or C-H*C*=C-O
43-39	aliphatic	tert. C-H, quat. C
31-25	aliphatic	sec. $-CH_2-$
17-14	aliphatic	prim. – CH_3

Figure 9 shows the FTIR spectra of fructose derived HT carbon at increasing reaction times. All spectra present some easily recognizable features, such as a broad intense band of O-H stretch centred around 3400 cm^{-1}, C-H stretch between 2960-2880 cm^{-1} and characteristic peak of C-O deformation in furan rings at 1020 cm^{-1}, confirming the structural motif of fused furan rings. A few peaks in the region between 1800 and 1500 cm^{-1}need special attention: C=O stretch at 1700 $cm^{-1}$and C=C stretch at 1610 cm^{-1}. These two peaks are a proof of the presence of aromatic units and carbonyl groups in saturated aliphatic ketones. An additional peak at 1665 cm^{-1} has been identified as C=O vibration of an aldehyde group like that of HMF, albeit not without ambiguity. In fact, this signal has been interpreted as a proof of HMF absorbed on the surface of the carbon spheres.[237] Nonetheless it is more likely it belongs to free aldehyde groups of furan rings covalently bonded to the polymeric structure of carbon, as no other peak of absorbed species like LA or FA reported by Tsilomelekis et al.[237] was detected in this study. 6h and 12h HT carbon spectra show a relative decrease in the intensity of the 1665 cm^{-1} and 1510 cm^{-1}, ascribed to furfural aldehyde group and furan ring stretch respectively, as well as a change in the 780-800 cm^{-1} band of vinyl C-H vibration. All these changes are compatible with an evolution of HT carbon towards a more

condensed structure where the reactive aldehyde group of furfural is consumed in condensation reactions and the furan ring is involved in cross-linking reactions.

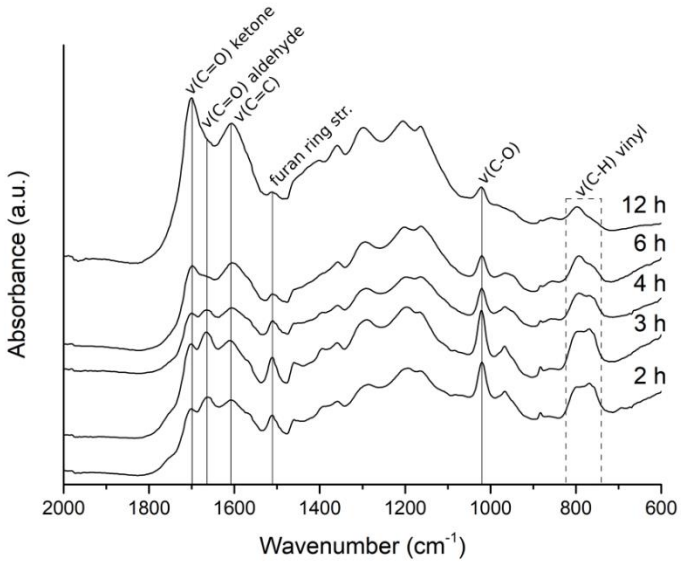

Figure 9 *FT-IR spectra of hydrothermal carbon derived from fructose at increasing reaction time.*

Scheme 8 illustrates three examples of possible chemical modification occurring in HT carbon after polymerization, due to prolonged stay under hydrothermal conditions. Condensation and cyclization can explain the simultaneous decline in furfural aldehyde and primary carbon signals observed in ^{13}C NMR and FT-IT spectra.

More details about the polymerization process can be withdrawn from MALDI-ToF mass spectrometry (**Figure 10**). Fru-3h and fru-4h HT carbon mass spectra present five equally spaced groups of peaks at 655 m/z, 866 m/z, 1077 m/z, 1289 m/z and 1499 m/z respectively. Interpreting these signals as belonging to a family of oligomers, the distance between each peak will correspond to increment of mass upon addition of a new unit, thus making the five identified species the trimer, tetramer, pentamer, hexamer and heptamer (3x, 4x, 5x, 6x and 7x) respectively. The average increment of the mass charge ratio is 211.1 m/z ± 0.4 m/z. Knowing that our system is rich in furan derivatives and ketoacids, we can reasonably assign this mass to a fragment with an empirical formula $[C_{10}H_{11}O_5]^+$.

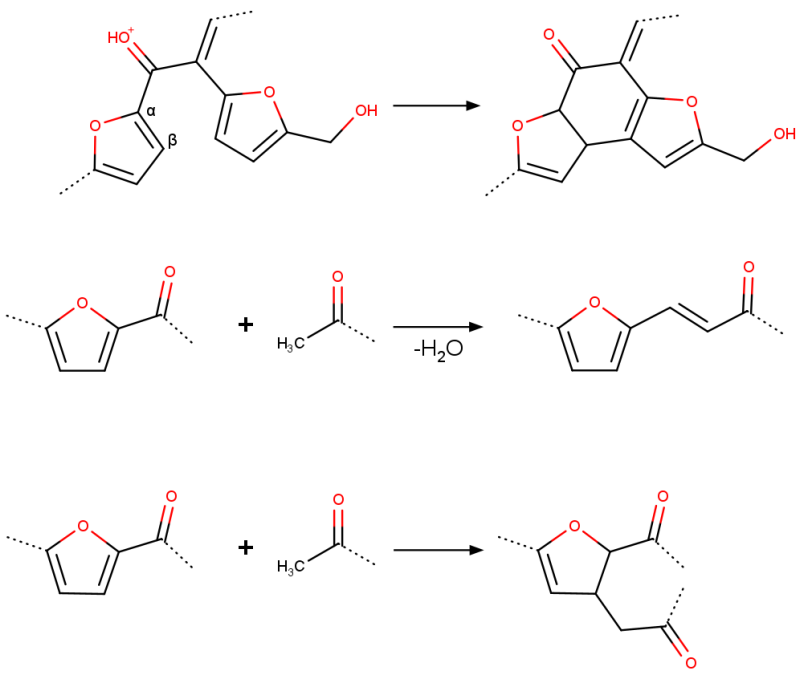

Scheme 8 Reaction schemes of possible post-polymerization modification occurring on HT carbon based on ^{13}C NMR and FT-IR spectra.

By means of a simple mathematical formula (Eq. 10) , it is possible to calculate the degree of unsaturation of an organic compound with such empirical formula.

$$degrees\ of\ unsaturation = \frac{2C - H - X + N + 2}{2}$$
$$C = n.of\ carbon\ atoms$$
$$H = n.of\ hydrogen\ atoms$$
$$X = n.of\ halogen\ atoms$$
$$N = n.of\ nitrogen\ atoms \qquad (\mathbf{10})$$

The result of this calculation is 5.5, indicating a high degree of unsaturation that is compatible with a structure composed of an unsaturated cycle linked aliphatic chains with carboxylic functionalities. Although a more in-depth structural characterization of the family of fragments found in this study is needed for a definitive identification, these results show that exose-derived hydrothermal carbon might form through polymerization of a single chemical species.

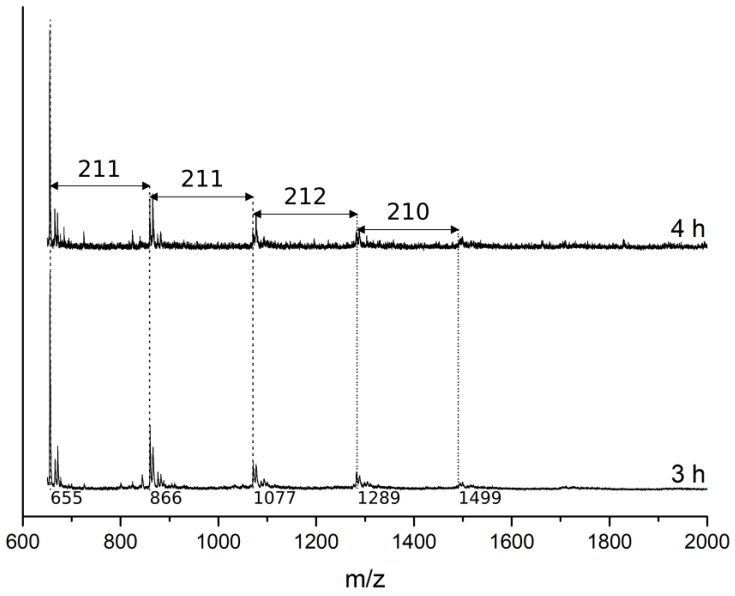

Figure 10 *MALDI-ToF mass spectra of fru-3h and fru-4h HT carbons showing evidence of oligomers with an average mass difference of 211 Da.*

As found in the analysis of the liquid phase, conversion of glucose is relatively slow and, at its highest point, HMF yield does not exceed 16%. This means that every polymerization process occurring on HMF is hindered by low concentration of the precursor. SEM micrographs and histograms of HT carbon particles size distribution are shown in **Figure 11**. These pictures show a slow and steady increase of the average diameter from 4 to 12 hours (0.137 μm to 0.355 μm). No HT carbon was recovered at 3 h. Therefore, nucleation occurs at a reaction time between 3 h and 4 h in a condition of low concentration of furan precursors, producing particles that are more than five time smaller than those obtained from fructose at the same time. As the reaction proceeds, concentration of furan species is kept low by slow rate of conversion of glucose and parallel consumption by rehydration, explaining the observed slow increase in size. Finally, it must be noted how relevant agglomeration of spheres becomes as the reaction time increase, as noted by Jung et al.[133]

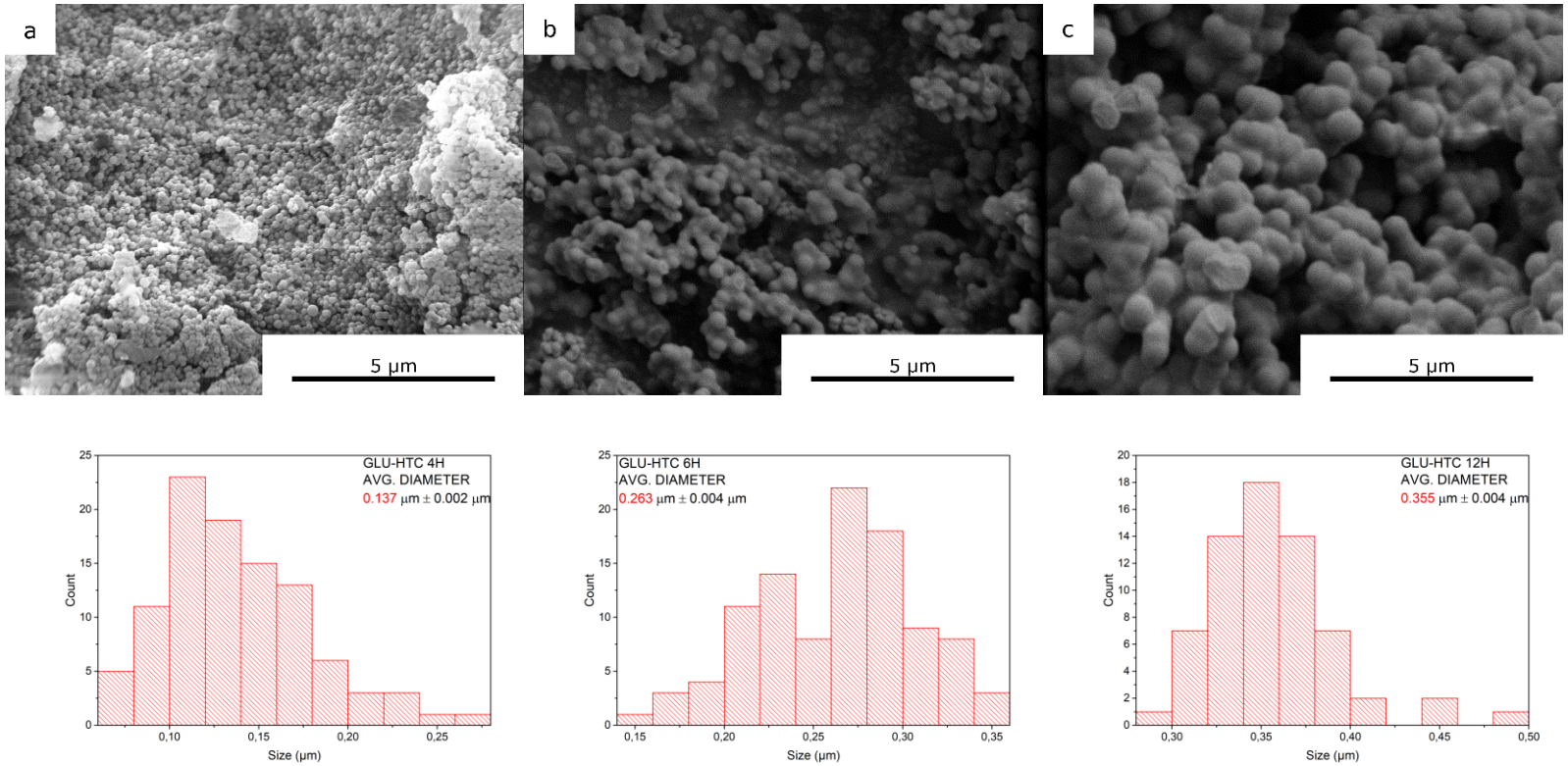

Figure 11 *SEM pictures of HT carbon obtained from glucose at 4 hours (a), 6 hours (b), 12 hours (c) with the relative histograms of particles diameter.*

Figure 12 shows CP-MAS spectra of HT carbons obtained from glucose in neutral initial pH. All spectra share a very similar structure with those of HT carbons obtained from hydrothermal conversion of fructose in the same conditions. Broad peaks point out to structure rich in oxygenated functional groups. Three main regions of interest can be highlighted: aliphatic carbons signals (δ < 100 ppm), heteroaromatic moieties (100 ppm < δ < 170 ppm) and carbonyl groups (δ > 170 ppm). These profiles are in fact hardly distinguishable from those of the spectra of fructose derived HT carbons, proving that the two kinds of carbons must share a similar chemical structure, with abundant oxygenated groups (ketones, aldehydes, carboxyl), (hetero)aromatic moieties and aliphatic chains. This, in turn, is evidence supporting the idea of a common conversion pathway of glucose and fructose to HT carbon.

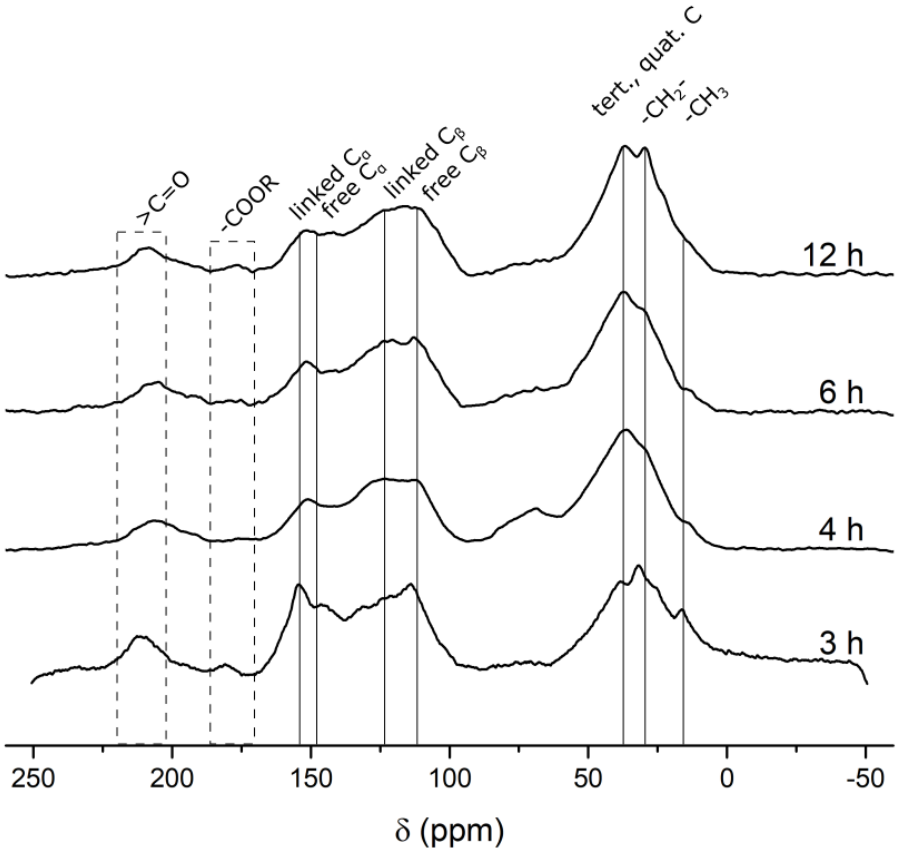

Figure 12 *Solid state ^{13}C CP-MAS spectra of hydrothermal carbon derived from glucose at increasing reaction time. Signals highlighted in the range between 0 ppm and 50 ppm belong to aliphatic carbons. Signals between 100 ppm and 160 ppm belong to sp^2 carbon atoms in furanic and arene structures.*

Figure 13 offers a different perspective on the same picture, showing FT-IR spectra of the same glucose-derived HT carbon samples. Again, all spectra present the easily recognizable features, such as a broad band of v(O-H) centred around 3400 cm^{-1}, v(C-H) vibrations between 2960-2880 cm^{-1} and characteristic peak of C-O stretch in furan rings at 1020 cm^{-1}, confirming the structural motif of fused furan rings. A few peaks in the region between 1800 and 1500 cm^{-1} need special attention: v(C=O) at 1700 cm^{-1} and v(C=C) at 1610 cm^{-1}. These two peaks suggest the presence of aromatic units (v(C=C)) and carbonyl groups (v(C=O)) in saturated aliphatic ketones. An additional peak at 1665 cm^{-1} may be identified as C=O vibration of an aldehyde group like that of HMF, possibly belonging to HMF-like ring covalently bonded to the polymeric structure of carbon. Further evidence of furan cycles come from a peak found at 1510 cm^{-1} belonging to furan stretching, and a couple of close peaks around 780-800 cm^{-1} identified as vinyl C-H vibration. Both these NMR and FT-IR spectra, as seen in the case of fructose, describe a coherent picture of a carbonaceous structure with furan cycles and aliphatic portion, possibly linking these cycles.

Moreover, both sets of spectra evolve in the same way under the influence of increasing reaction time. Some peaks appear to be notably smoothened out by longer residence in the reactor medium, such as primary aliphatic carbons (NMR), free furan C_β (NMR), furan ring stretching (FT-IR) and vinyl C-H vibration (FT-IR). On the other hand, some other peaks are enhanced by longer residence time, such as linked furan C_β (NMR) and C=C and C=O stretching (FT-IR). Assuming that, like in the case of fructose derived HT carbons, these spectra belong to a disordered carbonaceous structure made of furan units connected by aliphatic linkers and rich in carbonyl and carboxyl groups, this set of modifications can be interpreted as a sign of cross linking between adjacent furan units or furan-aliphatic β-linking. The resulting structure would allow less freedom of movement to the furan rings and would appear more extensively condensed, thus leading to the spectral differences described above.

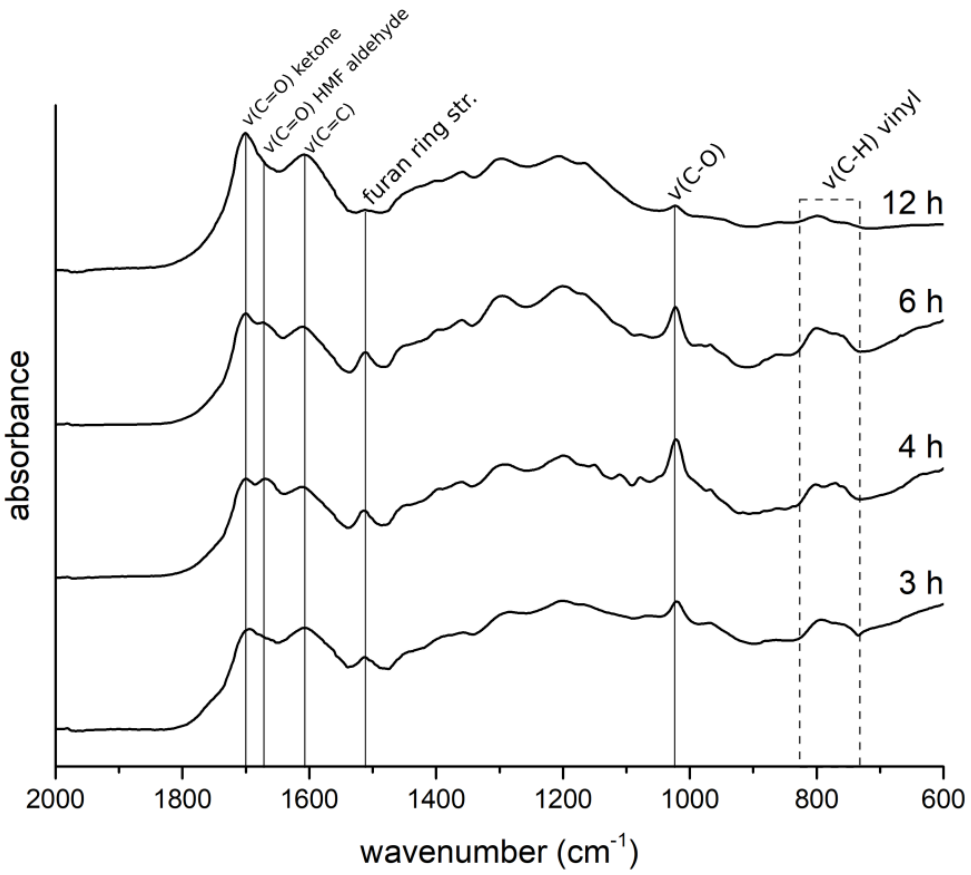

Figure 13 *FT-IR spectra of hydrothermal carbon derived from glucose at increasing reaction time.*

MALDI-ToF mass spectrometry of HT carbons exhibit some relevant features (**Figure 14**). Firstly, it shows the presence of large molecules in the mass-charge ratio range between 1000 m/z and 1800 m/z, proving that the carbonization of glucose to HT carbon proceeds via intermediate formation of soluble oligomers. Secondly, it can be noted that the oligomeric species change substantially throughout reaction time. The variety of peaks observed in glu-4h disappears in the later samples, pointing out to an extensive polymerization leading to consumption of oligomeric species. More interestingly, Glu-4h peaks at 995.6 m/z, 1163.6 m/z, 1329.6 m/z, 1494.4 m/z, 1660.3 m/z and 1829.3 m/z respectively are equally spaced. The average distance Δm/z between the six peaks equals 166.7 ± 0.7 m/z and all six peaks have mass/charge that are integer multiples of this value, meaning that the peaks belong to oligomers with a number of units ranging from 6 to 11. Maruani et al. detected, in similar conditions to this study, a family of glucose oligomers (Δm/z 162 Da) originating from glucose polymerization under hydrothermal conditions.[238] The mass increment of 162 Da

is quite close to the one observed here and the similarities between the two studies (hydrothermal conversion of glucose) might lead to think that we are in presence of glucose oligomers too. However, the observed masses and the mass increment itself do not match the ones observed by Maruani, making this interpretation unlikely. Poerschmann et al., on the other hand, reported several trace chemicals from hydrothermal conversion of fructose, glucose and xylose.[134] Among those, a molecule with a mass of 166 Da was found and its structure was identified as 1-(2-furyl)-1,4-pentanedione (**Scheme 9**). This species matches the mass of the fragment observed in MALDI-ToF very precisely; moreover, it would allow multiple self-aldol condensation, due to the presence of two carbonyl groups and six enolizable α-hydrogens on each monomer, explaining the presence of several oligomers. Moreover, it is structurally similar to the hypothetical monomer found in the MS analysis of fructose and both appear to be furfural or HMF derivatives. Its formation can be the result of a hydrolytic ring opening of a furan ring, as suggested by the presence of two ketone groups in γ position to each other. This mechanism of formation of oxygenated carbocycles species was also proposed by Shi as an explanation of several heteroaromatic oxygenated species in the reaction medium after hydrothermal carbonization of glucose.[136] At longer reaction time, only a small number of weak peaks are found in the mass spectra. Glu-6h spectrum presents two groups of peaks centred at 1068.8 m/z and 1289.4 m/z respectively. The latter appears as a group of five peaks, of which three are separated by a mass increment of ~16 Da, suggesting different degrees of oxidation within the same oligomer. Finally, glu-12h presents two weak peaks at 1092.3 m/z and 1288.5 m/z.

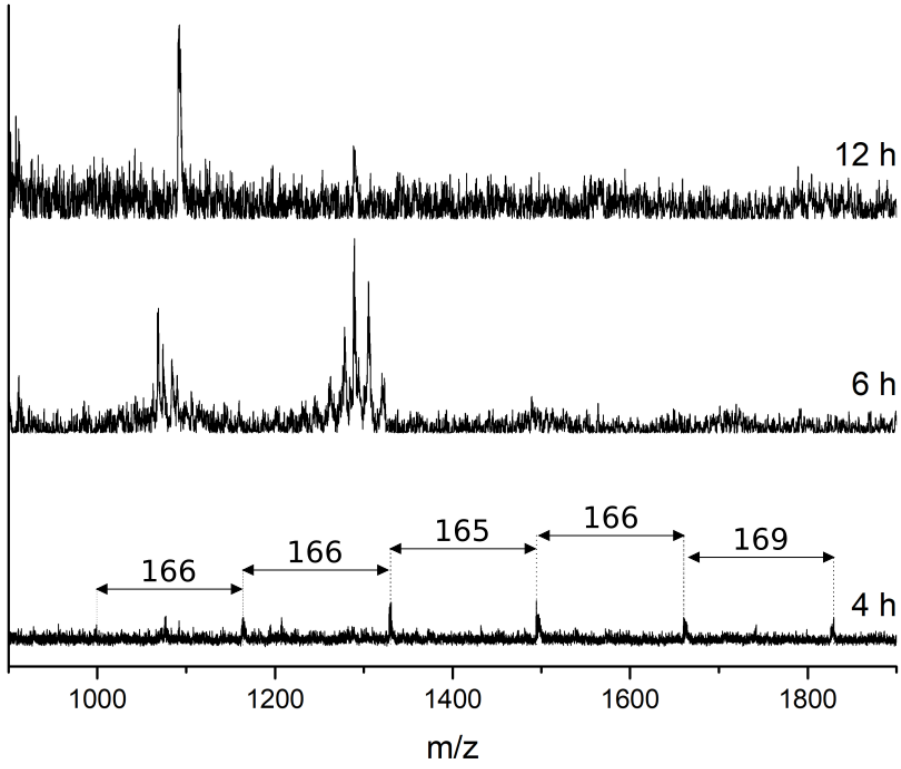

Figure 14 *MALDI-ToF mass spectra of glu-4h, glu-6h and glu-12h HT carbons. Glu-4h carbon shows evidence of oligomers with an average mass difference of 166 Da.*

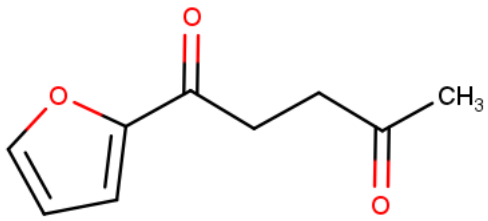

1-(2-furyl)-1,4-pentanedione

Scheme 9 *Tentative identification for the structure of the monomer with mass 166 Da, corresponding to the mass increment observed in glu-4h MALDI-ToF-MS fragments, as proposed by Poerschemann et al.*[134] .

The images of xylose HT carbons obtained with SEM (**Figure 15**) show the spherical morphology already observed in previous carbon samples. By comparison with fructose- and glucose-derived microspheres, it can be noticed that xylose microspheres tend to have

a more regular shape, with reduced tendency to form agglomerates or clusters, a characteristic that was also noted by Titirici.[31] The histograms below each micrographs report the distribution of particle size for each sample as well as their mean diameter and the standard errors. The size of the particles and the time scale of their evolution reflects the kinetics of xylose conversion to FF and seems to confirm, from the point of view of reactivity, the intermediate status of xylose, between fructose and glucose. In fact, xylose HT carbon particles, when compared with the analogous hexose derived particles at the same reaction time, are always smaller than fructose particles but larger than glucose ones.

The chemical structure of xylose-derived HT carbons was investigated through ^{13}C solid state NMR and infrared spectroscopy. **Figure 16** and **Figure 17** show the relative CP-MAS NMR and FT-IR spectra. Before entering in a deep analysis of the NMR peaks, it is necessary to make a clarification on the signals appearing in the 3 h sample in the rage between 50 ppm and 100 ppm. This is a region of aliphatic C-O bonds. The strength of the signals, overshadowing every other signal, suggests that they belong to unreacted xylose, largely present in on the HTC sample due to an incomplete washing of the unreacted precursor on the scarce carbon precipitate. Some weaker signals found in these regions in the 6 h and 12 h samples can also be attributed to xylose in traces. Xylose-derived HTC present the same three main regions previously observed in HMF-derived HTC: sp^3 carbons signals ($\delta < 100$ ppm), sp^2 aromatic carbons (100 ppm $< \delta <$ 170 ppm) and sp^2 carbonyl/carboxyl group ($\delta >$ 170 ppm). The aliphatic region presents a large, intense band where the contribution from primary and secondary sp^3 is less recognisable compared to the hexose-HTC spectra. The usual presence of aldehydes, ketones and carboxylic groups is confirmed by two signals in the range between 170 ppm and 210 ppm. Finally, the area around 100 ppm to 160 ppm is dominated by the furan sp^2 signals. Two peaks located around 150 ppm and 110 ppm have been identified as belonging to furan's C_α and C_β respectively. A very distinctive peak is found around 125 ppm. This is generally identified as a signal of sp^2 carbon in extended aromatic structures or long-range conjugated double bonds. The presence of this peak marks a difference with hexose-derived HT carbons. The difference must originate once again from the fact that xylose-derived carbon is based on FF instead of HMF. FF's free C5 allows a series of reactions that are not possible in HMF and other 2,5-disubstituted furans. In particular,

the spontaneous resinification reaction of FF in air has been explained as a consequence of C5 hydrogen abstraction by O_2 followed by radical attack on the aldehyde group;[239] alternatively, a nucleophilic attack of the 4-5 furan double bond on the aldehyde group, with a mechanism akin to aldol condensation, has been proposed as the responsible of the formation of soluble oligomers and insoluble resins in pure FF.[203]

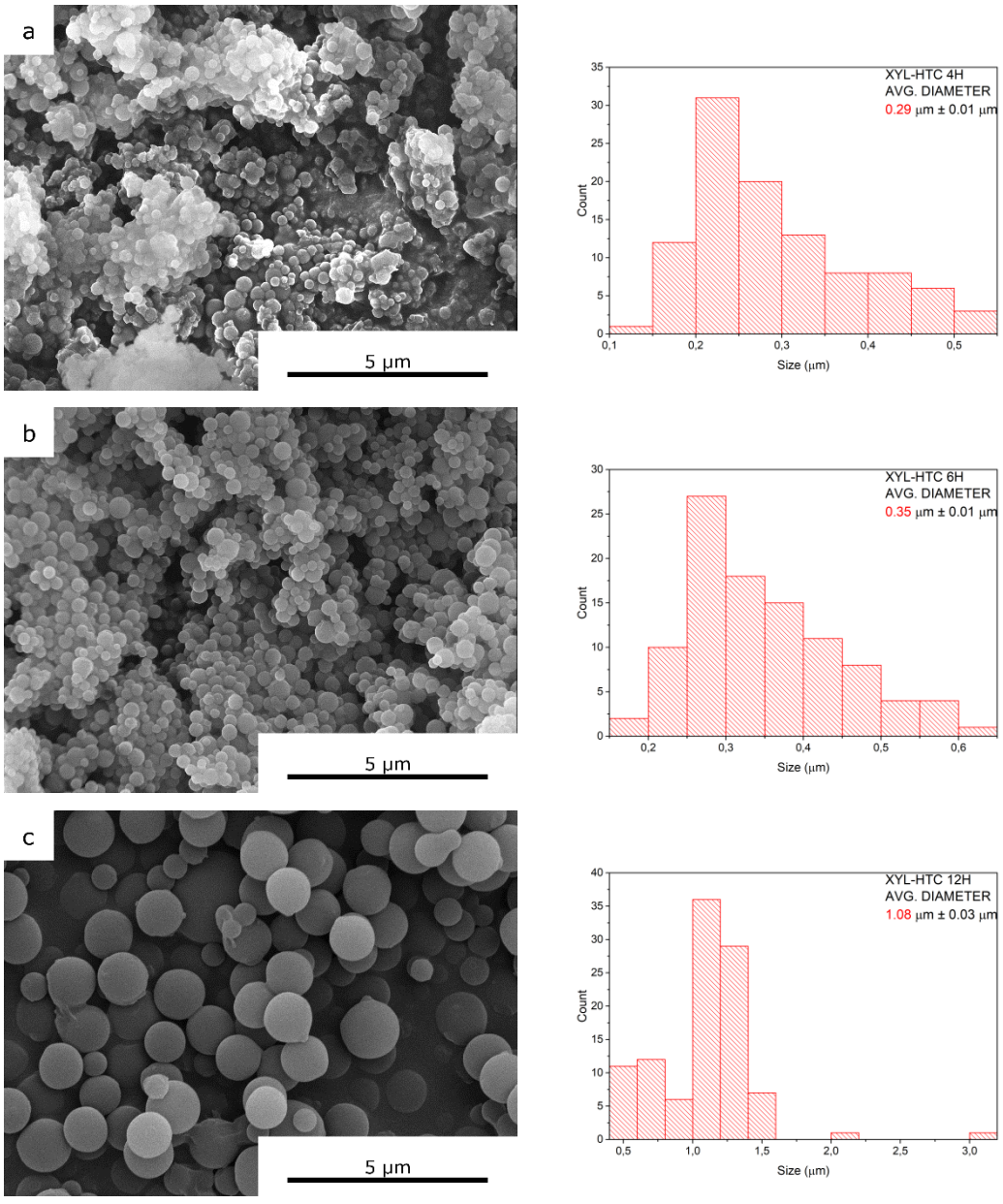

Figure 15 SEM pictures of xylose-derived HT carbon obtained at 4 hours (a), 6 hours (b), 12 hours (c) in plain water at 200 °C with the relative histograms of particles diameter

It is reasonable to suppose that such mechanisms may occur during hydrothermal conversion of xylose, where the FF is exposed to much more severe conditions, leading to the formation of extended chains of conjugated furans that ultimately aggregate and precipitate to form carbon spheres.

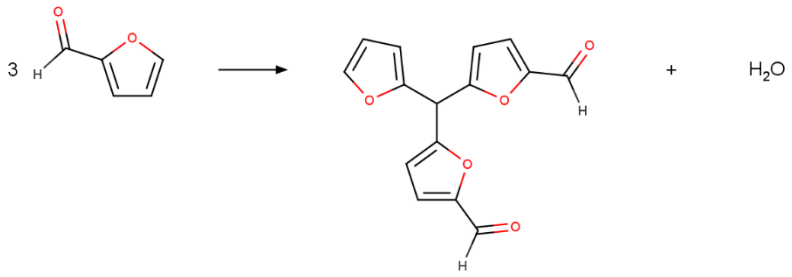

Scheme 10 *Mechanisms of FF spontaneous resinification by nucleophilic addition to the aldehyde group.*[203]

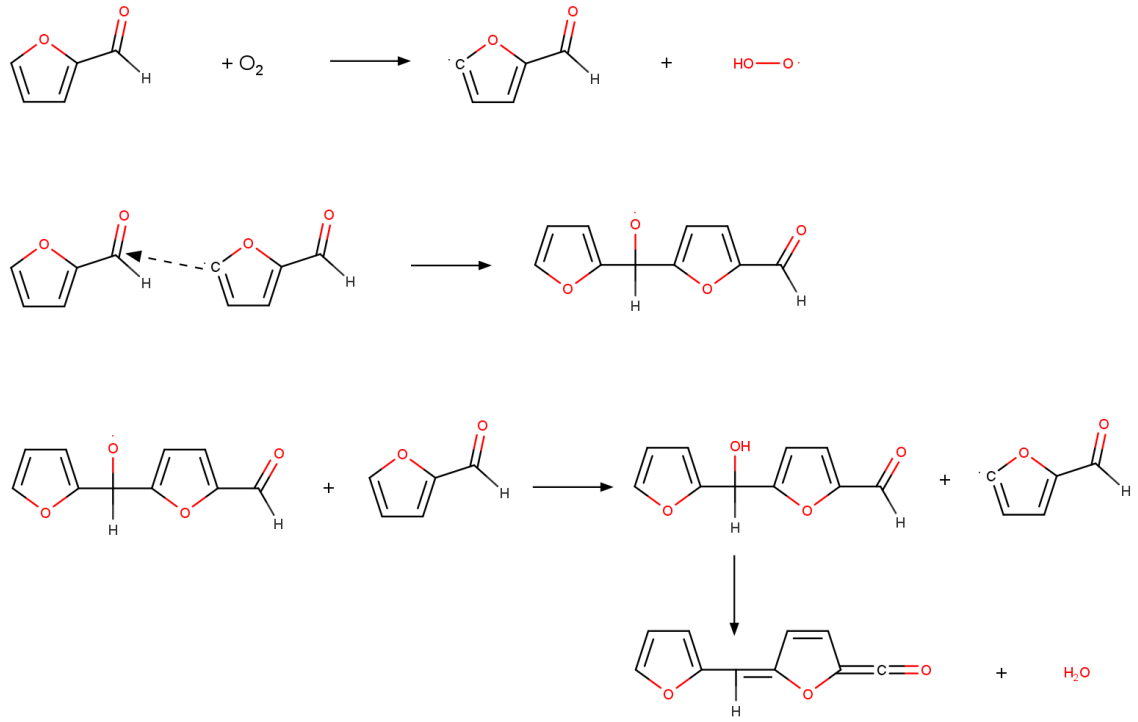

Scheme 11 *Mechanisms of FF spontaneous resinification by radical polymerization initiated by atmospheric oxygen.*[239]

Figure 17 shows FT-IR spectra of the xylose-derived HT carbon samples. Many spectral features are in common with previously observed fructose- and glucose-derived HT carbon,

such as three signals in the region between 1700 cm^{-1} and 1600 cm^{-1}: two of them at 1695 cm^{-1} and 1673 cm^{-1} are slightly overlapped and belong respectively to generic C=O stretching and furan-linked C=O stretching.[237] The latter disappears at 12 h possibly due to increased cross-linking. The third signal is found at 1612 cm^{-1} and belongs to aromatic or furan C=C stretching. A signal at 1460 cm^{-1} is characteristic of pentose-derived FF-based carbons and it can be interpreted as an aromatic stretching vibration.[240] A furan C-O stretching is observed at 1018 cm^{-1} and it is also common in all hexose and pentose carbons[241]. Finally, a couple of peaks at 883 cm^{-1} and 756 cm^{-1} are due to aromatic C-H out of plane vibration. The presence of these peaks marks another distinction with HMF-based carbons and indicates the more aromatic nature of FF carbons. It is also interesting to notice that these last two signals are less intense in the 12 h HT carbon, possibly suggesting a decline in the number of aromatic C-H bond due to an increased cross-linking between furan units.

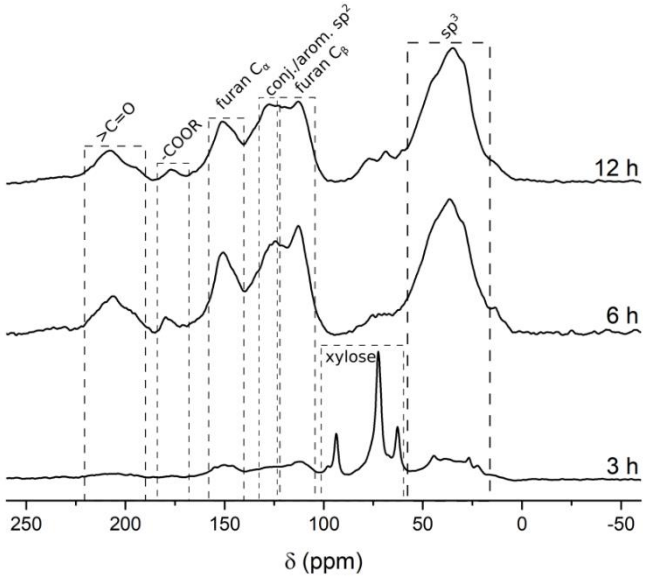

Figure 16 *Solid state ^{13}C CP-MAS spectra of xylose-derived hydrothermal carbon in plain water at 200 °C at 3 h, 6 h and 12 h.*

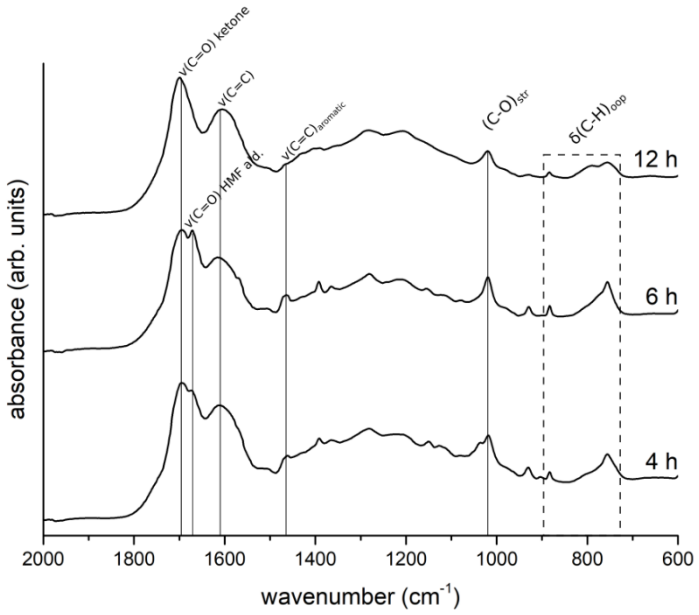

Figure 17 *FT-IR spectra of xylose-derived hydrothermal carbon in plain water at 200 °C at 4 h, 6 h and 12 h.*

The mass spectra obtained from MALDI-ToF analysis of xylose-derived carbons are showed in **Figure 17** and a summary of the main peaks is found in **Table 11**. The relative scarcity of notable signals suggests that xylose-derived HT carbons are far less soluble in THF than fructose- and glucose-derived HT carbons. The sparse peaks on each spectrum do not allow to make solid conclusions about the chemical structure of these soluble polymers. It can be noted, however, that the masses greatly increase from 4 h to 12 h due to extended polymerization reactions. A mass difference between two consecutive peaks in the 6 h sample equals 212 m/z. Although it is not possible to know from these results whether these two peaks actually belong to two oligomers or rather to unrelated species, it must be noted that a similar Δm was found in the fructose derived soluble oligomers. This mass value points to a fragment with a molecular formula of $[C_{10}H_{12}O_5]^+$ that is compatible with the nature of the chemicals in the reaction medium. In particular, a chemical species with 10 carbon atoms might be the result of a dimerization of furfural. Following this hypothesis, it can be argued

that the xyl-4h peaks at 1068 m/z and 1280 m/z are, respectively, pentamer (5x) and hexamer (6x) form of the 212 Da monomer.

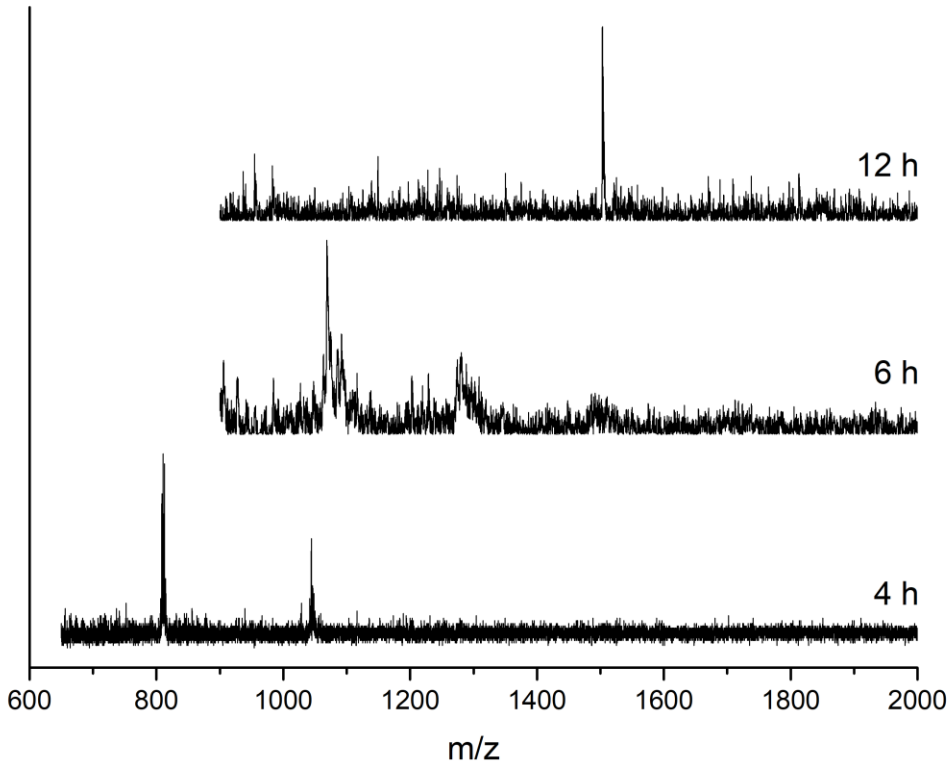

Figure 18 *MALDI-ToF mass spectra of XYL-4h, XYL-6h and XYL-12h HT carbons.*

Acid catalysis

Micrographs show that particles formed from fructose in presence of acidic catalyst are much bigger than those obtained in the same amount of time in uncatalyzed conditions. They have an average diameter of 6.6 μm and a broader size distribution (**Figure 19**), as opposed to 0.85 μm (**Figure 8a**). The larger size of carbon particles depends on the availability of HMF at the time of their formation. In fact, by looking back at the HPLC data, it is apparent that while HMF synthesis has just reached its peak after 3 hours in uncatalyzed conditions, a high concentration of HMF was already available at earlier times due to acid catalysis and it has been completely converted to other products (LevA+FA or HT carbon) after 3 hours (**Figure 4b**). HT carbon particles produced in these conditions have had more time and a higher concentration of HMF to grow in considerably larger size.

Table 11 *Summary of MALDI-ToF MS peaks obtained from xyl-HTC at various reaction time.*

m/z	Occurrence
810	XYL-4h
1044	XYL-4h
1068	XYL-6h
1280	XYL-6h
1503	XYL-12h

As for the chemical structure of these particles, there is no appreciable change in the chemical structure of HT carbon, indicating that acid plays no major role in the nucleation and growth process, apart from accelerating the formation of its primary building block, HMF.

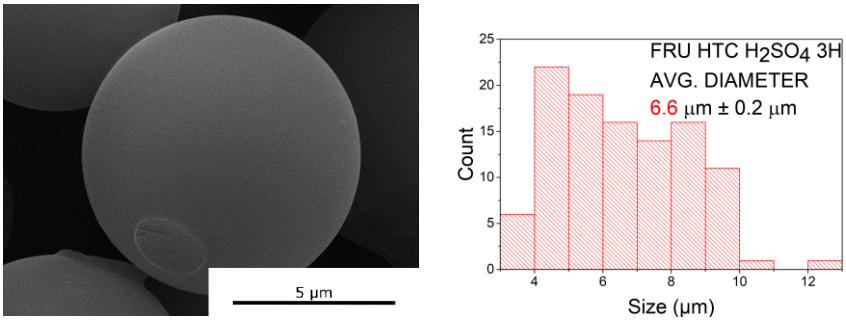

Figure 19 *SEM pictures of HT carbon obtained from fructose at 3 hours and initial pH 1.5 in presence of H_2SO_4 with the relative histogram of particles diameter.*

Figure 20 shows ^{13}C ss-NMR and FTIR spectra of HT carbon samples derived from fructose at acidic synthesis pH (1.5) and fixed reaction time (3 hours). An NMR spectrum of a sample

of carbon obtained at 3 hours without catalyst is shown in comparison, to demonstrate that the chemical structure of the three sample is nearly identical. It consists in an aliphatic portion with primary, secondary, tertiary and quaternary carbon atoms, a large aromatic portion and ketones and carboxylic functionalities. On the other hand, FT-IR presents some minor differences. In fact, it can be observed that C=C stretch peaks are slightly higher than C=O peaks, whereas the two peaks have roughly the same intensity in "uncatalyzed" HT carbons. This characteristic has also been noted by Reiche et al. and it suggests that a lower pH promotes a more condensed structure where extended conjugated or aromatic systems prevail over oxygen-rich structures. Moreover, the absence of the C=O vibration of an HMF aldehyde group at 1665 cm^{-1} indicates that this group is very reactive at low pH and easily undergoes condensation reactions.

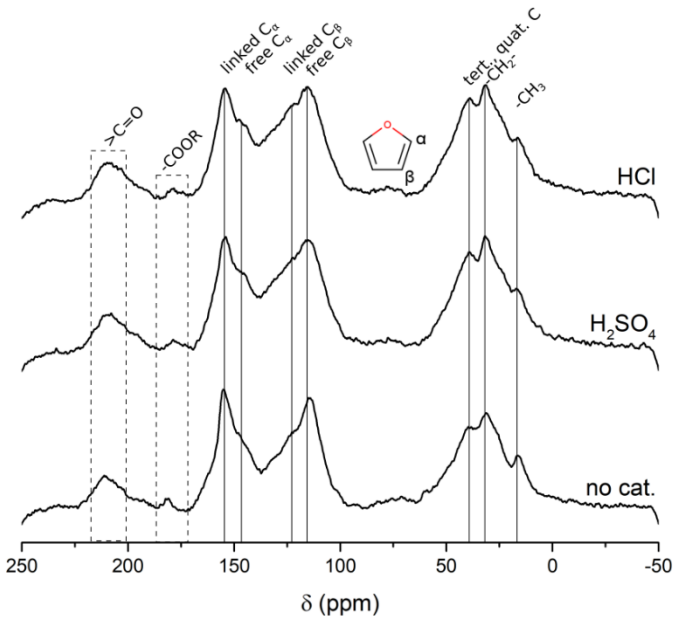

(a)

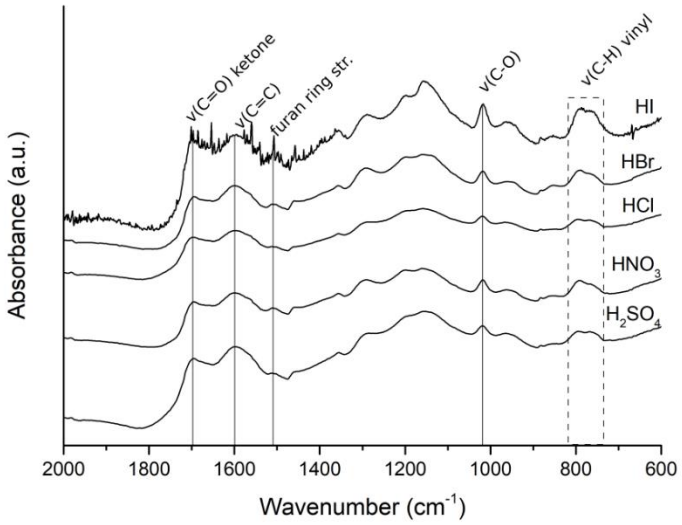

(b)

Figure 20 *^{13}C ss-NMR and FTIR spectra of HT carbon samples derived from fructose at acidic synthesis pH (1.5) and fixed reaction time (3 hours)*

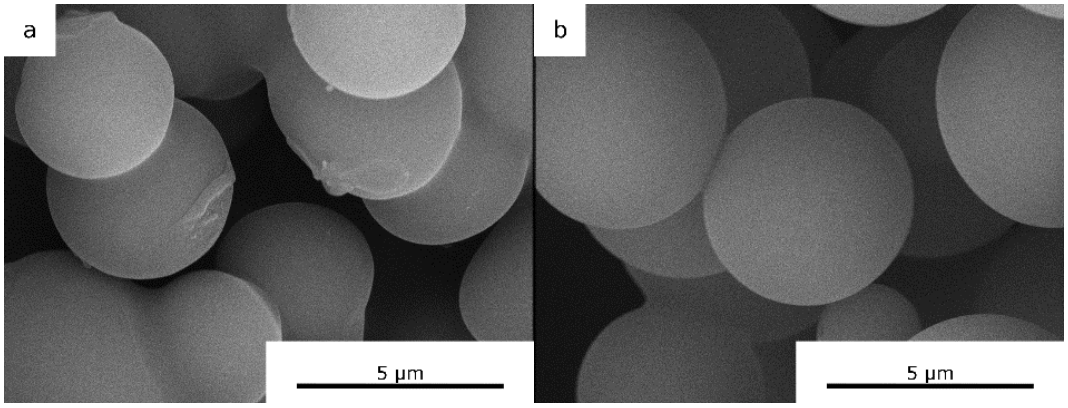

Figure 21 *SEM pictures of HT carbon obtained from glucose at 3 hours and initial pH 1.5 in presence of H_2SO_4 (a) and HNO_3 (b).*

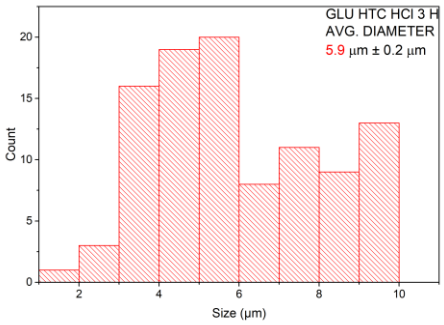

Figure 22 *Histogram of Glu-HTC-HCl-3h particles diameter.*

Addition of strong acids greatly accelerates the conversion of glucose in hydrothermal conversion, as seen in **Figure 5b**. Micrographs show that particles formed in presence of acidic catalyst are much bigger than those obtained in the same amount of time in uncatalyzed conditions. The average diameter of 5.9 µm is notably greater than that of uncatalyzed carbons and so is the size distribution. A larger availability of HMF at the time of spheres formation is most likely to be responsible for the increased diameters of carbon particles. The chemical structure of these particles, as shown by SS ^{13}C NMR and FT-IR, NMR, does not present a relevant variation in comparison to the HT carbon from uncatalyzed conversions (**Figure 23** and **Figure 24**). NMR spectra in particular seems very similar to the uncatalyzed counterpart, indicating that acid does not affect the chemistry of hydrothermal carbons and plays no major role in the nucleation and growth process, apart from accelerating the conversion of glucose and the formation of HMF.

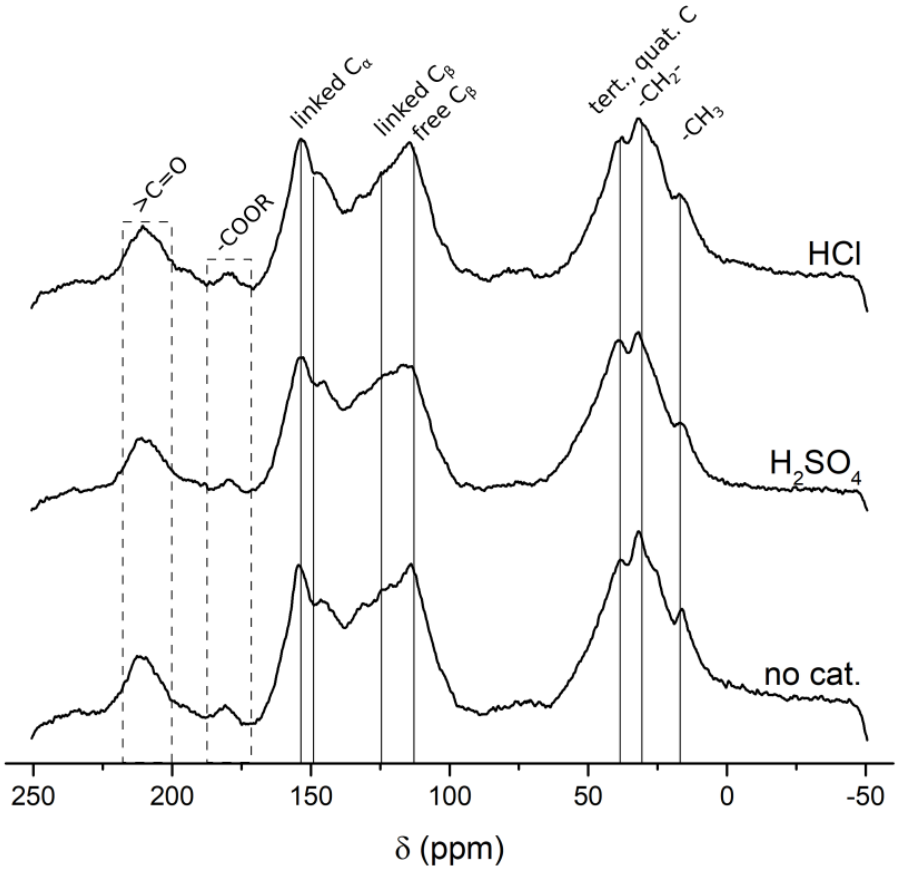

Figure 23 *Solid state ^{13}C CP-MAS spectra of hydrothermal carbon derived from glucose in presence of acidic catalysts (H_2SO_4 and HNO_3). Signals highlighted in the range between 0 ppm and 50 ppm belong to aliphatic carbons. Signals between 100 ppm and 160 ppm belong to sp^2 carbon atoms in furan and arene structures. NMR spectrum of 3h uncatalyzed carbon sample is show for comparison.*

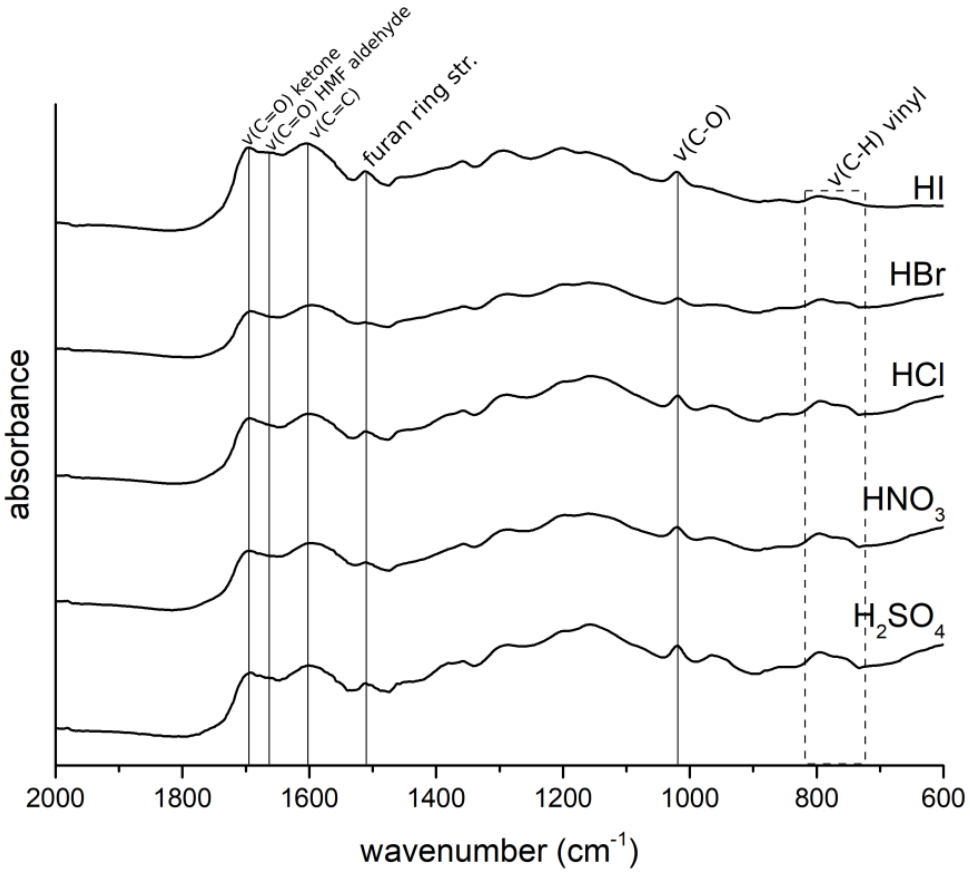

Figure 24 *FT-IR spectra of hydrothermal carbon derived from glucose in presence of acid catalysts at 3 h.*

Chapter 4 Kinetics study, conclusions and outlook

Kinetic modelling of experimental data

The experimental data gathered from HPLC, related to the concentration of species obtained by conversion of fructose, glucose and xylose as a function of reaction time, were modelled according three reaction networks showed below.

Fructose hydrothermal conversion (Reaction network 1):

$$Fru \xrightarrow{k_{1,F}} HMF \quad (\mathbf{11})$$

$$HMF \xrightarrow{k_{2,F}} LevA \quad (\mathbf{12})$$

$$HMF \xrightarrow{k_{3,F}} HTC \quad (\mathbf{13})$$

$$\frac{d[Fru]}{dt} = -k_{1,F}[Fru] \quad (\mathbf{14})$$

$$\frac{d[HMF]}{dt} = k_{1,F}[Fru] - k_{2,F}[HMF] - k_{3,F}[HMF] \quad (\mathbf{15})$$

$$\frac{d[LevA]}{dt} = k_{2,F}[HMF] \quad (\mathbf{16})$$

$$\frac{d[HTC]}{dt} = k_{3,F}[HMF] \quad (\mathbf{17})$$

Glucose hydrothermal conversion (Reaction network 2):

$$Glu \xrightarrow{k_{1,G}} HMF \quad (\mathbf{18})$$

$$HMF \xrightarrow{k_{2,G}} LevA \quad (\mathbf{19})$$

$$HMF \xrightarrow{k_{3,G}} HTC \quad (\mathbf{20})$$

$$\frac{d[Glu]}{dt} = -k_{1,G}[Fru] \quad (\mathbf{21})$$

$$\frac{d[HMF]}{dt} = k_{1,G}[Glu] - k_{2,G}[HMF] - k_{3,G}[HMF] \quad (\mathbf{22})$$

$$\frac{d[LevA]}{dt} = k_{2,G}[HMF] \quad (\mathbf{23})$$

$$\frac{d[HTC]}{dt} = k_{3,G}[HMF] \quad (\mathbf{24})$$

Xylose hydrothermal conversion (Reaction network 3):

$$Xyl \xrightarrow{k_{1,X}} FF \quad (\mathbf{25})$$

$$FF \xrightarrow{k_{2,X}} HTC \quad (\mathbf{26})$$

$$\frac{d[Xyl]}{dt} = -k_{1,X}[Xyl] \quad (\mathbf{27})$$

$$\frac{d[FF]}{dt} = k_{1,X}[Xyl] - k_{2,X}[FF] \quad (\mathbf{28})$$

$$\frac{d[HTC]}{dt} = k_{2,X}[FF] \quad (\mathbf{29})$$

For all three reaction networks, reactions were assumed to be first order, as in Tan-Soetedjo[242]. Moreover, AA was not included in these models for homogeneity, as it was not detected among the products of glucose conversion and only sparsely detected among the products of xylose conversion.

The reaction rates as well as the reaction rate constants are showed in Table 12. The reaction rate constants $k_{1,F}$, $k_{1,G}$ and $k_{1,X}$, relative to the degradation reactions of fructose, glucose and xylose, were obtained by linear fit of the logarithm of the experimental data versus time with the method of the least squares. The coefficients of determination R^2 for $k_{1,F}$, $k_{1,G}$ and $k_{1,X}$ were 0.6966, 0.7113 and 0.7545. The value of $k_{2,F} + k_{3,F}$ was obtained by linear fit of logarithm the HMF experimental data versus time, with a coefficient of determination R^2 of

0.6633; subsequently, single values of $k_{2,F}$ and $k_{3,F}$ were obtained by inserting $k_{2,F} + k_{3,F}$ in the expressions of reaction rates for LevA and HTC calculated at different reaction times and averaging the results. The reaction rate constants $k_{2,G}$ and $k_{3,G}$ were obtained in the same way (with $k_{2,G} + k_{3,G}$ R^2= 0.9693). Finally, $k_{2,X}$ was obtained by linear fit of logarithm the FF experimental data versus time, with a coefficient of determination R^2 of 0.9530. Low coefficients of determination found in some cases are to be ascribed to the small set of experimental data rather than inaccuracy of the models, as the reaction networks used to model experimental data were tested before in previous works.[98], [133], [243] Despite this, reaction rate constants are in agreement with previous studies[98], [243] and outline a picture that is coherent with the observations made in the previous chapter. In this picture, among sugar dehydrations, fructose exhibits the highest reaction rate constant, followed by xylose and glucose. The reaction rate constants of HMF rehydration to LevA and HTC formation found from fitting of fructose and glucose data are in good agreement with each other, thus proving the validity of the models. Finally, the reaction rate constant associated with the formation of furfural-derived HTC appears to be lower than that of HMF-derived HTC, seemingly suggesting a slightly higher stability of FF, although the associated uncertainties do not allow to give a conclusive answer.

Table 12 Summary of reaction rates of reaction network 1, 2 and 3 and their relative estimated reaction rate constants

	Reaction rates	**Reaction rate constants [s^{-1}]**	**Standard error [s^{-1}]**
Reaction network 1 (fructose)	$C_{FRU}(t) = c_{0,F}e^{-t\,k_{1,F}}$ $C_{HMF}(t) = \frac{c_{0,F}k_{1,F}}{k_{1,F}-k_{2,F}-k_{3,F}}\left[e^{-t(k_{2,F}+k_{3,F})} - e^{-t\,k_{1,F}}\right]$ $C_{LevA}(t) = \frac{c_{0,F}k_{2,F}}{k_{2,F}+k_{3,F}} - \frac{c_{0,F}k_{2,F}}{(-k_{1,F}+k_{2,F}+k_{3,F})(k_{2,F}+k_{3,F})}\left[-k_{1,F}e^{-t(k_{2,F}+k_{3,F})} - (k_{2,F}+k_{3,F})e^{-t\,k_{1,F}}\right]$ $C_{HTC}(t) = \frac{c_{0,F}k_{3,F}}{k_{2,F}+k_{3,F}} - \frac{c_{0,F}k_{3,F}}{(-k_{1,F}+k_{2,F}+k_{3,F})(k_{2,F}+k_{3,F})}\left[-k_{1,F}e^{-t(k_{2,F}+k_{3,F})} - (k_{2,F}+k_{3,F})e^{-t\,k_{1,F}}\right]$	$k_{1,F}$ 7.6 · 10-5 $k_{2,F}$ 1.4 · 10-5 $k_{3,F}$ 4.3 · 10-5	2.4 · 10-5 6.6 · 10-6 2.7 · 10-5
Reaction network 2 (glucose)	$C_{GLU}(t) = c_{0,G}e^{-k_{1,G}\,t}$ $C_{HMF}(t) = \frac{c_{0,G}k_{1,G}}{k_{1,G}-k_{2,G}-k_{3,G}}\left[e^{-t(k_{2,G}+k_{3,G})} - e^{-k_{1,G}\,t}\right]$ $C_{LevA}(t) = \frac{c_{0,G}k_{2,G}}{k_{2,G}+k_{3,G}} - \frac{c_{0,G}k_{2,G}}{(-k_{1,G}+k_{2,G}+k_{3,G})(k_{2,G}+k_{3,G})}\left[-k_{1,F}e^{-t(k_{2,F}+k_{3,F})} - (k_{2,F}+k_{3,F})e^{-k_{1,F}\,t}\right]$ $C_{HTC}(t) = \frac{c_{0,G}k_{3,G}}{k_{2,G}+k_{3,G}} - \frac{c_{0,G}k_{3,G}}{(-k_{1,G}+k_{2,G}+k_{3,G})(k_{2,G}+k_{3,G})}\left[-k_{1,F}e^{-t(k_{2,F}+k_{3,F})} - (k_{2,F}+k_{3,F})e^{-k_{1,F}\,t}\right]$	$k_{1,G}$ 1.8 · 10-5 $k_{2,G}$ 1.7 · 10-5 $k_{3,G}$ 7.7 · 10-5	5.7 · 10-6 7.8 · 10-6 1.7 · 10-5
Reaction network 3 (xylose)	$C_{XYL}(t) = c_{0,X}e^{-k_{1X}\,t}$ $C_{FF}(t) = \frac{c_{0,X}k_{1,X}}{k_{1,X}-k_{2,X}}[e^{-t\,k_{2,X}} - e^{-t\,k_{1,X}}]$ $C_{HTC}(t) = c_{0,X} - \frac{c_{0,X}}{-k_{1,X}+k_{2,X}}\left[-k_{1,X}e^{-t\,k_{2,X}} + k_{2,X}e^{-t\,k_{1,X}}\right]$	$k_{1,X}$ 3.9 · 10-5 $k_{2,X}$ 3.7 · 10-5	1.1 · 10-5 4.5 · 10-6

Conclusions and outlook

The aim of this thesis was to elucidate the mechanisms of hydrothermal conversion of sugars and understand how different reaction parameters affect the yields of conversion of water-soluble products and the chemistry and morphology of HT carbon.

The three monosaccharides chosen for this study were fructose, glucose and xylose. Glucose is a model molecule to understand the mechanism of cellulosic biomass conversion. Fructose is strictly related to glucose and, according to current understanding of hydrothermal carbonization mechanisms, isomerization of glucose to fructose is a supposedly obliged step of the glucose conversion. Therefore, fructose allows to evaluate the reactivity of a hexose in a simplified model that skips the isomerization step. Xylose, instead, was chosen to model the behaviour of C_5 sugars-containing hemicellulose.

All three monosaccharides were tested in plain water against increasing reaction time (2-12 h), in order to trace a profile of how soluble and insoluble product yields evolve through time. Fructose and glucose conversions were also tested in presence of strong acid catalysts (sulfuric acid, nitric acid, hydrochloric acid, hydrobromic acid and hydroiodic acid) at a fixed reaction time (3 h) and an initial pH value of 1.5 in order to differentiate the contribution of acid catalysis on a ketose and an aldose. Finally, the hydrothermal reactivity of fructose was also tested in presence of different headspace feed gas (air, N_2 and CO_2), each one at two levels of pressure (1 bar and 2 bar).

Fructose conversion in hydrothermal conditions proved to be relatively fast. Complete conversion in plain water is achieved after 3 h. HMF yields peaks at 3 h reaching a value of 52.7% and declines very fast, disappearing from the reaction medium after 4 h. Its decline is connected to the appearance of LevA, FA and HT carbon.

No unreacted fructose and no HMF were detected when the experiments were performed in presence of strong acids and a strong increase in the LevA and FA was observed. On the contrary, HT carbon yields were similar to those observed, suggesting that HMF rehydration to LevA is more pH-dependent that HT carbon formation. Also, notably, the nature of the acid

employed as catalyst does not seem to have a great impact on the product yields, indicating that fructose and HMF are too reactive to appreciate any anion effect in their conversion.

Pressure experiments demonstrated that a slight increase in the starting pressure leads to an increase in the total yields; moreover, a CO_2 atmosphere causes the same changes in the product yields observed with strong acids, that is a decrease of HMF and an increased production of LevA and FA, proving to act as a weak acid catalyst.

Fructose-derived HT carbon shows the well-known morphology of carbon spheres and, from a chemical point of view, it is composed of heteroaromatic structures and aliphatic linkers with abundant ketone and carboxylic functionalities. The increase of reaction time leads to some structural changes, such as evidences of cross-linking between furan units and a more condensed character. From a morphological point of view, this is reflected to a growth in the particle diameter and an extensive agglomeration of particles. Acid catalysis does not affect the chemical structure of the particle but it leads to a great increase of their average diameter. MALDI-ToF mass spectrometry of the THF-soluble fraction of HT carbon showed the existence of a group of oligomers in a mass range between 600 Da and 1500 Da with a regular mass increase 211 Da. This finding suggest that insoluble HT carbon may originate from the growth and precipitation of HMF-derived polymers with a well-defined structure.

Glucose hydrothermal conversion observed as a function of reaction time clarifies that glucose conversion in plain water is comparatively much slower than fructose conversion. Complete conversion is achieved after 6 h and the highest yield of HMF (15.9%) is found at 4 h. Since fructose is detected as a product in this conversion, these observations confirm that glucose dehydration proceeds via a slow step of isomerization to fructose. The extra step of conversion required by glucose can be appreciated by addition of strong acid catalysts. In this case, in fact, besides the obvious acceleration of glucose conversion in presence of strong acids, we were able to observe differences in product yields among different acids, as an effect of the anion. Larger anions, with better leaving group qualities such as sulfate or iodide led to a greater glucose conversion, suggesting that anions might play a role in stabilizing or destabilizing the transition states in the dehydration reaction.

Glucose-derived HT carbon appears to be morphologically and structurally very similar to fructose HT carbon; moreover, they show a similar evolution in function of reaction time to a more condensed and cross-linked structure. The smaller mean diameter of the particles is consistent with the hypothesis that the rate of particle growth is connected to HMF concentration. As further evidence to support this hypothesis, glucose-derived HT carbon particles in presence of acid catalyst have a diameter that is similar the fructose-HT particles obtained in analogous conditions. MALDI-ToF analysis revealed again the presence of a family of oligomers in a mass range of 1000 Da to 1800 Da. A comparison with previous literature allowed for a tentative identification of the monomer. The hypothetical structure is similar to the one identified from fructose HT carbon whose structure is compatible with FT-IR and NMR spectra and similar to the hypothetical monomer identified in hydrothermal conversion of fructose.

The study of xylose conversion in plain water highlights that the structural differences of this sugar with the two hexoses previously studied has a profound impact on its reactivity and the properties and behaviours of the related products. Xylose conversion is kinetically slightly faster than glucose and slower than fructose. The reduced presence of other chemical species also indicates that FF, the dehydration product of xylose, is a less unstable and reactive molecule than HMF. HT carbon also forms in lesser amount. As a consequence, FF has a more pronounced tendency to accumulate in the reaction medium when compared to HMF.

Microscopic observations of the xylose-derived HT carbon show that the carbon spheres appear to be more regular and with a reduced tendency to agglomerate at longer reaction times. Investigations on the chemical structure of this HT carbon shows many similarities with C_6 sugars-derived HT carbons and an important difference: a more condensed character that can be ascribed to a free furfural C_α making a ring-ring coupling possible, with the formation of an extensive conjugated system. MALDI-ToF mass spectrometry of this material showed some large molecules in the mass range between 800 Da and 1500 Da.

The results of this study clarify the chemical relationship between glucose and fructose in hydrothermal conditions. Glucose and fructose belong to the same chemical pathway. The

modelling of experimental data confirms that glucose conversion is kinetically slower than fructose conversion. The reason of this lies in the isomerization step of glucose to fructose, a kinetically slow step that hinders glucose conversion and all subsequent transformations. This step is catalysed by acids and anions can contribute to stabilization of transition states. Fructose and HMF are relatively unstable and fast reacting species, particularly in acidic conditions. Among the two main HMF-consuming reactions, rehydration to LevA is more dependent to pH than HT carbon formation. These findings confirm previous studies and suggest future directions to investigate in order to furtherly optimize the process of biomass conversion. If HMF is the target molecule, a multi-stage hydrothermal conversion of cellulose that divides the process in cellulose hydrolysis to glucose, glucose isomerization to fructose, followed by fructose dehydration to HMF, might be a way to maximize yields and thus compensate for the rise of production costs. LevA production might allow a less strict control of the reaction phases, due to the greater chemical stability of this species, but the formation of HT carbon as unwanted by-product should be kept in control. In any case, the choice of adequate acid catalyst for each phase of the conversion is extremely important: this study showed the combination of a weak acid like CO_2 and a pressurized environment could have a beneficial effect in terms of sugar conversion and more research should be dedicated to this topic. Finally, it is advisable to focus more attention in future research on the importance of other secondary reaction pathways such as retro-aldol condensation of sugars, with formation of C_2, C_3 C_4 saccharides and subsequent oxidations or rearrangements, on the overall conversion of C_6 and C_5 saccharides.

The results of morphological and structural analysis of fructose, glucose and xylose are in good agreement with previous studies on this topic, but they also underline a probably overlooked aspect of this material, that is its tendency to evolve in time under the effect of prolonged exposure to reaction conditions. Future development of industrial or energetic applications for this material should hold this aspect in consideration, in the perspective of a fine tuning of HT carbon chemical properties.

Moreover, the identification of groups of oligomers with a repetitive chemical structure is a promise for a definitive and unambiguous identification of the chemical structure of HT carbon, which, in turn, will potentially allow for a stricter and more tailored control of its

chemical and physical properties. Of course, more research is needed in this direction. Tandem mass spectrometry can be employed to identify the real chemical structure of these oligomers. Furtherly, once the chemical structures of the oligomers and the monomer are known, the existence of a real causal relationship between these species and HT carbon should be assessed. A comparison between an empirical formula of HT carbon, obtained from elemental analysis data and the chemical structure of the monomer would show if the former can be interpreted as a polymeric form of the latter. Moreover, a laboratorial synthesis of the supposed monomer and its exposure to hydrothermal conditions should clarify if there is an actual formation of HT carbon-like materials.

In the perspective of translating the information gathered in the present study to more complex matrices such as real biomass, we must consider the possibility of interaction between different sugars in the reaction medium. In principle, it is possible to hypothesize of some sort of interaction and cross-condensation that could potentially decrease the yield of conversion to more desirable products such as HMF and levulinic acid. A study on the impact of a cross-condensation reactions between glucose and fructose was covered in two independent studies, by Tan-Soetedjo and Steinbach.[63], [242] In the study by Tan-Soetedjo, an equimolar mixture of glucose and fructose was subject of hydrothermal conversion, whereas Steinbach calculated the amount fraction of products in a mixture by combining the results obtained by independent hydrothermal conversion of glucose and sucrose. Both theoretical and experimental results showed that hydrothermal conversion of sucrose can be described by the conversion of glucose and fructose behaving independently from each other and cross-reactions do not take place to a considerable extent. These results are promising as they suggest that that no significant interaction will take place between other sugars in hydrothermal conditions. This hypothesis however needs to be verified by experimental observations, especially in the perspective of hydrothermal of real biomass, where a mixture of different sugars is very likely to form in the reaction medium.

From the point of view of reaction times, an investigation on hydrothermal conversion of more complex substrates like polysaccharides or real biomass would see all reaction steps described in this study shifted to larger times. In fact, hydrothermal conversion of real biomass will require the hydrolysis of large bundles of polymeric fibres. Lu and Berge

showed than predicting properties of hydrothermal products based on the feedstock composition only provides satisfactory results in few cases, like energy content of solid products.[244] Other properties, such as functional groups, are much more influenced by increasing complexity of the substrate and are not very well predicted by the sum of individual components. It is probable that some of the deviations of physical or chemical properties from those derived from pure compounds arises from the hindered access of water to large bundles of fibres, triggering pyrolysis reactions that greatly change the chemistry of the system. Starch for example, among the polymers of glucose, when subject of hydrothermal treatment, behaves in a similar way to its monomer,[31], [240] producing carbon spheres that are very close in morphology and chemical structure to those obtained by hydrothermal carbonization of glucose. Cellulose, on the other hand, due to its insolubility in water and extended and compact crystalline structure, only undergoes heterogeneous hydrolysis on the surface of fibres that are in contact with the water medium; the inner part of the fibres which is not exposed to water, undergoes pyrolysis.[49] Paksung compared the behaviour of microcrystalline cellulose and alpha cellulose and demonstrated that a higher degree of polymerization of cellulose is a major hindrance to the heterogeneous hydrolysis of cellulose.[245] Therefore it is advisable, in order to more easily translate the information gathered on hydrothermal carbonization of pure saccharides, to design a multi-steps process where depolymerization and hydrolysis are treated separately from dehydration reactions.

Chapter 5 Experimental methods

Preparation of aqueous and solid samples

D-(+)-glucose (99.5%), D-(-)-fructose (99%), D(+)-xylose (99%) levulinic acid (98%), formic acid, 5-hydroxymethyl-furfural (99%), Furfural (99%), sulfuric acid (98%), nitric acid (65%), hydrobromic acid (48%) and hydroiodic acid (57%) were obtained from Sigma-Aldrich Corp. Hydrochloric acid (37%) was obtained from VWR Chemicals. A typical experiment involved the preparation of 150 mL of a 10% w/w fructose. The solution was then transferred to a 200 mL Teflon-lined stainless-steel autoclave and heated in an oven to a temperature of 200 °C. After the target temperature was reached, it was kept for a variable amount of time, ranging from 2 h to 12 h. In catalyzed reactions, an adequate volume of concentrated acid (H_2SO_4, HNO_3, HCl, HBr, HI) was added in order to reach a targeted pH of 1.5. In these cases, the reaction time was 3 h. After reaching the desired reaction time, reaction was quenched by immersing the autoclave into icy water. Then, the reaction medium was vacuum-filtered to separate the aqueous phase from the solid, brownish-black solid precipitate of hydrothermal carbon. Occasionally, when precipitate was too finely dispersed, a centrifugation step (14500 rpm for 30 min) was required before filtration to separate it from the solution. The solution was then collected and analyzed via HPLC. The precipitate was washed several times with hot deionized water, until the washing solution was neutral. Finally, the HTC powder collected was dried at 80 °C overnight and then weighed and stored for further analysis. A series of experiments involving pressure and atmosphere control as described below was carried out using a Parr 5513 100 mL reactor filled with 40 ml of 10% w/w fructose solution. The reactor was filled with air, N2 or CO2, under atmospheric pressure or slight overpressure (2 bar). The system was heated to 200 °C in 45 minutes and then kept at the same temperature for 2 h. The solution was subsequently allowed to cool down to room temperature and analyzed via HPLC. The amount of HT carbon formed was not taken into account in this last series of experiments. In this reactor, in fact, the HT carbon deposited as a thick layer on the reactor walls and stirrer instead of precipitating as a fine powder. Its quantitative recovery was deemed to be unreliable both with mechanic methods and chemical dissolution with strong bases that would have

partially dissolved the carbon and altered its chemical properties. Therefore, HT carbon yields were omitted from the subsequent calculations. Each experiment in this study was performed in duplicate.

Analysis of aqueous phase

Samples were analyzed through HPLC analysis on an Agilent LC 1260 Infinity II system equipped with 1260 Infinity II variable wavelength detector and 1260 Infinity II RI detector. Separation of the complex mixture of soluble products was performed with an Aminex HPX-87H column, using 5 mM H_2SO_4 as the mobile phase at a flow rate of 0.6 mL min^{-1}, at a working temperature of 65 °C and detected through UV (254 nm) and RI detector. All analytes were quantified by means of a calibration curve.

Uncertainties on measurements

Each experiment was performed in double. The uncertainties associated with molar yields shown in **Tables 3**, **Table 4**, **Table 7** and **Table 11** were calculated as square root of sum of the squares of uncertainty of the average of two measurements and the uncertainties derived from the calibration curve as shown in **Equation 30**.

$$\sigma_{i,tot} = \sqrt{\sigma_{i,cal1}^2 + \sigma_{i,cal2}^2 + \sigma_{i,av}^2} \quad (\mathbf{30})$$

The sums of product yields ($m_i/m_{precursor}$) and unreacted precursor ($m_{p,u}/m_{precursor}$, if present) (**Equation 31**) along with their uncertainties are shown in **Tables 13**, **Table 14** and **Table 15.** The uncertainty of each sum is calculated as square root of the sum of squared uncertainty of each addend.

$$sum\ [\%] = \frac{\sum m_i + m_{p,u}}{m_{precursor}} \cdot 100 \quad (\mathbf{31})$$

Table 13 *Sum of product yields and unreacted precursors with uncertainties in reaction time experiments*

	2h		3h		4h		6h		12h	
	Sum [%]	u/c (k=1) [%]	Sum [%]	u/c (k=1) [%]	Sum [%]	u/c (k=1) [%]	Sum [%]	u/c (k=1) [%]	Sum [%]	u/c (k=1) [%]
glucose	105	7	107	5	105	2	100	8	96	1
fructose	105	2	118	14	106	6	105	8	111,8	0,9
xylose	95,8	0,3	91	1	90	12	80	7	78,4	0,5

Slight deviations from theoretical 100% (**Table 13**) can be ascribed to:

- Propagation of error;
- Estimate of molar yield of HTC based on the assumption of a chemical structure of a polymer of HMF units (fructose and glucose) and furfural units (xylose);
- Unspecified and therefore not quantified conversion products.

Table 14 *Sum of product yields and unreacted precursors with uncertainties in reaction acid catalysis experiments*

	H_2SO_4		HNO_3		HCl		HBr		HI	
	Sum [%]	u/c (k=1) [%]	Sum [%]	u/c (k=1) [%]	Sum [%]	u/c (k=1) [%]	Sum [%]	u/c (k=1) [%]	Sum [%]	u/c (k=1) [%]
glucose	120	9	112	13	113	15	115	6	128	13
fructose	153,2	0,3	148	8	151,9	0,3	151	5	159,8	0,8

Table 14 shows larger deviations from theoretical 100%, despite uncertainties comparatively similar to those of the time experiments, pointing out to a systematic error. These deviations were likely caused by loss of water vapour during reaction, resulting in a more concentrated final solution and an overestimation of the concentration of water-soluble products. The loss of water vapour was caused by a limitation of the employed reactors that could not sustain higher pressures reached in the acid-catalyzed systems.

Table 15 *Sum of product yields and unreacted precursors with uncertainties in reaction acid catalysis experiments*

	1 bar		2 bar		1 bar		2 bar		1 bar		2 bar	
	Sum [%]	u/c (k=1) [%]	Sum [%]	u/c (k=1) [%]	Sum [%]	u/c (k=1) [%]	Sum [%]	u/c (k=1) [%]	Sum [%]	u/c (k=1) [%]	Sum [%]	u/c (k=1) [%]
fructose	27,6	0,8	31	2	29	3	34	8	28	2	30	3

Table 15 shows the sums of products yields and unreacted precursors in the feed gas series of experiments. In this case, the hydrothermal carbon was not measured and therefore the sums only account for the water-soluble products.

Analysis of hydrothermal carbon

FT-IR

Fourier transform infrared spectroscopy (FT-IR) is an analytical technique to investigate the chemical structures of compounds and materials. The principle of this technique is the ability of infrared radiation of being absorbed by the sample at given frequencies corresponding to vibrational states of the molecule investigation.[246]

FTIR spectra were obtained from powder samplers using a Bruker Tensor 27 FTIR spectrometer equipped with ATR (attenuated total reflectance) detector in the range of 400 to 4000 cm^{-1}, with scan rate of 20 scans min^{-1}

Solid state ^{13}C NMR

Nuclear Magnetic Resonance (NMR) spectroscopy is a powerful technique to investigate individual atoms, molecules as well as structural and dynamic information. NMR exploits the physical property of atom nuclei with non-zero spin to align to an external magnetic field and develop different energy levels. By perturbing this alignment with a radiofrequency pulse and detecting the waves emitted by nuclei in response to this perturbation, we are able to collect information about the chemical environment of each atom. In fact, the total magnetic field experienced by a nucleus includes local magnetic fields induced by electrons in the molecular orbitals, which varies according to the local geometry and affecting the spin energy levels (and resonance frequencies). The different frequencies of the same kind of nucleus due to the variation in electron distribution results in chemical shifts, which are diagnostic to the chemical structure, and the size of the shift is relative to a standard in a magnetic field.[247]

In solid-state NMR, anisotropic interactions modify the resonance frequency of all sites in the material and often contribute to a line-broadening effect in NMR spectra. Different

acquisition methods have been developed to reduce the large anisotropic interactions between nuclei and to increase the signal to noise ratio (S/N), such as cross-polarisation (CP), magic angle spinning (MAS) and two-dimensional phase adjusted spinning sidebands (2D-PASS). SS-NMR ^{13}C CP-MAS spectra were obtained on Bruker AV600 NEO Spectrometer.

Scanning electron microscopy

Electron microscopy is a useful tool to study the morphology and structure of carbon materials. SEM images are obtained by means of a focused electron beam that is used to illuminate/image the sample. The electron beam is scattered from the atoms contained in the sample. The scattered electrons are detected and converted into an image. Due to electrons being readily absorbed by air, electron microscopy is carried out under ultrahigh vacuum.[248] A schematic of the main working components of a scanning electron microscope can be seen in **Figure 25**.

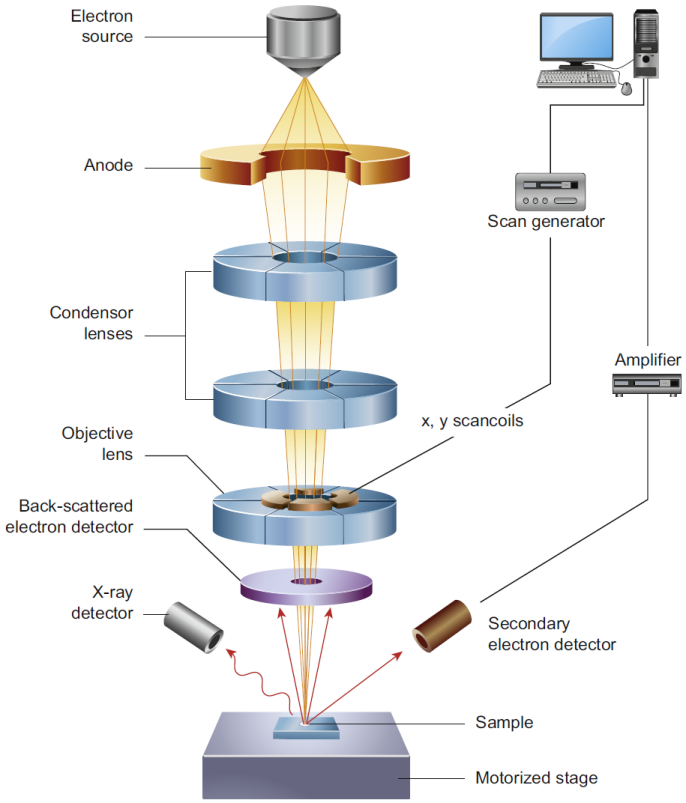

Figure 25 *Schematic of the working components of a scanning electron microscope. Reproduced from Inkson,*[249] *Copyright 2016 Elsevier.*

Micrograph images were obtained with FEI Quanta 3D Scanning Electron Microscope (SEM). Powder samples were supported on sticky carbon tape on top of a steel stub and sputter coated with gold.

MALDI-ToF Mass Spectrometry

Mass spectrometry is an analytical technique that analyzes mass-to-charge molecular fragments or molecular ions of a sample in order to get information about the chemical structure of the sample. A mass spectrometer must include a source of ions and a detector. Time of flight is a type of detector used in mass spectrometry that is able to discriminate between different ions by measuring the time that they need to reach the sensor, which is a function of their mass. Matrix-assisted laser desorption ionization is a soft ionization technique based on the use on a laser to cause "soft" desorption of ions from a matrix.[250]

Samples were run on a Micromass MALDI-ToF mass spectrometer operating in linear positive mode (pulse 800, detector 2300, N_2 laser 337 nm). 1 mg of sample was dissolved into 0.5 ml of THF. 5 µL was removed and 5 µL of CHCA (10 mg mL^{-1} in 50:50 water:acetonitrile) was added. Sample was vortexed for 30 s and then 1 µL of the mixture was spotted onto the MALDI plate. Sample was left to air dry. Where necessary, samples were re-spotted and again left to air dry.

Chapter 6 References

[1] N. Watts *et al.*, "The 2018 report of the Lancet Countdown on health and climate change: shaping the health of nations for centuries to come," *The Lancet*, vol. 392, no. 10163, pp. 2479–2514, 2018.

[2] A. L. Burrell, J. P. Evans, and M. G. de Kauwe, "Anthropogenic climate change has driven over 5 million km2 of drylands towards desertification," *Nat Commun*, vol. 11, no. 1, pp. 1–11, 2020.

[3] R. S. Nerem, B. D. Beckley, J. T. Fasullo, B. D. Hamlington, D. Masters, and G. T. Mitchum, "Climate-change–driven accelerated sea-level rise detected in the altimeter era," *Proceedings of the national academy of sciences*, vol. 115, no. 9, pp. 2022–2025, 2018.

[4] S. Kabasci, "Biobased plastics," in *Plastic waste and recycling*, Elsevier, 2020, pp. 67–96.

[5] A. J. Hunt, *Element recovery and sustainability*, no. 22. Royal Society of Chemistry, 2013.

[6] T. J. Brown, R. A. Shaw, T. Bide, E. Petravratzi, E. R. Raycraft, and A. S. Walters, *World mineral production 2007-11*. British Geological Survey, 2013.

[7] J. Xie and Y.-C. Lu, "A retrospective on lithium-ion batteries," *Nat Commun*, vol. 11, no. 1, pp. 1–4, 2020.

[8] H. Vikström, S. Davidsson, and M. Höök, "Lithium availability and future production outlooks," *Appl Energy*, vol. 110, pp. 252–266, 2013.

[9] R. S. Kalyoncu and H. A. Taylor Jr, "Natural graphite," in *Kirk-Othmer Encyclopedia of Chemical Technology*, 2000.

[10] B. Khassab, "The paradox of sustainability in the extraction of''green minerals''from highly volatile contexts: A case study of graphite mining in Cabo Delgado province, Mozambique," 2021.

[11] N. Savage, "Fuel options: the ideal biofuel," *Nature*, vol. 474, no. 7352, pp. S9–S11, 2011.

[12] L. Reijnders, "Conditions for the sustainability of biomass based fuel use," *Energy Policy*, vol. 34, no. 7, pp. 863–876, 2006, doi: https://doi.org/10.1016/j.enpol.2004.09.001.

[13] J. Hill, E. Nelson, D. Tilman, S. Polasky, and D. Tiffany, "Environmental, economic, and energetic costs and benefits of biodiesel and ethanol biofuels," *Proceedings of the national academy of sciences*, vol. 103, no. 30, pp. 11206–11210, 2006.

[14] S. N. Gebremariam and J. M. Marchetti, "Economics of biodiesel production," *Energy Convers Manag*, vol. 168, pp. 74–84, 2018.

[15] R. Geyer, "Earth and Plastic," in *Earth 2020. An Insider's Guide to a Rapidly Changing Planet*, P. Tortell, Ed. OpenBook Publishers, 2020, pp. 213–220.

[16] T. D. Nielsen, J. Hasselbalch, K. Holmberg, and J. Stripple, "Politics and the plastic crisis: A review throughout the plastic life cycle," *Wiley Interdiscip Rev Energy Environ*, vol. 9, no. 1, p. e360, 2020.

[17] M. MacLeod, H. P. H. Arp, M. B. Tekman, and A. Jahnke, "The global threat from plastic pollution," *Science (1979)*, vol. 373, no. 6550, pp. 61–65, 2021.

[18] M.-M. Titirici, A. Funke, and A. Kruse, "Hydrothermal carbonization of biomass," in *Recent advances in Thermo-chemical conversion of biomass*, Elsevier, 2015, pp. 325–352.

[19] Q. Wang, H. Li, L. Chen, and X. Huang, "Monodispersed hard carbon spherules with uniform nanopores," *Carbon N Y*, vol. 39, no. 14, pp. 2211–2214, 2001.

[20] X. Sun and Y. Li, "Colloidal carbon spheres and their core/shell structures with noble-metal nanoparticles," *Angewandte Chemie*, vol. 116, no. 5, pp. 607–611, 2004.

[21] M. M. Titirici, A. Thomas, and M. Antonietti, "Back in the black: Hydrothermal carbonization of plant material as an efficient chemical process to treat the CO2problem?," *New Journal of Chemistry*, vol. 31, no. 6, pp. 787–789, 2007, doi: 10.1039/b616045j.

[22] A. Kruse and N. Dahmen, "Hydrothermal biomass conversion: Quo vadis?," *J Supercrit Fluids*, vol. 134, pp. 114–123, 2018.

[23] Y. Shen, "A review on hydrothermal carbonization of biomass and plastic wastes to energy products," *Biomass Bioenergy*, vol. 134, p. 105479, 2020.

[24] J. Pérez, J. Munoz-Dorado, T. de la Rubia, and J. Martinez, "Biodegradation and biological treatments of cellulose, hemicellulose and lignin: an overview," *International microbiology*, vol. 5, no. 2, pp. 53–63, 2002.

[25] J. Ralph, C. Lapierre, and W. Boerjan, "Lignin structure and its engineering," *Curr Opin Biotechnol*, vol. 56, pp. 240–249, 2019, doi: https://doi.org/10.1016/j.copbio.2019.02.019.

[26] M.-M. Titirici and M. Antonietti, "Chemistry and materials options of sustainable carbon materials made by hydrothermal carbonization," *Chem Soc Rev*, vol. 39, no. 1, pp. 103–116, 2010.

[27] T. Werpy and G. Petersen, "Top value added chemicals from biomass: volume I--results of screening for potential candidates from sugars and synthesis gas," National Renewable Energy Lab., Golden, CO (US), 2004.

[28] S. Román, J. M. v Nabais, C. Laginhas, B. Ledesma, and J. F. González, "Hydrothermal carbonization as an effective way of densifying the energy content of biomass," *Fuel Processing Technology*, vol. 103, pp. 78–83, 2012, doi: https://doi.org/10.1016/j.fuproc.2011.11.009.

[29] A. Álvarez-Murillo, S. Román, B. Ledesma, and E. Sabio, "Study of variables in energy densification of olive stone by hydrothermal carbonization," *J Anal Appl Pyrolysis*, vol. 113, pp. 307–314, 2015.

[30] J. A. Rice and P. MacCarthy, "Comments on the literature of the humin fraction of humus," *Geoderma*, vol. 43, no. 1, pp. 65–73, 1988.

[31] M.-M. Titirici, M. Antonietti, and N. Baccile, "Hydrothermal carbon from biomass: a comparison of the local structure from poly-to monosaccharides and pentoses/hexoses," *Green Chemistry*, vol. 10, no. 11, pp. 1204–1212, 2008.

[32] C. Falco, N. Baccile, and M. M. Titirici, "Morphological and structural differences between glucose, cellulose and lignocellulosic biomass derived hydrothermal carbons," *Green Chemistry*, vol. 13, no. 11, pp. 3273–3281, 2011, doi: 10.1039/c1gc15742f.

[33] S. A. Nicolae, P. Á. Szilágyi, and M. M. Titirici, "Soft templating production of porous carbon adsorbents for CO2 and H2S capture," *Carbon N Y*, vol. 169, pp. 193–204, 2020, doi: https://doi.org/10.1016/j.carbon.2020.07.064.

[34] Z. C. Yang *et al.*, "Intrinsically fluorescent carbon dots with tunable emission derived from hydrothermal treatment of glucose in the presence of monopotassium phosphate," *Chemical Communications*, vol. 47, no. 42, pp. 11615–11617, 2011, doi: 10.1039/c1cc14860e.

[35] S. Sahu, B. Behera, T. K. Maiti, and S. Mohapatra, "Simple one-step synthesis of highly luminescent carbon dots from orange juice: application as excellent bio-imaging agents," *Chemical communications*, vol. 48, no. 70, pp. 8835–8837, 2012.

[36] X. T. Zheng, A. Ananthanarayanan, K. Q. Luo, and P. Chen, "Glowing graphene quantum dots and carbon dots: properties, syntheses, and biological applications," *small*, vol. 11, no. 14, pp. 1620–1636, 2015.

[37] S. C. Ray, A. Saha, N. R. Jana, and R. Sarkar, "Fluorescent carbon nanoparticles: synthesis, characterization, and bioimaging application," *The Journal of Physical Chemistry C*, vol. 113, no. 43, pp. 18546–18551, 2009.

[38] S. N. Baker and G. A. Baker, "Luminescent Carbon Nanodots: Emergent Nanolights," *Angewandte Chemie International Edition*, vol. 49, no. 38, pp. 6726–6744, 2010, doi: https://doi.org/10.1002/anie.200906623.

[39] Y. Chen, Y. Wu, B. Weng, B. Wang, and C. Li, "Facile synthesis of nitrogen and sulfur co-doped carbon dots and application for Fe(III) ions detection and cell imaging,"

Sens Actuators B Chem, vol. 223, pp. 689–696, 2016, doi: https://doi.org/10.1016/j.snb.2015.09.081.

[40] N. Wang, Y. Wang, T. Guo, T. Yang, M. Chen, and J. Wang, "Green preparation of carbon dots with papaya as carbon source for effective fluorescent sensing of Iron (III) and Escherichia coli," *Biosens Bioelectron*, vol. 85, pp. 68–75, 2016.

[41] T. N. J. I. Edison, R. Atchudan, J. J. Shim, S. Kalimuthu, B. C. Ahn, and Y. R. Lee, "Turn-off fluorescence sensor for the detection of ferric ion in water using green synthesized N-doped carbon dots and its bio-imaging," *J Photochem Photobiol B*, vol. 158, pp. 235–242, 2016, doi: 10.1016/j.jphotobiol.2016.03.010.

[42] J. Liao, Z. Cheng, and L. Zhou, "Nitrogen-doping enhanced fluorescent carbon dots: green synthesis and their applications for bioimaging and label-free detection of Au3+ ions," *ACS Sustain Chem Eng*, vol. 4, no. 6, pp. 3053–3061, 2016.

[43] M. Jahanbakhshi and B. Habibi, "A novel and facile synthesis of carbon quantum dots via salep hydrothermal treatment as the silver nanoparticles support: Application to electroanalytical determination of H2O2 in fetal bovine serum," *Biosens Bioelectron*, vol. 81, pp. 143–150, 2016.

[44] J. Li, L. Zhang, P. Li, Y. Zhang, and C. Dong, "One step hydrothermal synthesis of carbon nanodots to realize the fluorescence detection of picric acid in real samples," *Sens Actuators B Chem*, vol. 258, pp. 580–588, 2018.

[45] Y. Guo, L. Yang, W. Li, X. Wang, Y. Shang, and B. Li, "Carbon dots doped with nitrogen and sulfur and loaded with copper(II) as a 'turn-on' fluorescent probe for cystein, glutathione and homocysteine," *Microchimica Acta*, vol. 183, no. 4, pp. 1409–1416, 2016, doi: 10.1007/s00604-016-1779-6.

[46] R. Atchudan, T. N. J. I. Edison, S. Perumal, and Y. R. Lee, "Green synthesis of nitrogen-doped graphitic carbon sheets with use of Prunus persica for supercapacitor applications," *Appl Surf Sci*, vol. 393, pp. 276–286, 2017, doi: 10.1016/j.apsusc.2016.10.030.

[47] H. W. Blanch, B. A. Simmons, and D. Klein-Marcuschamer, "Biomass deconstruction to sugars," *Biotechnol J*, vol. 6, no. 9, pp. 1086–1102, Sep. 2011, doi: https://doi.org/10.1002/biot.201000180.

[48] Y. Matsumura *et al.*, "Supercritical water treatment of biomass for energy and material recovery," *Combustion Science and Technology*, vol. 178, no. 1–3, pp. 509–536, 2006.

[49] F. Buendia-Kandia, G. Mauviel, E. Guedon, E. Rondags, D. Petitjean, and A. Dufour, "Decomposition of cellulose in hot-compressed water: detailed analysis of the products and effect of operating conditions," *Energy & Fuels*, vol. 32, no. 4, pp. 4127–4138, 2017.

[50] A. Funke and F. Ziegler, "Hydrothermal carbonization of biomass: a summary and discussion of chemical mechanisms for process engineering," *Biofuels, Bioproducts and Biorefining*, vol. 4, no. 2, pp. 160–177, 2010.

[51] S. K. Hoekman, A. Broch, and C. Robbins, "Hydrothermal carbonization (HTC) of lignocellulosic biomass," *Energy & Fuels*, vol. 25, no. 4, pp. 1802–1810, 2011.

[52] M. Nagamori and T. Funazukuri, "Glucose production by hydrolysis of starch under hydrothermal conditions," *Journal of Chemical Technology & Biotechnology: International Research in Process, Environmental & Clean Technology*, vol. 79, no. 3, pp. 229–233, 2004.

[53] M. T. Reza, B. Wirth, U. Lüder, and M. Werner, "Behavior of selected hydrolyzed and dehydrated products during hydrothermal carbonization of biomass," *Bioresour Technol*, vol. 169, pp. 352–361, 2014.

[54] K. Nakason, B. Panyapinyopol, V. Kanokkantapong, N. Viriya-empikul, W. Kraithong, and P. Pavasant, "Characteristics of hydrochar and hydrothermal liquid products from hydrothermal carbonization of corncob," *Biomass Convers Biorefin*, vol. 8, no. 1, pp. 199–210, 2018.

[55] K. Nakason, B. Panyapinyopol, V. Kanokkantapong, N. Viriya-empikul, W. Kraithong, and P. Pavasant, "Characteristics of hydrochar and liquid fraction from hydrothermal carbonization of cassava rhizome," *Journal of the Energy Institute*, vol. 91, no. 2, pp. 184–193, 2018.

[56] K. Nakason, B. Panyapinyopol, V. Kanokkantapong, N. Viriya-empikul, W. Kraithong, and P. Pavasant, "Hydrothermal carbonization of unwanted biomass materials: Effect of process temperature and retention time on hydrochar and liquid fraction," *Journal of the Energy Institute*, vol. 91, no. 5, pp. 786–796, 2018, doi: https://doi.org/10.1016/j.joei.2017.05.002.

[57] X. Lu, P. Pellechia, J. R. V. ; Flora, and N. Berge, "Influence of reaction time and temperature on product formation associated with the hydrothermal carbonization of cellulose," *Bioresour Technol*, vol. 138, pp. 180–190, 2013.

[58] F. S. Asghari and H. Yoshida, "Dehydration of fructose to 5-hydroxymethylfurfural in sub-critical water over heterogeneous zirconium phosphate catalysts," *Carbohydr Res*, vol. 341, no. 14, pp. 2379–2387, 2006.

[59] S. K. R. Patil and C. R. F. Lund, "Formation and growth of humins via aldol addition and condensation during acid-catalyzed conversion of 5-hydroxymethylfurfural," *Energy and Fuels*, vol. 25, no. 10, pp. 4745–4755, 2011, doi: 10.1021/ef2010157.

[60] R. Becker, U. Dorgerloh, E. Paulke, J. Mumme, and I. Nehls, "Hydrothermal carbonization of biomass: major organic components of the aqueous phase," *Chem Eng Technol*, vol. 37, no. 3, pp. 511–518, 2014.

[61] M. T. Reza, E. Rottler, L. Herklotz, and B. Wirth, "Hydrothermal carbonization (HTC) of wheat straw: Influence of feedwater pH prepared by acetic acid and potassium hydroxide," *Bioresour Technol*, vol. 182, pp. 336–344, 2015.

[62] R. van Putten *et al.*, "Dehydration of different ketoses and aldoses to 5-hydroxymethylfurfural," *ChemSusChem*, vol. 6, no. 9, pp. 1681–1687, 2013.

[63] D. Steinbach, A. Kruse, J. Sauer, and P. Vetter, "Sucrose Is a Promising Feedstock for the Synthesis of the Platform Chemical Hydroxymethylfurfural," *Energies (Basel)*, vol. 11, no. 3, p. 645, 2018, [Online]. Available: https://www.mdpi.com/1996-1073/11/3/645

[64] C. A. L. de Bruyn and W. A. van Ekenstein, "Action des alcalis sur les sucres, II. Transformation réciproque des uns dans les autres des sucres glucose, fructose et mannose," *Recueil des Travaux Chimiques des Pays-Bas*, vol. 14, no. 7, pp. 203–216, 1895.

[65] J. C. Speck, "The Lobry De Bruyn-Alberda Van Ekenstein Transformation," in *Advances in Carbohydrate Chemistry*, vol. 13, M. L. Wolfrom, Ed. Academic Press, 1958, pp. 63–103. doi: https://doi.org/10.1016/S0096-5332(08)60352-5.

[66] H. Ost, "Umwandlung der Dextrose in Lävulose u. Nachweis der Lävulose," *Angewandte Chemie*, vol. 18, no. 30, pp. 1170–1174, 1905.

[67] D. W. Harris and M. S. Feather, "Mechanism of the interconversion of D-glucose, D-mannose, and D-fructose in acid solution," *J Am Chem Soc*, vol. 97, no. 1, pp. 178–181, 1975.

[68] R. S. Assary, T. Kim, J. J. Low, J. Greeley, and L. A. Curtiss, "Glucose and fructose to platform chemicals: understanding the thermodynamic landscapes of acid-catalysed reactions using high-level ab initio methods," *Physical Chemistry Chemical Physics*, vol. 14, no. 48, pp. 16603–16611, 2012, doi: 10.1039/C2CP41842H.

[69] L. Yang, G. Tsilomelekis, S. Caratzoulas, and D. G. Vlachos, "Mechanism of Brønsted Acid-Catalyzed Glucose Dehydration," *ChemSusChem*, vol. 8, no. 8, pp. 1334–1341, 2015, doi: https://doi.org/10.1002/cssc.201403264.

[70] A. E. Stütz, *Glycoscience: epimerisation, isomerisation and rearrangement reactions of carbohydrates*, vol. 215. Springer, 2003.

[71] J. Zhang and E. Weitz, "An in Situ NMR Study of the Mechanism for the Catalytic Conversion of Fructose to 5-Hydroxymethylfurfural and then to Levulinic Acid Using 13C Labeled d-Fructose," *ACS Catal*, vol. 2, no. 6, pp. 1211–1218, Jun. 2012, doi: 10.1021/cs300045r.

[72] A. S. Amarasekara, L. D. Williams, and C. C. Ebede, "Mechanism of the dehydration of d-fructose to 5-hydroxymethylfurfural in dimethyl sulfoxide at 150°C: an NMR study," *Carbohydr Res*, vol. 343, no. 18, pp. 3021–3024, 2008, doi: https://doi.org/10.1016/j.carres.2008.09.008.

[73] Y. Román-Leshkov, C. J. Barrett, Z. Y. Liu, and J. A. Dumesic, "Production of dimethylfuran for liquid fuels from biomass-derived carbohydrates," *Nature*, vol. 447, no. 7147, pp. 982–985, 2007.

[74] O. Casanova, S. Iborra, and A. Corma, "Biomass into chemicals: aerobic oxidation of 5-hydroxymethyl-2-furfural into 2, 5-furandicarboxylic acid with gold nanoparticle catalysts," *ChemSusChem: Chemistry & Sustainability Energy & Materials*, vol. 2, no. 12, pp. 1138–1144, 2009.

[75] E. de de Jong, M. A. Dam, L. Sipos, and G.-J. Gruter, "Furandicarboxylic acid (FDCA), a versatile building block for a very interesting class of polyesters," in *Biobased monomers, polymers, and materials*, ACS Publications, 2012, pp. 1–13.

[76] R. Beerthuis, G. Rothenberg, and N. R. Shiju, "Catalytic routes towards acrylic acid, adipic acid and ε-caprolactam starting from biorenewables," *Green Chemistry*, vol. 17, no. 3, pp. 1341–1361, 2015.

[77] J. J. Bozell and G. R. Petersen, "Technology development for the production of biobased products from biorefinery carbohydrates-the US Department of Energy's 'Top 10' revisited," *Green Chemistry*, vol. 12, no. 4, pp. 539–554, 2010.

[78] D. J. Hayes, J. Ross, M. H. B. Hayes, and S. Fitzpatrick, "The Biofine process: production of levulinic acid, furfural and formic acid from lignocellulosic feedstocks," *Biorefineries-Industrial Processes and Products*, vol. 1, 2005, doi: 10.1002/9783527619849.

[79] S. Krawielitzki, "AVA Biochem, Pioneer in Industrial Biobased Furan Chemistry," *CHIMIA International Journal for Chemistry*, vol. 74, no. 10, pp. 776–778, 2020.

[80] C. Rosenfeld, J. Konnerth, W. Sailer-Kronlachner, P. Solt, T. Rosenau, and H. W. G. van Herwijnen, "Current Situation of the Challenging Scale-Up Development of Hydroxymethylfurfural Production," *ChemSusChem*, vol. 13, no. 14, pp. 3544–3564, 2020, doi: https://doi.org/10.1002/cssc.202000581.

[81] R. van Putten, J. C. van der Waal, M. Harmse, H. H. van de Bovenkamp, E. de Jong, and H. J. Heeres, "A comparative study on the reactivity of various ketohexoses to furanics in methanol," *ChemSusChem*, vol. 9, no. 14, pp. 1827–1834, 2016.

[82] Avantium, "YXY® Technology," 2021. https://www.avantium.com/technologies/yxy/

[83] GFBiochemicals, "GFBiochemicals and American Process Inc enter into a joint development agreement to create the largest integrated cellulosic bio-refinery in the world." 2017. [Online]. Available: http://www.gfbiochemicals.com/_media/Document/2017/4/26/_GFBIOCHEMICALS%20AND%20AMERICAN%20PROCESS%20INC%20ENTER%20INTO%20A%20JOINT%20DEVELOPMENT%20A....pdf

[84] F. D. Pileidis and M. Titirici, “Levulinic acid biorefineries: new challenges for efficient utilization of biomass,” *ChemSusChem*, vol. 9, no. 6, pp. 562–582, 2016.

[85] G. C. Hayes and C. R. Becer, “Levulinic acid: A sustainable platform chemical for novel polymer architectures,” *Polym Chem*, vol. 11, no. 25, pp. 4068–4077, 2020.

[86] M. G. Banwell, B. Pollard, X. Liu, and L. A. Connal, “Exploiting Nature’s Most Abundant Polymers: Developing New Pathways for the Conversion of Cellulose, Hemicellulose, Lignin and Chitin into Platform Molecules (and Beyond),” *Chemistry–An Asian Journal*, vol. 16, no. 6, pp. 604–620, 2021.

[87] P. Bajpai, “Structure of Lignocellulosic Biomass,” in *Pretreatment of Lignocellulosic Biomass for Biofuel Production*, Singapore: Springer Singapore, 2016, pp. 7–12. doi: 10.1007/978-981-10-0687-6_2.

[88] P. Sudarsanam, R. Zhong, S. van den Bosch, S. M. Coman, V. I. Parvulescu, and B. F. Sels, “Functionalised heterogeneous catalysts for sustainable biomass valorisation,” *Chem Soc Rev*, vol. 47, no. 22, pp. 8349–8402, 2018, doi: 10.1039/C8CS00410B.

[89] H. J. Brownlee and C. S. Miner, “Industrial development of furfural,” *Ind Eng Chem*, vol. 40, no. 2, pp. 201–204, 1948.

[90] C. D. Hurd and L. L. Isenhour, “Pentose reactions. I. Furfural formation,” *J Am Chem Soc*, vol. 54, no. 1, pp. 317–330, 1932.

[91] E. E. Hughes and S. F. Acree, “Quantitative formation of furfural and methylfurfural from pentoses and methylpentoses,” *J. Res. Natl. Bur. Stand*, vol. 23, pp. 293–298, 1939.

[92] H. E. Hoydonckx, W. M. van Rhijn, W. van Rhijn, D. E. de Vos, and P. A. Jacobs, “Furfural and derivatives,” in *Ullmann’s encyclopedia of industrial chemistry*, 2000.

[93] F. C. Beall and H. W. Eickner, “Thermal degradation of wood components: a review of the literature,” 1970.

[94] E. R. Garrett and B. H. Dvorchik, “Kinetics and mechanisms of the acid degradation of the aldopentoses to furfural,” *J Pharm Sci*, vol. 58, no. 7, pp. 813–820, 1969, doi: https://doi.org/10.1002/jps.2600580703.

[95] M. S. Feather, D. W. Harris, and S. B. Nichols, “Routes of conversion of D-xylose, hexuronic acids, and L-ascorbic acid to 2-furaldehyde,” *J Org Chem*, vol. 37, no. 10, pp. 1606–1608, 1972.

[96] M. J. Antal Jr, T. Leesomboon, W. S. Mok, and G. N. Richards, “Mechanism of formation of 2-furaldehyde from D-xylose,” *Carbohydr Res*, vol. 217, pp. 71–85, 1991.

[97] M. R. Nimlos, X. Qian, M. Davis, M. E. Himmel, and D. K. Johnson, “Energetics of Xylose Decomposition as Determined Using Quantum Mechanics Modeling,” *J Phys Chem A*, vol. 110, no. 42, pp. 11824–11838, 2006, doi: 10.1021/jp0626770.

[98] Q. Jing and X. LÜ, "Kinetics of Non-catalyzed Decomposition of D-xylose in High Temperature Liquid Water," *Chin J Chem Eng*, vol. 15, no. 5, pp. 666–669, 2007, doi: https://doi.org/10.1016/S1004-9541(07)60143-8.

[99] P. J. Oefner, A. H. Lanziner, G. Bonn, and O. Bobleter, "Quantitative studies on furfural and organic acid formation during hydrothermal, acidic and alkaline degradation ofD-xylose," *Monatshefte für Chemie / Chemical Monthly*, vol. 123, no. 6, pp. 547–556, 1992, doi: 10.1007/BF00816848.

[100] M. Kabbour and R. Luque, "Furfural as a platform chemical: From production to applications," *Biomass, Biofuels, Biochemicals*, pp. 283–297, 2020.

[101] A. S. Mamman *et al.*, "Furfural: Hemicellulose/xylosederived biochemical," *Biofuels, Bioproducts and Biorefining: Innovation for a sustainable economy*, vol. 2, no. 5, pp. 438–454, 2008.

[102] B. Danon, G. Marcotullio, and W. de Jong, "Mechanistic and kinetic aspects of pentose dehydration towards furfural in aqueous media employing homogeneous catalysis," *Green Chemistry*, vol. 16, no. 1, pp. 39–54, 2014.

[103] J. Lange, E. van der Heide, J. van Buijtenen, and R. Price, "Furfural—a promising platform for lignocellulosic biofuels," *ChemSusChem*, vol. 5, no. 1, pp. 150–166, 2012.

[104] X. Li, P. Jia, and T. Wang, "Furfural: A Promising Platform Compound for Sustainable Production of C4 and C5 Chemicals," *ACS Catal*, vol. 6, no. 11, pp. 7621–7640, Nov. 2016, doi: 10.1021/acscatal.6b01838.

[105] G. H. C. Dubbink *et al.*, "Furfural to FDCA: systematic process design and techno-economic evaluation," *Biofuels, Bioproducts and Biorefining*, vol. 15, no. 4, pp. 1021–1030, Jul. 2021, doi: https://doi.org/10.1002/bbb.2204.

[106] G. Zang, A. Shah, and C. Wan, "Techno-economic analysis of an integrated biorefinery strategy based on one-pot biomass fractionation and furfural production," *J Clean Prod*, vol. 260, p. 120837, 2020, doi: https://doi.org/10.1016/j.jclepro.2020.120837.

[107] K. Dalvand, J. Rubin, S. Gunukula, M. Clayton Wheeler, and G. Hunt, "Economics of biofuels: Market potential of furfural and its derivatives," *Biomass Bioenergy*, vol. 115, pp. 56–63, 2018, doi: https://doi.org/10.1016/j.biombioe.2018.04.005.

[108] F. Jin, Z. Zhou, H. Enomoto, T. Moriya, and H. Higashijima, "Conversion mechanism of cellulosic biomass to lactic acid in subcritical water and acid–base catalytic effect of subcritical water," *Chem Lett*, vol. 33, no. 2, pp. 126–127, 2004.

[109] X. Yan, F. Jin, K. Tohji, T. Moriya, and H. Enomoto, "Production of lactic acid from glucose by alkaline hydrothermal reaction," *J Mater Sci*, vol. 42, no. 24, pp. 9995–9999, 2007.

[110] X. Yan, F. Jin, and K. Tohji, "Hydrothermal Conversion of Carbohydrate Biomass to Lactic Acid," *AIChE Journal*, vol. 56, no. 10, pp. 2727–2733, 2010, doi: 10.1002/aic.

[111] M. Dusselier, P. van Wouwe, A. Dewaele, E. Makshina, and B. F. Sels, "Lactic acid as a platform chemical in the biobased economy: the role of chemocatalysis," *Energy Environ Sci*, vol. 6, no. 5, pp. 1415–1442, 2013.

[112] A. v Bavykina, M. G. Goesten, F. Kapteijn, M. Makkee, and J. Gascon, "Efficient production of hydrogen from formic acid using a Covalent Triazine Framework supported molecular catalyst," *ChemSusChem*, vol. 8, no. 5, pp. 809–812, 2015.

[113] M. Iguchi, Y. Himeda, Y. Manaka, K. Matsuoka, and H. Kawanami, "Simple Continuous High-Pressure Hydrogen Production and Separation System from Formic Acid under Mild Temperatures," *ChemCatChem*, vol. 8, no. 5, pp. 886–890, 2016, doi: https://doi.org/10.1002/cctc.201501296.

[114] F. Jin, Z. Zhou, A. Kishita, and H. Enomoto, "Hydrothermal conversion of biomass into acetic acid," *J Mater Sci*, vol. 41, no. 5, pp. 1495–1500, 2006, doi: 10.1007/s10853-006-7493-8.

[115] D. J. Hayes, S. Fitzpatrick, M. H. B. Hayes, and J. R. H. Ross, "The biofine process–production of levulinic acid, furfural, and formic acid from lignocellulosic feedstocks," *Biorefineries–Industrial Processes and Product*, vol. 1, pp. 139–164, 2006.

[116] W. S. L. Mok, M. J. Antal Jr, and M. Jones Jr, "Formation of acrylic acid from lactic acid in supercritical water," *J Org Chem*, vol. 54, no. 19, pp. 4596–4602, 1989.

[117] T. M. Aida, A. Ikarashi, Y. Saito, M. Watanabe, R. L. Smith Jr, and K. Arai, "Dehydration of lactic acid to acrylic acid in high temperature water at high pressures," *J Supercrit Fluids*, vol. 50, no. 3, pp. 257–264, 2009.

[118] M. J. Antal, W. S. L. Mok, and G. N. Richards, "Mechanism of formation of 5-(hydroxymethyl)-2-furaldehyde from d-fructose and sucrose," *Carbohydr Res*, vol. 199, no. 1, pp. 91–109, 1990, doi: 10.1016/0008-6215(90)84096-D.

[119] F. Jin, Z. Zhou, T. Moriya, H. Kishida, H. Higashijima, and H. Enomoto, "Controlling hydrothermal reaction pathways to improve acetic acid production from carbohydrate biomass," *Environ Sci Technol*, vol. 39, no. 6, pp. 1893–1902, 2005.

[120] S. S. Bang and D. Johnston, "Environmental effects of sodium acetate/formate deicer, Ice Shear™," *Arch Environ Contam Toxicol*, vol. 35, no. 4, pp. 580–587, 1998.

[121] L. G. Terry, K. Conaway, J. Rebar, and A. J. Graettinger, "Alternative deicers for winter road Maintenance—A Review," *Water Air Soil Pollut*, vol. 231, no. 8, pp. 1–29, 2020.

[122] N. Baccile, G. Laurent, F. Babonneau, F. Fayon, M. M. Titirici, and M. Antonietti, "Structural characterization of hydrothermal carbon spheres by advanced solid-state MAS 13C NMR investigations," *Journal of Physical Chemistry C*, vol. 113, no. 22, pp. 9644–9654, 2009, doi: 10.1021/jp901582x.

[123] I. v Sumerskii, S. M. Krutov, and M. Y. Zarubin, "Humin-like substances formed under the conditions of industrial hydrolysis of wood," *Russian Journal of Applied Chemistry*, vol. 83, no. 2, pp. 320–327, 2010.

[124] S. K. R. Patil, J. Heltzel, and C. R. F. Lund, "Comparison of structural features of humins formed catalytically from glucose, fructose, and 5-hydroxymethylfurfuraldehyde," *Energy & Fuels*, vol. 26, no. 8, pp. 5281–5293, 2012.

[125] I. van Zandvoort *et al.*, "Formation, molecular structure, and morphology of humins in biomass conversion: Influence of feedstock and processing conditions," *ChemSusChem*, vol. 6, no. 9, pp. 1745–1758, 2013, doi: 10.1002/cssc.201300332.

[126] I. van Zandvoort, E. R. H. van Eck, P. de Peinder, H. J. Heeres, P. C. A. Bruijnincx, and B. M. Weckhuysen, "Full, reactive solubilization of humin byproducts by alkaline treatment and characterization of the alkali-treated humins formed," *ACS Sustain Chem Eng*, vol. 3, no. 3, pp. 533–543, 2015, doi: 10.1021/sc500772w.

[127] Y. Qi, B. Song, and Y. Qi, "The roles of formic acid and levulinic acid on the formation and growth of carbonaceous spheres by hydrothermal carbonization," *RSC Adv*, vol. 6, no. 104, pp. 102428–102435, 2016.

[128] A. B. Brown, B. J. McKeogh, G. A. Tompsett, R. Lewis, N. A. Deskins, and M. T. Timko, "Structural analysis of hydrothermal char and its models by density functional theory simulation of vibrational spectroscopy," *Carbon N Y*, vol. 125, pp. 614–629, 2017.

[129] L. J. R. Higgins, A. P. Brown, J. P. Harrington, A. B. Ross, B. Kaulich, and B. Mishra, "Evidence for a core-shell structure of hydrothermal carbon," *Carbon N Y*, vol. 161, pp. 423–431, 2020.

[130] Z. Cheng, J. Everhart, G. Tsilomelekis, V. Nikolakis, B. Saha, and D. Vlachos, "Structural Analysis of Humins Formed in the Brønsted-Catalyzed Dehydration of Fructose," *Green Chemistry*, 2018, doi: 10.1039/C7GC03054A.

[131] M. Sevilla and A. B. Fuertes, "The production of carbon materials by hydrothermal carbonization of cellulose," *Carbon N Y*, vol. 47, no. 9, pp. 2281–2289, 2009, doi: https://doi.org/10.1016/j.carbon.2009.04.026.

[132] A. J. Romero-Anaya, M. Ouzzine, M. A. Lillo-Rodenas, and A. Linares-Solano, "Spherical carbons: Synthesis, characterization and activation processes," *Carbon N Y*, vol. 68, pp. 296–307, 2014.

[133] D. Jung, M. Zimmermann, and A. Kruse, "Hydrothermal carbonization of fructose: Growth mechanism and kinetic model," *ACS Sustain Chem Eng*, vol. 6, no. 11, pp. 13877–13887, 2018.

[134] J. Poerschmann, B. Weiner, R. Koehler, and F.-D. Kopinke, "Hydrothermal Carbonization of Glucose, Fructose, and Xylose Identification of Organic Products with Medium Molecular Masses," *ACS Sustain Chem Eng*, vol. 5, no. 8, pp. 6420–6428, 2017.

[135] N. Shi *et al.*, "Molecular structure and formation mechanism of hydrochar from hydrothermal carbonization of carbohydrates," *Energy & Fuels*, vol. 33, no. 10, pp. 9904–9915, 2019.

[136] N. Shi *et al.*, "Formation of soluble furanic and carbocyclic oxy-organics during the hydrothermal carbonization of glucose," *Energy & Fuels*, vol. 34, no. 2, pp. 1830–1840, 2020.

[137] N. Shi *et al.*, "Characterization of the Soluble Products Formed during the Hydrothermal Conversion of Biomass-Derived Furanic Compounds by Using LC–MS/MS," *ACS Omega*, vol. 5, no. 36, pp. 23322–23333, 2020, doi: 10.1021/acsomega.0c03169.

[138] L. Wei, M. Sevilla, A. B. Fuertes, R. Mokaya, and G. Yushin, "Hydrothermal carbonization of abundant renewable natural organic chemicals for high-performance supercapacitor electrodes," *Adv Energy Mater*, vol. 1, no. 3, pp. 356–361, 2011.

[139] C. Falco *et al.*, "Hydrothermal carbons from hemicellulose-derived aqueous hydrolysis products as electrode materials for supercapacitors," *ChemSusChem*, vol. 6, no. 2, pp. 374–382, 2013.

[140] X. Tong *et al.*, "Tailoring the physicochemical properties of chitosan-derived N-doped carbon by controlling hydrothermal carbonization time for high-performance supercapacitor application," *Carbohydr Polym*, vol. 207, pp. 764–774, 2019.

[141] V. Hoffmann *et al.*, "Conductive Carbon Materials from the Hydrothermal Carbonization of Vineyard Residues for the Application in Electrochemical Double-Layer Capacitors (EDLCs) and Direct Carbon Fuel Cells (DCFCs)," *Materials*, vol. 12, no. 10, p. 1703, 2019, [Online]. Available: https://www.mdpi.com/1996-1944/12/10/1703

[142] J. Zhang, Z. Chen, G. Wang, L. Hou, and C. Yuan, "Eco-friendly and scalable synthesis of micro-/mesoporous carbon sub-microspheres as competitive electrodes for supercapacitors and sodium-ion batteries," *Appl Surf Sci*, vol. 533, p. 147511, 2020, doi: https://doi.org/10.1016/j.apsusc.2020.147511.

[143] M. K. Rybarczyk, Y. Li, M. Qiao, Y.-S. Hu, M.-M. Titirici, and M. Lieder, "Hard carbon derived from rice husk as low cost negative electrodes in Na-ion batteries," *Journal of Energy Chemistry*, vol. 29, pp. 17–22, 2019.

[144] S. A. Nicolae *et al.*, "Recent advances in hydrothermal carbonisation: from tailored carbon materials and biochemicals to applications and bioenergy," *Green Chemistry*, vol. 22, no. 15, pp. 4747–4800, 2020.

[145] S.-A. Wohlgemuth, R. J. White, M.-G. Willinger, M.-M. Titirici, and M. Antonietti, "A one-pot hydrothermal synthesis of sulfur and nitrogen doped carbon aerogels with

enhanced electrocatalytic activity in the oxygen reduction reaction," *Green Chemistry*, vol. 14, no. 5, pp. 1515–1523, 2012, doi: 10.1039/C2GC35309A.

[146] Y. Pang, K. Wang, H. Xie, Y. Sun, M.-M. Titirici, and G.-L. Chai, "Mesoporous Carbon Hollow Spheres as Efficient Electrocatalysts for Oxygen Reduction to Hydrogen Peroxide in Neutral Electrolytes," *ACS Catal*, vol. 10, no. 14, pp. 7434–7442, 2020, doi: 10.1021/acscatal.0c00584.

[147] I.-A. Baragau *et al.*, "Efficient Continuous Hydrothermal Flow Synthesis of Carbon Quantum Dots from a Targeted Biomass Precursor for On–Off Metal Ions Nanosensing," *ACS Sustain Chem Eng*, vol. 9, no. 6, pp. 2559–2569, 2021, doi: 10.1021/acssuschemeng.0c08594.

[148] Y. Li, D. Li, Y. Rao, X. Zhao, and M. Wu, "Superior CO2, CH4, and H2 uptakes over ultrahigh-surface-area carbon spheres prepared from sustainable biomass-derived char by CO2 activation," *Carbon N Y*, vol. 105, pp. 454–462, 2016, doi: https://doi.org/10.1016/j.carbon.2016.04.036.

[149] F. Schipper, S. Kubo, and T. P. Fellinger, "Nitrogen-doped porous carbon via ammonothermal carbonization for supercapacitors," *J Solgel Sci Technol*, vol. 89, no. 1, pp. 101–110, 2019, doi: 10.1007/s10971-018-4837-1.

[150] Z. Zhang, N. Sun, and W. Wei, "Facile and controllable synthesis of ordered mesoporous carbons with tunable single-crystal morphology for CO2 capture," *Carbon N Y*, vol. 161, pp. 629–638, 2020, doi: https://doi.org/10.1016/j.carbon.2020.02.009.

[151] X. Lu, J. R. V. Flora, and N. D. Berge, "Influence of process water quality on hydrothermal carbonization of cellulose," *Bioresour Technol*, vol. 154, pp. 229–239, 2014, doi: 10.1016/j.biortech.2013.11.069.

[152] S. Reiche, N. Kowalew, and R. Schlögl, "Influence of Synthesis pH and Oxidative Strength of the Catalyzing Acid on the Morphology and Chemical Structure of Hydrothermal Carbon," *ChemPhysChem*, vol. 16, no. 3, pp. 579–587, 2015, doi: https://doi.org/10.1002/cphc.201402834.

[153] P. Körner, S. Beil, and A. Kruse, "Effect of salt on the formation of 5-hydroxymethylfurfural from ketohexoses under aqueous conditions," *React Chem Eng*, vol. 4, no. 4, pp. 747–762, 2019, doi: 10.1039/C8RE00300A.

[154] Z. C. Zhao, H., Holladay, J.E., Brown, H., Zhang, "Metal chlorides in ionic liquid solvents convert sugar to 5-hydroxymethyfurfural," *Science (1979)*, vol. 316, no. 5831, pp. 1597–600, 2007.

[155] V. Choudhary *et al.*, "Insights into the Interplay of Lewis and Brønsted Acid Catalysts in Glucose and Fructose Conversion to 5-(Hydroxymethyl)furfural and Levulinic Acid in Aqueous Media," *J Am Chem Soc*, vol. 135, no. 10, pp. 3997–4006, 2013, doi: 10.1021/ja3122763.

[156] S. Hu, Z. Zhang, J. Song, Y. Zhou, and B. Han, "Efficient conversion of glucose into 5-hydroxymethylfurfural catalyzed by a common Lewis acid SnCl4 in an ionic liquid," *Green Chemistry*, vol. 11, no. 11, pp. 1746–1749, 2009, doi: 10.1039/B914601F.

[157] Y. Jiang *et al.*, "Speciation and kinetic study of iron promoted sugar conversion to 5-hydroxymethylfurfural (HMF) and levulinic acid (LA)," *Organic Chemistry Frontiers*, vol. 2, no. 10, pp. 1388–1396, 2015, doi: 10.1039/C5QO00194C.

[158] W. Weiqi and W. Shubin, "Experimental and kinetic study of glucose conversion to levulinic acid catalyzed by synergy of Lewis and Brønsted acids," *Chemical Engineering Journal*, vol. 307, pp. 389–398, 2017, doi: https://doi.org/10.1016/j.cej.2016.08.099.

[159] H. Lin, Q. Xiong, Y. Zhao, J. Chen, and S. Wang, "Conversion of carbohydrates into 5-hydroxymethylfurfural in a green reaction system of CO2-water-isopropanol," *AIChE Journal*, vol. 63, no. 1, pp. 257–265, 2016, doi: 10.1002/aic.

[160] X. Fu, J. Dai, X. Guo, J. Tang, L. Zhu, and C. Hu, "Suppression of oligomer formation in glucose dehydration by CO2and tetrahydrofuran," *Green Chemistry*, vol. 19, no. 14, pp. 3334–3343, 2017, doi: 10.1039/c7gc01115f.

[161] L. Yang, J. Su, S. Carl, J. G. Lynam, X. Yang, and H. Lin, "Catalytic conversion of hemicellulosic biomass to lactic acid in pH neutral aqueous phase media," *Appl Catal B*, vol. 162, pp. 149–157, 2015, doi: https://doi.org/10.1016/j.apcatb.2014.06.025.

[162] Q. Hou *et al.*, "Tin phosphate as a heterogeneous catalyst for efficient dehydration of glucose into 5-hydroxymethylfurfural in ionic liquid," *Appl Catal B*, vol. 224, pp. 183–193, 2018, doi: https://doi.org/10.1016/j.apcatb.2017.09.049.

[163] A. Dibenedetto, M. Aresta, L. di Bitonto, and C. Pastore, "Organic Carbonates: Efficient Extraction Solvents for the Synthesis of HMF in Aqueous Media with Cerium Phosphates as Catalysts," *ChemSusChem*, vol. 9, no. 1, pp. 118–125, 2016, doi: https://doi.org/10.1002/cssc.201501181.

[164] H. Li, S. Saravanamurugan, S. Yang, and A. Riisager, "Direct transformation of carbohydrates to the biofuel 5-ethoxymethylfurfural by solid acid catalysts," *Green Chemistry*, vol. 18, no. 3, pp. 726–734, 2016, doi: 10.1039/C5GC01043H.

[165] K. Dong, J. Zhang, W. Luo, L. Su, and Z. Huang, "Catalytic conversion of carbohydrates into 5-hydroxymethyl furfural over sulfonated hyper-cross-linked polymer in DMSO," *Chemical Engineering Journal*, vol. 334, pp. 1055–1064, 2018, doi: https://doi.org/10.1016/j.cej.2017.10.092.

[166] J. Howard, D. W. Rackemann, J. P. Bartley, C. Samori, and W. O. S. Doherty, "Conversion of Sugar Cane Molasses to 5-Hydroxymethylfurfural Using Molasses and Bagasse-Derived Catalysts," *ACS Sustain Chem Eng*, vol. 6, no. 4, pp. 4531–4538, 2018, doi: 10.1021/acssuschemeng.7b02746.

[167] J. Wang, L. Zhu, Y. Wang, H. Cui, Y. Zhang, and Y. Zhang, "Fructose dehydration to 5-HMF over three sulfonated carbons: effect of different pore structures," *Journal of Chemical Technology & Biotechnology*, vol. 92, no. 6, pp. 1454–1463, 2017, doi: https://doi.org/10.1002/jctb.5144.

[168] X. Qi, H. Guo, L. Li, and R. L. Smith, "Acid-catalyzed dehydration of fructose into 5-hydroxymethylfurfural by cellulose-derived amorphous carbon," *ChemSusChem*, vol. 5, no. 11, pp. 2215–2220, 2012, doi: 10.1002/cssc.201200363.

[169] Y. Yu and H. Wu, "Significant Differences in the Hydrolysis Behavior of Amorphous and Crystalline Portions within Microcrystalline Cellulose in Hot-Compressed Water," *Ind Eng Chem Res*, vol. 49, no. 8, pp. 3902–3909, 2010, doi: 10.1021/ie901925g.

[170] A. G. Demesa, A. Laari, E. Tirronen, and I. Turunen, "Comparison of solvents for the recovery of low-molecular carboxylic acids and furfural from aqueous solutions," *Chemical Engineering Research and Design*, vol. 93, pp. 531–540, 2015, doi: https://doi.org/10.1016/j.cherd.2014.04.033.

[171] Y. Román-Leshkov, J. N. Chheda, and J. A. Dumesic, "Phase Modifiers Promote Efficient Production of Hydroxymethylfurfural from Fructose," *Science (1979)*, vol. 312, no. 5782, pp. 1933–1937, 2006, doi: doi:10.1126/science.1126337.

[172] T. Shimanouchi, Y. Kataoka, M. Yasukawa, T. Ono, and Y. Kimura, "Simplified model for extraction of 5-hydroxymethylfurfural from fructose: use of water/oil biphasic system under high temperature and pressure conditions," *Solvent Extraction Research and Development, Japan*, vol. 20, pp. 205–212, 2013.

[173] J. M. R. Gallo, D. M. Alonso, M. A. Mellmer, and J. A. Dumesic, "Production and upgrading of 5-hydroxymethylfurfural using heterogeneous catalysts and biomass-derived solvents," *Green Chemistry*, vol. 15, no. 1, pp. 85–90, 2013, doi: 10.1039/C2GC36536G.

[174] L. C. Blumenthal *et al.*, "Systematic Identification of Solvents Optimal for the Extraction of 5-Hydroxymethylfurfural from Aqueous Reactive Solutions," *ACS Sustain Chem Eng*, vol. 4, no. 1, pp. 228–235, 2016, doi: 10.1021/acssuschemeng.5b01036.

[175] E. Weingart, L. Teevs, R. Krieg, and U. Prüße, "Hexafluoroisopropanol as a Low-Boiling Extraction Solvent for 5-Hydroxymethylfurfural Production," *Energy Technology*, vol. 6, no. 2, pp. 432–440, 2018, doi: https://doi.org/10.1002/ente.201700569.

[176] E. C. Sindermann, A. Holbach, A. de Haan, and N. Kockmann, "Single stage and countercurrent extraction of 5-hydroxymethylfurfural from aqueous phase systems," *Chemical Engineering Journal*, vol. 283, pp. 251–259, 2016, doi: https://doi.org/10.1016/j.cej.2015.07.029.

[177] S. Mohammad, G. Grundl, R. Müller, W. Kunz, G. Sadowski, and C. Held, "Influence of electrolytes on liquid-liquid equilibria of water/1-butanol and on the partitioning of 5-hydroxymethylfurfural in water/1-butanol," *Fluid Phase Equilib*, vol. 428, pp. 102–111, 2016, doi: https://doi.org/10.1016/j.fluid.2016.05.001.

[178] G. Grundl, M. Müller, D. Touraud, and W. Kunz, "Salting-out and salting-in effects of organic compounds and applications of the salting-out effect of Pentasodium phytate in different extraction processes," *J Mol Liq*, vol. 236, pp. 368–375, 2017, doi: https://doi.org/10.1016/j.molliq.2017.03.091.

[179] F. Liu, S. Sivoththaman, and Z. Tan, "Solvent extraction of 5-HMF from simulated hydrothermal conversion product," *Sustainable Environment Research*, vol. 24, no. 2, 2014.

[180] T. Brouwer, M. Blahusiak, K. Babic, and B. Schuur, "Reactive extraction and recovery of levulinic acid, formic acid and furfural from aqueous solutions containing sulphuric acid," *Sep Purif Technol*, vol. 185, pp. 186–195, 2017, doi: https://doi.org/10.1016/j.seppur.2017.05.036.

[181] J. Slak, B. Pomeroy, A. Kostyniuk, M. Grilc, and B. Likozar, "A review of bio-refining process intensification in catalytic conversion reactions, separations and purifications of hydroxymethylfurfural (HMF) and furfural," *Chemical Engineering Journal*, vol. 429, p. 132325, 2022.

[182] C. H. J. T. Dietz, F. Gallucci, M. van Sint Annaland, C. Held, and M. C. Kroon, "110th Anniversary: Distribution Coefficients of Furfural and 5-Hydroxymethylfurfural in Hydrophobic Deep Eutectic Solvent + Water Systems: Experiments and Perturbed-Chain Statistical Associating Fluid Theory Predictions," *Ind Eng Chem Res*, vol. 58, no. 10, pp. 4240–4247, Mar. 2019, doi: 10.1021/acs.iecr.8b06234.

[183] X. Sun, Z. Liu, Z. Xue, Y. Zhang, and T. Mu, "Extraction of 5-HMF from the conversion of glucose in ionic liquid [Bmim]Cl by compressed carbon dioxide," *Green Chemistry*, vol. 17, no. 5, pp. 2719–2722, 2015, doi: 10.1039/C5GC00092K.

[184] A. Sarwono, Z. Man, A. Idris, A. S. Khan, N. Muhammad, and C. D. Wilfred, "Optimization of ionic liquid assisted sugar conversion and nanofiltration membrane separation for 5-hydroxymethylfurfural," *Journal of Industrial and Engineering Chemistry*, vol. 69, pp. 171–178, 2019, doi: https://doi.org/10.1016/j.jiec.2018.09.020.

[185] M. Sevilla and A. B. Fuertes, "Chemical and structural properties of carbonaceous products obtained by hydrothermal carbonization of saccharides," *Chemistry–A European Journal*, vol. 15, no. 16, pp. 4195–4203, 2009.

[186] M. Li, W. Li, and S. Liu, "Hydrothermal synthesis, characterization, and KOH activation of carbon spheres from glucose," *Carbohydr Res*, vol. 346, no. 8, pp. 999–1004, 2011, doi: https://doi.org/10.1016/j.carres.2011.03.020.

[187] H. Simsir, N. Eltugral, and S. Karagoz, "Hydrothermal carbonization for the preparation of hydrochars from glucose, cellulose, chitin, chitosan and wood chips via low-temperature and their characterization," *Bioresour Technol*, vol. 246, pp. 82–87, 2017, doi: https://doi.org/10.1016/j.biortech.2017.07.018.

[188] J. Wang and J. Qiu, "A review of carbon dots in biological applications," *J Mater Sci*, vol. 51, no. 10, pp. 4728–4738, 2016, doi: 10.1007/s10853-016-9797-7.

[189] M. Heidari, A. Dutta, B. Acharya, and S. Mahmud, "A review of the current knowledge and challenges of hydrothermal carbonization for biomass conversion," *Journal of the Energy Institute*, vol. 92, no. 6, pp. 1779–1799, 2019, doi: https://doi.org/10.1016/j.joei.2018.12.003.

[190] N. Baccile, G. Laurent, F. Babonneau, F. Fayon, M.-M. Titirici, and M. Antonietti, "Structural Characterization of Hydrothermal Carbon Spheres by Advanced Solid-State MAS13C NMR Investigations," *The Journal of Physical Chemistry C*, vol. 113, no. 22, pp. 9644–9654, 2009, doi: 10.1021/jp901582x.

[191] Y. Gao *et al.*, "Effect of residence time on chemical and structural properties of hydrochar obtained by hydrothermal carbonization of water hyacinth," *Energy*, vol. 58, pp. 376–383, 2013, doi: https://doi.org/10.1016/j.energy.2013.06.023.

[192] S. E. Elaigwu and G. M. Greenway, "Chemical, structural and energy properties of hydrochars from microwave-assisted hydrothermal carbonization of glucose," *International Journal of Industrial Chemistry*, vol. 7, no. 4, pp. 449–456, 2016, doi: 10.1007/s40090-016-0081-0.

[193] F. Liu, R. Yu, X. Ji, and M. Guo, "Hydrothermal carbonization of holocellulose into hydrochar: Structural, chemical characteristics, and combustion behavior," *Bioresour Technol*, vol. 263, pp. 508–516, 2018, doi: https://doi.org/10.1016/j.biortech.2018.05.019.

[194] F. S. Asghari and H. Yoshida, "Kinetics of the Decomposition of Fructose Catalyzed by Hydrochloric Acid in Subcritical Water: Formation of 5-Hydroxymethylfurfural, Levulinic, and Formic Acids," *Ind Eng Chem Res*, vol. 46, no. 23, pp. 7703–7710, 2007, doi: 10.1021/ie061673e.

[195] G. Garrote, H. Dominguez, and J. C. Parajo, "Hydrothermal processing of lignocellulosic materials," *Holz als Roh- und Werkstoff*, vol. 57, no. 3, pp. 191–202, 1999.

[196] Y. Ogihara, R. L. Smith, H. Inomata, and K. Arai, "Direct observation of cellulose dissolution in subcritical and supercritical water over a wide range of water densities (550–1000 kg/m3)," *Cellulose*, vol. 12, no. 6, pp. 595–606, 2005, doi: 10.1007/s10570-005-9008-1.

[197] M. Sasaki, Z. Fang, Y. Fukushima, T. Adschiri, and K. Arai, "Dissolution and Hydrolysis of Cellulose in Subcritical and Supercritical Water," *Ind Eng Chem Res*, vol. 39, no. 8, pp. 2883–2890, 2000, doi: 10.1021/ie990690j.

[198] F. M. Relvas, A. R. C. Morais, and R. Bogel-Lukasik, "Selective hydrolysis of wheat straw hemicellulose using high-pressure CO2 as catalyst," *RSC Adv*, vol. 5, no. 90, pp. 73935–73944, 2015, doi: 10.1039/C5RA14632A.

[199] S. Motokucho, H. Morikawa, H. Nakatani, and B. A. J. Noordover, "Efficient and environmental-friendly dehydration of fructose to 5-hydroxymethyl-2-furfural in water under high pressure of CO2," *Tetrahedron Lett*, vol. 57, no. 42, pp. 4742–4745, 2016, doi: https://doi.org/10.1016/j.tetlet.2016.09.036.

[200] R. Lee, J. Harris, P. Champagne, and P. G. Jessop, "CO2-Catalysed conversion of carbohydrates to 5-hydroxymethyl furfural," *Green Chemistry*, vol. 18, no. 23, pp. 6305–6310, 2016, doi: 10.1039/C6GC01853J.

[201] H. Labauze, S. Camy, P. Floquet, B. Benjelloun-Mlayah, and J.-S. Condoret, "Kinetic Study of 5-Hydroxymethylfurfural Synthesis from Fructose in High Pressure CO2–Water Two-Phase System," *Ind Eng Chem Res*, vol. 58, no. 1, pp. 92–100, 2019, doi: 10.1021/acs.iecr.8b04694.

[202] D. Jung, P. Körner, and A. Kruse, "Kinetic study on the impact of acidity and acid concentration on the formation of 5-hydroxymethylfurfural (HMF), humins, and levulinic acid in the hydrothermal conversion of fructose," *Biomass Convers Biorefin*, vol. 11, no. 4, pp. 1155–1170, 2021, doi: 10.1007/s13399-019-00507-0.

[203] A. Gandini and M. N. Belgacem, "Furans in polymer chemistry," *Prog Polym Sci*, vol. 22, no. 6, pp. 1203–1379, 1997, doi: https://doi.org/10.1016/S0079-6700(97)00004-X.

[204] A. P. Dunlop, "Furfural formation and behavior," *Ind Eng Chem*, vol. 40, no. 2, pp. 204–209, 1948.

[205] H. R. Holgate, J. C. Meyer, and J. W. Tester, "Glucose hydrolysis and oxidation in supercritical water," *AIChE Journal*, vol. 41, no. 3, pp. 637–648, 1995, doi: https://doi.org/10.1002/aic.690410320.

[206] A. P. Dunlop and F. N. Peters Jr, "Thermal stability of furfural," *Ind Eng Chem*, vol. 32, no. 12, pp. 1639–1641, 1940.

[207] D. L. Williams and A. P. Dunlop, "Kinetics of furfural destruction in acidic aqueous media," *Ind Eng Chem*, vol. 40, no. 2, pp. 239–241, 1948.

[208] A. P. Dunlop, P. R. Stout, and S. Swadesh, "Autoxidation of Furfural," *Ind Eng Chem*, vol. 38, no. 7, pp. 705–708, 1946.

[209] J. Yu and P. E. Savage, “Decomposition of Formic Acid under Hydrothermal Conditions,” *Ind Eng Chem Res*, vol. 37, no. 1, pp. 2–10, 1998, doi: 10.1021/ie970182e.

[210] B. F. M. Kuster and H. M. G. Temmink, “The influence of pH and weak-acid anions on the dehydration of d-fructose,” *Carbohydr Res*, vol. 54, no. 2, pp. 185–191, 1977, doi: https://doi.org/10.1016/S0008-6215(00)84808-9.

[211] G. R. Akien, L. Qi, and I. T. Horváth, “Molecular mapping of the acid catalysed dehydration of fructose,” *Chemical communications*, vol. 48, no. 47, pp. 5850–5852, 2012, doi: 10.1039/C2CC31689G.

[212] D. A. Skoog, D. M. West, F. J. Holler, and S. R. Crouch, *Fundamentals of analytical chemistry*. Cengage learning, 2013.

[213] J. Kielland, “Individual activity coefficients of ions in aqueous solutions,” *J Am Chem Soc*, vol. 59, no. 9, pp. 1675–1678, 1937.

[214] C. D. Kennedy, “Ionic strength and the dissociation of acids,” *Biochem Educ*, vol. 18, no. 1, pp. 35–40, 1990, doi: https://doi.org/10.1016/0307-4412(90)90017-I.

[215] W. E. Dasent, *Inorganic energetics: an introduction*. CUP Archive, 1982.

[216] D. D. Perrin, “Dissociation constants of inorganic acids and bases in aqueous solution,” *Pure and Applied Chemistry*, vol. 20, no. 2, pp. 133–236, 1969.

[217] M. B. Smith, *March’s advanced organic chemistry: reactions, mechanisms, and structure*. John Wiley & Sons, 2020.

[218] J. C. Slater, “Atomic radii in crystals,” *J Chem Phys*, vol. 41, no. 10, pp. 3199–3204, 1964.

[219] F. H. Allen, D. G. Watson, L. Brammer, A. G. Orpen, and R. Taylor, “Typical interatomic distances: organic compounds,” 2006.

[220] P. Körner, D. Jung, and A. Kruse, “The effect of different Brønsted acids on the hydrothermal conversion of fructose to HMF,” *Green Chemistry*, vol. 20, no. 10, pp. 2231–2241, 2018, doi: 10.1039/c8gc00435h.

[221] J. B. Binder and R. T. Raines, “Simple Chemical Transformation of Lignocellulosic Biomass into Furans for Fuels and Chemicals,” *J Am Chem Soc*, vol. 131, no. 5, pp. 1979–1985, 2009, doi: 10.1021/ja808537j.

[222] T. Ståhlberg, S. Rodriguez-Rodriguez, P. Fristrup, and A. Riisager, “Metal-Free Dehydration of Glucose to 5-(Hydroxymethyl)furfural in Ionic Liquids with Boric Acid as a Promoter,” *Chemistry – A European Journal*, vol. 17, no. 5, pp. 1456–1464, 2011, doi: https://doi.org/10.1002/chem.201002171.

[223] H. D. Phan, T. Yokoyama, and Y. Matsumoto, “Direct participation of counter anion in acid hydrolysis of glycoside,” *Org Biomol Chem*, vol. 10, no. 36, pp. 7382–7391, 2012, doi: 10.1039/C2OB25451D.

[224] H. D. Phan, T. Yokoyama, and Y. Matsumoto, “Effect of Increasing the Common Anion Concentration on the Acid Hydrolysis of Glycosides,” *J Carbohydr Chem*, vol. 32, no. 4, pp. 223–239, 2013, doi: 10.1080/07328303.2013.800085.

[225] C. Wang, L. Fu, X. Tong, Q. Yang, and W. Zhang, “Efficient and selective conversion of sucrose to 5-hydroxymethylfurfural promoted by ammonium halides under mild conditions,” *Carbohydr Res*, vol. 347, no. 1, pp. 182–185, 2012, doi: https://doi.org/10.1016/j.carres.2011.11.013.

[226] P. Wrigstedt, J. Keskiväli, M. Leskelä, and T. Repo, “The Role of Salts and Brønsted Acids in Lewis Acid-Catalyzed Aqueous-Phase Glucose Dehydration to 5-Hydroxymethylfurfural,” *ChemCatChem*, vol. 7, no. 3, pp. 501–507, 2015.

[227] J. B. Binder, A. v Cefali, J. J. Blank, and R. T. Raines, “Mechanistic insights on the conversion of sugars into 5-hydroxymethylfurfural,” *Energy Environ Sci*, vol. 3, no. 6, pp. 765–771, 2010, doi: 10.1039/B923961H.

[228] P. Wrigstedt, J. Keskiväli, J. E. Perea-Buceta, and T. Repo, “One-Pot Transformation of Carbohydrates into Valuable Furan Derivatives via 5-Hydroxymethylfurfural,” *ChemCatChem*, vol. 9, no. 22, pp. 4244–4255, 2017, doi: https://doi.org/10.1002/cctc.201701106.

[229] S. Imamura, “Catalytic and Noncatalytic Wet Oxidation,” *Ind Eng Chem Res*, vol. 38, no. 5, pp. 1743–1753, May 1999, doi: 10.1021/ie980576l.

[230] D. J. Wuebbles, D. W. Fahey, and K. A. Hibbard, “Climate science special report: fourth national climate assessment, volume I,” 2017.

[231] “Carbon Dioxide,” *NIST Chemistry WebBook, SRD 69*, 2021.

[232] J. T. Edsall, “Carbon dioxide, carbonic acid, and bicarbonate ion: physical properties and kinetics of interconversion,” *CO2: Chemical, Biological and Physiological Aspects*, pp. 15–27, 1969.

[233] R. Wiebe and V. L. Gaddy, “The solubility in water of carbon dioxide at 50, 75 and 100, at pressures to 700 atmospheres,” *J Am Chem Soc*, vol. 61, no. 2, pp. 315–318, 1939.

[234] R. Wiebe, “The Binary System Carbon Dioxide-Water under Pressure,” *Chem Rev*, vol. 29, no. 3, pp. 475–481, 1941.

[235] I. van Zandvoort, E. J. Koers, M. Weingarth, P. C. A. Bruijnincx, M. Baldus, and B. M. Weckhuysen, “Structural characterization of 13C-enriched humins and alkali-treated 13C humins by 2D solid-state NMR,” *Green Chemistry*, vol. 17, no. 8, pp. 4383–4392, 2015, doi: 10.1039/c5gc00327j.

[236] C. Falco *et al.*, "Hydrothermal Carbon from Biomass: Structural Differences between Hydrothermal and Pyrolyzed Carbons via 13C Solid State NMR," *Langmuir*, vol. 27, no. 23, pp. 14460–14471, 2011, doi: 10.1021/la202361p.

[237] G. Tsilomelekis *et al.*, "Molecular structure, morphology and growth mechanisms and rates of 5-hydroxymethyl furfural (HMF) derived humins," *Green Chemistry*, vol. 18, no. 7, pp. 1983–1993, 2016, doi: 10.1039/C5GC01938A.

[238] V. Maruani, S. Narayanin-Richenapin, E. Framery, and B. Andrioletti, "Acidic Hydrothermal Dehydration of d-Glucose into Humins: Identification and Characterization of Intermediates," *ACS Sustain Chem Eng*, vol. 6, no. 10, pp. 13487–13493, 2018, doi: 10.1021/acssuschemeng.8b03479.

[239] K. J. Zeitsch, *The chemistry and technology of furfural and its many by-products*. Elsevier, 2000.

[240] L. Yu, C. Falco, J. Weber, R. J. White, J. Y. Howe, and M. M. Titirici, "Carbohydrate-derived hydrothermal carbons: A thorough characterization study," *Langmuir*, vol. 28, no. 33, pp. 12373–12383, 2012, doi: 10.1021/la3024277.

[241] J. Ryu, Y.-W. Suh, D. J. Suh, and D. J. Ahn, "Hydrothermal preparation of carbon microspheres from mono-saccharides and phenolic compounds," *Carbon N Y*, vol. 48, no. 7, pp. 1990–1998, 2010, doi: https://doi.org/10.1016/j.carbon.2010.02.006.

[242] J. N. M. Tan-Soetedjo, H. H. van de Bovenkamp, R. M. Abdilla, C. B. Rasrendra, J. van Ginkel, and H. J. Heeres, "Experimental and Kinetic Modeling Studies on the Conversion of Sucrose to Levulinic Acid and 5-Hydroxymethylfurfural Using Sulfuric Acid in Water," *Ind Eng Chem Res*, vol. 56, no. 45, pp. 13228–13239, 2017, doi: 10.1021/acs.iecr.7b01611.

[243] Q. He, Y. Yu, J. Wang, X. Suo, and Y. Liu, "Kinetic Study of the Hydrothermal Carbonization Reaction of Glucose and Its Product Structures," *Ind Eng Chem Res*, vol. 60, no. 12, pp. 4552–4561, Mar. 2021, doi: 10.1021/acs.iecr.0c06280.

[244] X. Lu and N. D. Berge, "Influence of feedstock chemical composition on product formation and characteristics derived from the hydrothermal carbonization of mixed feedstocks," *Bioresour Technol*, vol. 166, pp. 120–131, 2014, doi: http://doi.org/10.1016/j.biortech.2014.05.015.

[245] N. Paksung, J. Pfersich, P. J. Arauzo, D. Jung, and A. Kruse, "Structural Effects of Cellulose on Hydrolysis and Carbonization Behavior during Hydrothermal Treatment," *ACS Omega*, vol. 5, no. 21, pp. 12210–12223, Jun. 2020, doi: 10.1021/acsomega.0c00737.

[246] P. R. Griffiths, J. A. de Haseth, and J. D. Winefordner, "Fourier transform infrared spectrometry. ISBN," &, vol. 560, 2007.

[247] L. F. Gladden, “Nuclear magnetic resonance in chemical engineering: Principles and applications,” *Chem Eng Sci*, vol. 49, no. 20, pp. 3339–3408, 1994, doi: https://doi.org/10.1016/0009-2509(94)00129-4.

[248] B. D. Fahlman, “Materials Characterization,” in *Materials Chemistry*, Dordrecht: Springer Netherlands, 2018, pp. 643–741. doi: 10.1007/978-94-024-1255-0_7.

[249] B. J. Inkson, “2 - Scanning electron microscopy (SEM) and transmission electron microscopy (TEM) for materials characterization,” in *Materials Characterization Using Nondestructive Evaluation (NDE) Methods*, G. Hübschen, I. Altpeter, R. Tschuncky, and H.-G. Herrmann, Eds. Woodhead Publishing, 2016, pp. 17–43. doi: https://doi.org/10.1016/B978-0-08-100040-3.00002-X.

[250] S. Hosseini and S. O. Martinez-Chapa, “Principles and Mechanism of MALDI-ToF-MS Analysis,” in *Fundamentals of MALDI-ToF-MS Analysis: Applications in Bio-diagnosis, Tissue Engineering and Drug Delivery*, Singapore: Springer Singapore, 2017, pp. 1–19. doi: 10.1007/978-981-10-2356-9_1.

Chapter 7 Appendix

List of publications

Modugno, P. and Titirici, M.-M. (2021), Influence of Reaction Conditions on Hydrothermal Carbonization of Fructose. ChemSusChem.

Modugno, P., Szego, A. E., Titirici, M. M., & Hedin, N. (2019). Hydrothermal carbonisation and its role in catalysis.

Nicolae, S. A., Au, H., **Modugno, P**., Luo, H., Szego, A. E., Qiao, M., ... & Titirici, M. M. (2020). Recent advances in hydrothermal carbonisation: from tailored carbon materials and biochemicals to applications and bioenergy. Green Chemistry, 22(15), 4747-4800.

Pfersich, J., Arauzo, P. J., Lucian, M., **Modugno, P**., Titirici, M. M., Fiori, L., & Kruse, A. (2020). Hydrothermal conversion of spent sugar beets into high-value platform molecules. Molecules, 25(17), 3914.